

REGULATION OF FATTY ACID TRANSPORT ACROSS THE MITOCHONDRIAL
MEMBRANES IN HUMAN AND RODENT SKELETAL MUSCLE

A Thesis

Presented to

The Faculty of Graduate Studies

of

The University of Guelph

by

VERONIC BEZAIRE

In partial fulfilment of requirements

for the degree of

Doctor of Philosophy

April, 2005

© Veronic Bezaire, 2005

ABSTRACT

REGULATION OF FATTY ACID TRANSPORT ACROSS THE MITOCHONDRIAL MEMBRANES IN HUMAN AND RODENT SKELETAL MUSCLE

Veronic S. Bezaire
University of Guelph, 2005

Advisor:
Lawrence L. Spriet

This thesis is an investigation of the role and regulation of carnitine palmitoyltransferase I (CPTI), fatty acid translocase (FAT/CD36) and uncoupling protein 3 (UCP3) and their impact on fatty acid (FA) transport across the mitochondrial membranes and metabolism in human and rodent skeletal muscle.

The regulation of CPTI activity was examined in intermyofibrillar (IMF) and subsarcolemmal (SS) mitochondria isolated from human and rat skeletal muscle. Maximal CPTI activity and sensitivity to inhibitor malonyl-CoA (M-CoA) was similar between IMF and SS mitochondria from both species. Moderate intensity concentrations of exercise-related metabolites calcium, AMP, ADP and inorganic phosphate failed to override M-CoA inhibition in IMF and SS mitochondria. This data suggests that the regulation of FA transport across the mitochondria during moderate intensity exercise remains unclear.

Following the recent identification of FAT/CD36 in rat skeletal mitochondria, the presence and role of FAT/CD36 in human skeletal muscle mitochondria was investigated. *In vitro* treatment of mitochondria with specific FAT/CD36 inhibitor sulfo-N-succimidyl-oleate (SSO) decreased palmitate oxidation by 95% ($P < 0.01$) without affecting mitochondrial octanoate oxidation demonstrating the specificity of SSO towards FAT/CD36. Furthermore, treatment of mitochondria with SSO had no effect on maximal

and submaximal CPTI activity but did inhibit palmitoylcarnitine oxidation by 92% ($P < 0.001$). Therefore, it was hypothesized that FAT/CD36 is required for palmitate oxidation and functions downstream of CPTI, possibly in the transfer of palmitoylcarnitine from CPTI to CPTII in the intermembrane space of human skeletal muscle mitochondria.

Given the strong link between FA levels and UCP3 expression, the effects of a physiological overexpression of uncoupling protein 3 (UCP3) and ablation of UCP3 on FA transport and oxidation capacity in mouse skeletal muscle were examined. UCP3 overexpression improved serum lipid profile and increased capacity for LCFA uptake ($P < 0.05$) and oxidation ($P < 0.05$) resulting in decreased intramuscular triglyceride stores ($P < 0.05$). High energy phosphagens, coenzyme A and carnitine levels were increased ($P < 0.05$) with UCP3 overexpression but unchanged with UCP3 ablation. Despite the lack of change with UCP3 ablation, this study supports an important role for UCP3 in FA metabolism.

PUBLICATIONS

This thesis is based on the following publications:

Bezaire V, Heigenhauser GJ, Spriet LL. Regulation of CPT I activity in intermyofibrillar and subsarcolemmal mitochondria from human and rat skeletal muscle. (2004) Am J Physiol (Endocrinol & Metab) **286(1)**: E85-91.

Bezaire V, Spriet LL, Campbell S, Sabet N, Gerrits M, Bonen A and Harper M-E. Constitutive UCP3 overexpression at physiological levels increases mouse skeletal muscle capacity for fatty acid transport and oxidation. (2005) FASEB J Published online April 6th.

Bezaire V, Bruce CR, Heigenhauser GJ, Tandon NN, Glatz JFC, Luiken JJF, Bonen A and Spriet LL. Identification of fatty acid translocase on human skeletal muscle mitochondrial membranes: Essential role in fatty acid transport. (2005) Submitted

I would like to acknowledge the work completed by the following individuals:

Dr. Shannon Campbell: Completion of Western blot analysis of FAT/CD36, FABPpm, FABPc on the muscle of Ucp3-tg, wild-type and Ucp3 (-/-) mice.

Dr. Martin Gerrits: Completion of additional indirect calorimetry measurements of Ucp3-tg, wild-type and Ucp3 (-/-) mice.

ACKNOWLEDGEMENTS

I would like to thank my advisor Dr. Lawrence Spriet for giving me the opportunity to discover what I love to do. His guidance and enthusiasm for research have been inspiring.

I am grateful to my thesis committee, Drs Dave Dyck and George Heigenhauser for their availability, thoughtful insight, and support over the past four years.

I would also like to acknowledge my collaborators in these studies: Dr. Mary-ellen Harper (University of Ottawa) and Dr. Arend Bonen (University of Guelph) for giving me the opportunity to expand my horizons.

I have been fortunate to work on a daily basis with a fantastic group of students in the Spriet and Dyck labs. Long hours in the laboratory have gone by quickly thanks to their company and friendship. I would also like to extend my appreciation to the department of Human Biology and Nutritional Sciences for providing a healthy and motivating work environment.

Lastly I would like to thank my family, for their support and interest in my research. J'apprécie que vous me posiez des questions au sujet de ma recherche en sachant que vous ne comprendriez pas la réponse. Stephen, thank you for your love, support, and patience. Thank you for your trust in me and my abilities. I could not have done this without you.

TABLE OF CONTENTS

ACKNOWLEDGEMENTS	i
TABLE OF CONTENTS	ii
LIST OF TABLES	viii
LIST OF FIGURES	ix
CHAPTER ONE	
INTRODUCTION & LITERATURE REVIEW	1
1.1 Introduction.....	2
1.2 Mitochondria	4
<i>1.2.1 Overview</i>	<i>4</i>
<i>1.2.2 Mitochondrial Subfractions Properties</i>	<i>6</i>
<i>1.2.3 Hypothesized Roles of Mitochondrial Subfractions.....</i>	<i>7</i>
<i>1.2.4 Isolation of Mitochondrial Subfractions.....</i>	<i>8</i>
1.3 Carnitine Palmitoyltransferase I (CPTI).....	10
<i>1.3.1 Overview</i>	<i>10</i>
<i>1.3.2 Tissue Expression of CPTI Isoforms.....</i>	<i>11</i>
<i>1.3.3 Identification</i>	<i>11</i>
<i>1.3.4 Structure of CPT Components</i>	<i>12</i>
<i>1.3.5 Molecular Mechanisms of Action</i>	<i>14</i>
<i>1.3.6 Regulation of CPTI</i>	<i>15</i>
1.4 Fatty Acid Translocase (FAT/CD36)	18
<i>1.4.1 Overview</i>	<i>18</i>

1.4.2 Tissue Expression.....	18
1.4.3 Structure.....	19
1.4.4 Role in lipid metabolism	21
1.4.5 Regulation of FAT/CD36.....	23
1.5 Uncoupling Protein 3 (UCP3)	25
1.5.1 Overview	25
1.5.2 Uncoupling and UCP1.....	26
1.5.3 Location/Structure of UCP3	28
1.5.4 Tissue Expression of Novel Uncoupling Proteins.....	28
1.5.5 UCP3 as an Uncoupler.....	29
1.5.6 Role in Protecting Against Reactive Oxygen Species	31
1.5.7 Role as LCFA anion exporter	33
 CHAPTER TWO	
AIMS OF THESIS	37
2.1 Aims of thesis.....	38
 CHAPTER THREE	
REGULATION OF CPTI ACTIVITY IN INTERMYOFIBRILLAR AND	
SUBSARCOLEMMA MITOCHONDRIA FROM HUMAN AND RAT	
SKELETAL MUSCLE.....	40
3.1 Abstract.....	41
3.2 Introduction.....	43
3.3 Methods.....	45
3.3.1 Subjects	45

3.3.2 <i>Experimental protocol</i>	46
3.3.3 <i>Animals and tissue extraction</i>	46
3.3.4 <i>Isolation of mitochondria</i>	47
3.3.5 <i>Determination of CPTI (EC 2.3.1.21) activity</i>	48
3.3.6 <i>Statistics</i>	49
3.4 Results	50
3.4.1 <i>Human skeletal muscle</i>	50
3.4.2 <i>Rat soleus and RG muscles</i>	54
3.5 Discussion	59
3.5.1 <i>IMF and SS mitochondria extraction</i>	59
3.5.2 <i>CPTI activity in human muscle IMF and SS mitochondria</i>	60
3.5.3 <i>CPTI activity in rat muscle IMF and SS mitochondria</i>	61
3.5.4 <i>Regulation of CPTI activity</i>	63
3.5.5 <i>Summary</i>	64
 CHAPTER FOUR	
IDENTIFICATION OF FATTY ACID TRANSLOCASE ON HUMAN SKELETAL	
MUSCLE MITOCHONDRIAL MEMBRANES: ESSENTIAL ROLE IN FATTY	
ACID TRANSPORT	65
4.1 Abstract	66
4.2 Introduction	67
4.3 Methods	69
4.3.1 <i>Subjects</i>	69
4.3.2 <i>Experimental protocols</i>	70

4.3.3 Isolation of mitochondria from skeletal muscle.....	70
4.3.4 Mitochondrial lipid oxidation measurements	72
4.3.5 Enzymatic activities	74
4.3.6 Western Blotting.....	75
4.3.7 Statistics	76
4.4 Results	76
4.4.1 Identification of FAT/CD36 in pure human skeletal muscle mitochondria	76
4.4.2 Assessment of FAT/CD36 function in LCFA mitochondrial transport	78
4.4.3 Relationships between palmitate oxidation, FAT/CD36 content and markers of oxidative capacity	81
4.5 Discussion.....	85
4.5.1 Mitochondrial LCFA transport: roles for CPTI and FAT/CD36	85
4.5.2 FAT/CD36 and mitochondrial LCFA transport	87
4.5.3 CPT and FAT/CD36 cooperation: structural feasibility	88
4.5.4 Correlation studies of FAT/CD36 and oxidative capacity	89
4.5.5 Summary	90
 CHAPTER FIVE	
CONSTITUTIVE UCP3 OVEREXPRESSION AT PHYSIOLOGICAL LEVELS INCREASES MOUSE SKELETAL MUSCLE CAPACITY FOR FATTY ACID TRANSPORT AND OXIDATION.....	
91	91
5.1 Abstract.....	92
5.2 Introduction.....	93
5.3 Methods.....	94

5.3.1 Treatment of animals	94
5.3.2 Indirect Calorimetry	95
5.3.3 Collection of Tissue Samples	96
5.3.4 Collection of Blood and Serum Analysis	96
5.3.5 Isolation of Mitochondria from Skeletal Muscle	97
5.3.6 Western blots of UCP3 protein	97
5.3.7 Enzyme Activity measurements	98
5.3.8 Muscle metabolite and fuel determinations	100
5.3.9 Western blot analyses of key proteins involved in LCFA uptake and metabolism	101
5.3.10 Statistics	101
5.4 Results	102
5.4.1 Food intake, body and tissue weights	102
5.4.2 In vivo studies of metabolic rate, and respiratory exchange ratio (RER)	102
5.4.3 Blood analysis	103
5.4.4 Western blots analyses	104
5.4.5 Enzymatic activities	107
5.4.6 Intramuscular triglyceride content (IMTG)	111
5.4.7 High energy phosphagens and related metabolites	111
5.5 Discussion	114
5.5.1 Serum analyses	116
5.5.2 Expression of fatty acid binding proteins and transporter	117
5.5.3 Intramuscular fuel handling and storage	118

5.5.4 Mitochondrial adaptations.....	119
5.5.5 High energy phosphate adaptations	120
5.5.6 Transgenic mouse models	122
5.5.7 Role of UCP3 in LCFA handling.....	123
5.5.8 Summary	124
CHAPTER SIX	
DISCUSSION AND CONCLUSIONS	126
6.1 Summary of results	127
6.2 Mitochondrial subfractions.....	128
6.3 Concerted regulation of CPTI, FAT/CD36 and UCP3 during low LCFA flux conditions	130
6.4 Concerted regulation of CPTI, FAT/CD36 and UCP3 during acutely elevated LCFA flux conditions	133
6.5 Concerted regulation of CPTI, FAT/CD36 and UCP3 during chronically elevated LCFA flux	136
6.6 Future work	139
6.7 Conclusions	140
REFERENCES.....	142
APPENDIX 1.....	172
APPENDIX 2.....	178
APPENDIX 3.....	180

LIST OF TABLES

Table 3.1. Subject characteristics.....	50
Table 3.2. Enzymatic activities and response to 0.7 μ M M-CoA in IMF and SS mitochondria isolated from human vastus lateralis muscles of recreationally active subjects.....	51
Table 3.3. Enzymatic activities and response to 2 μ M M-CoA in IMF and SS mitochondria of rat soleus and RG muscle.....	55
Table 5.1. Food intake, body and fat pad weights of WT, UCP3-tg and UCP3 (-/-) mice.....	102
Table 5.2. 24h VO_2 and respiratory exchange ratio (RER) of WT, UCP3-tg and UCP3 (-/-) mice measured in the 24h period preceding sacrifice.....	103
Table 5.3. Serum analytes of WT, UCP3-tg, and UCP3 (-/-) mice measured immediately post-decapitation in the fed state.....	104
Table 5.4. Western blot analyses of LCFA transporter protein and AMPK in mixed gastrocnemius muscle of WT, UCP3-tg, and UCP3 (-/-) mice.....	106
Table 5.5. High energy phosphagen muscle content of WT, UCP3-tg, and UCP3 (-/-) mice measured in freeze-dried mixed quadriceps muscle following a perchloric acid extraction.....	112
Table 5.6. Muscle metabolites of WT, UCP3-tg, and UCP3 (-/-) mice measured in freeze-dried mixed quadriceps muscle following a perchloric acid extraction.	113

LIST OF FIGURES

Figure 1.1 Electron micrograph of IMF and SS mitochondria.	5
Figure 1.2. Topology of CPTI. A) Polytopic (hair-pin) topology of CPTI.....	13
Figure 1.3. Regulation of CPTI activity in skeletal muscle.	17
Figure 1.4. Structure of FAT/CD36 its key features.....	21
Figure 1.5. Regulation of FAT/CD36 by insulin and muscle contraction.	24
Figure 1.6. Electron transport chain and the proton leak process through UCP.....	27
Figure 1.7. HNE stimulates proton conductance through UCP/ANT.....	32
Figure 1.8. Hypotheses of UCP3 as a LCFA anion exporter.....	35
Figure 3.1. Effects of M-CoA on CPTI activity of IMF (filled) and SS (open) mitochondria isolated from human vastus lateralis of recreationally active males.	52
Figure 3.2. CPTI activity of IMF (filled) and SS (open) mitochondria isolated from human vastus lateralis of recreationally active males in the presence of physiological concentrations of calcium, free AMP, ADP, and Pi, with 0.7 μ M M-CoA.....	53
Figure 3.3. Effect of pH on CPTI activity of IMF (filled) and SS (open) mitochondria isolated from human vastus lateralis of recreationally active males.....	54
Figure 3.4. Effects of M-CoA on CPTI activity of IMF (filled) and SS (open) mitochondria isolated from rat soleus (A) and RG (B).....	56
Figure 3.5. CPTI activity of IMF (filled) and SS (open) mitochondria isolated from rat soleus (A) and RG (B) skeletal muscle with physiological concentrations of calcium, free AMP, ADP, and Pi, with M-CoA.	58

Figure 4.1. Representative Western blot of FAT/CD36 (A), COXIV (B), Na ⁺ /K ⁺ ATPase (C), and SERCA1 (D).	77
Figure 4.2. Effect of SSO on palmitate oxidation. Activity is expressed as a percentage of maximal palmitate oxidation.	78
Figure 4.3. Effect of 200 μM SSO on octanoate oxidation.	79
Figure 4.4. Effect of SSO on maximal and submaximal CPTI activity (A) and palmitoylcarnitine oxidation (B).	80
Figure 4.5. Simple linear regression analysis between palmitate oxidation and VO ₂ peak (A), CPTI (B), β-HAD (C) and CS (D); N = 14.	83
Figure 4.6. Multiple regression analysis of CPTI and FAT/CD36 on predicted mitochondrial palmitate oxidation.	84
Figure 4.7. Schematic representation of FAT/CD36 facilitating palmitoylcarnitine from CPTI to CPTII.	84
Figure 5.1. Western blot of skeletal muscle mitochondrial UCP3 protein.	105
Figure 5.2. HSL (A) and CPTI (B) enzymatic activity measured in gastrocnemius muscle of WT, UCP3-tg, and UCP3 (-/-).	108
Figure 5.3. β-HAD (A) and citrate synthase (B) activity measured in red quadriceps homogenate of WT, UCP3-tg, and UCP3 (-/-).	110
Figure 5.4. Intramuscular triglyceride content of gastrocnemius muscle from WT, UCP3-tg, and UCP3 (-/-) as measured by lipid extraction.	111
Figure 6.1. Concerted regulation of CPTI, FAT/CD36 and UCP3 in conditions of resting low LCFA flux.	132

Figure 6.2. Concerted regulation of CPTI, FAT/CD36 and UCP3 in conditions of acutely elevated LCFA flux.....	135
Figure 6.3. Concerted regulation of CPTI, FAT/CD36 and UCP3 in conditions of chronically elevated LCFA flux.....	138

CHAPTER ONE
INTRODUCTION & LITERATURE REVIEW

1.1 Introduction

Energy allows the body to function. A balance must be met between energy-producing and energy-requiring pathways for proper functioning. In the body, energy takes the form of adenosine-triphosphate (ATP). The triphosphate molecule has stored energy in its phosphate bounds. The hydrolysis of the phosphates releases the energy and allows it to be utilized by energy-requiring pathways. Thus the generation of energy, or ATP synthesis, is imperative, and skeletal muscle by virtue of its mass, is a major energy-producing tissue. Energy enters the body as foodstuff ingested in our daily diet. Fats, carbohydrates (CHO) and proteins, are the main forms of energy found in the diet, with the first two providing the body with the majority of its energy. Fat stores in the body are virtually unlimited. They are available in large amounts in the North American diet and are stored in adipocytes, the bloodstream and muscles. Due to their abundance, fat stores are preferentially used during prolonged periods of exercise and fasting.

The first potential site of regulation in skeletal muscle fat metabolism and oxidation during exercise is adipose tissue lipolysis and long-chain fatty acids (LCFA) delivery to the muscle. Briefly, increases in plasma norepinehrine and epinephrine during exercise override the inhibition of lipolysis by these same hormones at lower concentrations and the inhibition by adenosine and a constant or decreasing insulin concentration. The net result is the activation of hormone sensitive lipase (HSL) and ultimately triglyceride (TG) degradation to LCFA and glycerol. The LCFA must then be released from the adipose tissue into the blood, a function of plasma LCFA concentration and muscle blood flow.

Once in proximity of muscle cells, LCFA must cross the sarcolemma. This step is the second regulation point in fat metabolism and oxidation. Cellular uptake of LCFA requires specific machinery on the muscle membrane. The LCFA binding protein in the plasma membrane (FABPpm), the fatty acid translocase (FAT/CD36) and the fatty acid transport protein (FATP) are the main transport proteins which regulate cellular LCFA uptake (1; 2). FAT/CD36 has been shown to translocate to the cell membrane from a cytosolic pool in response to various stimuli like muscle contraction (3; 4) or insulin (5).

LCFA are chaperoned by FABP in the cytosol where they have two fates: esterification or oxidation. These two processes appear to occur simultaneously but the oxidation to storage ratio determines which of two processes is favoured (6). In resting conditions, storage of LCFA as intramuscular TG (IMTG) droplets is favoured. In exercise conditions, the oxidation process is favoured over storage resulting in energy production. IMTG droplets must be hydrolyzed prior to oxidation by muscle HSL, the third important point of fat metabolism regulation, catalyzes this reaction (7). HSL is the muscle version of adipose tissue HSL and breaks down IMTG to LCFA and glycerol. It has a neutral pH optimum and is covalently activated by the action of a kinase that adds a phosphate and deactivated by a phosphatase that removes a phosphate as described for adipose tissue HSL. Regulation of HSL during exercise is a result of calcium, epinephrine and AMP activated protein kinase (AMPK) (8).

LCFA entry into mitochondria through the carnitine palmitoyltransferase (CPT) system is the fourth important site of control for fat metabolism. LCFA are activated via binding with coenzyme A (CoA), converted to a fatty acyl carnitine through the action of carnitine palmitoyltransferase I (CPTI) complex and moved across the mitochondrial

membranes while bound to carnitine (9). Inside the mitochondria, the carnitine is removed by carnitine palmitoyltransferase II (CPTII), the CoA is bound to LCFA, and the long chain fatty acyl-CoA (LCFA-CoA) molecules can be metabolized in the β -oxidation pathway with the production of reducing equivalents (NADH, FADH₂) and acetyl-CoA (A-CoA). The A-CoA is further metabolized in the tricarboxylic (TCA) pathway with the production of additional reducing equivalents. The electron transport chain (ETC), including oxygen, accepts the reducing equivalents to generate the proton motive force, which provides the chemical energy used to synthesize ATP from inorganic phosphate (P_i) and ADP in the process of oxidative phosphorylation.

While skeletal muscle handles the oxidation and storage both of LCFA and CHO, this thesis focuses on three proteins involved in the movement of LCFA across the mitochondrial membranes of skeletal muscle. Specifically, the role of CPTI, FAT/CD36, and uncoupling protein 3 (UCP3) is investigated in individual studies. Their involvement in LCFA transport and impact on fat metabolism is examined in rodent and human skeletal muscle.

1.2 Mitochondria

1.2.1 Overview

Mitochondria are known as the energy producing organelles of the cell. Oxidation of both LCFA through the beta-oxidation pathway and CHO through the TCA cycle takes place in the mitochondria. It is in this organelle that CO₂ is generated and that reducing equivalents (FADH₂ and NADH) enter the ETC for the production of ATP. Beta-oxidation of a LCFA to LCFA-CoA generates one molecule of FADH₂ and NADH.

The A-CoA molecule derived from β -oxidation or glycolysis enters the TCA cycle and yields 2 CO₂ molecules, 3 NADH and 1 FADH₂ molecule. The transfer of electrons from the reducing equivalents to O₂ by the electron carriers of the ETC results in the generation of ATP.

The mitochondrion is a complex organelle with its own DNA, the result of an endosymbiotic event (10). There are several theories regarding the structure of mitochondria inside the muscle cell. Studies by Kirkwood et al. (11; 12) and Skulachev (13) demonstrated that rat skeletal mitochondria most likely exist as a reticular structure. However, pioneering morphological studies by Hoppeler and colleagues have demonstrated the presence of two different subfractions of mitochondria but data on their similarities and differences is limited (14-16).

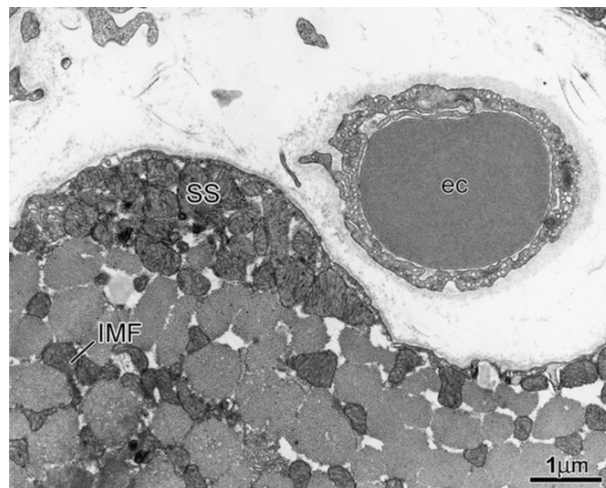


Figure 1.1 Electron micrograph of IMF and SS mitochondria. IMF, intermyofibrillar; SS, subsarcolemmal; ec, erythrocyte. From Hoppeler et al 2003 (17).

The different populations differ primarily by their localization: intermyofibrillar (IMF) mitochondria are located deeper in the cell, associated with the myofibrils while the subsarcolemmal (SS) mitochondria are more superficial, located just beneath the sarcolemma. Studies looking specifically at the functional differences of IMF and SS mitochondria are fairly recent but essential in order to understand the roles of two mitochondrial subfractions.

1.2.2 Mitochondrial Subfractions Properties

The roles of two distinct mitochondrial fractions in skeletal muscle is unclear. Several parameters have been studied in both mitochondrial fractions to elucidate their respective roles. Mitochondrial respiration has been examined extensively in IMF and SS mitochondria. The majority of reports demonstrate that in a variety of tissues, IMF mitochondria display increased state 3 and state 4 respiration when compared to SS mitochondria (18-22) with the exception being duckling mitochondria where the reverse was observed (23). Moreover it has been found in regards to the respiratory control ratio (RCR), an indicator of coupling of respiration and phosphorylation. Researchers have shown increased RCR in IMF than SS mitochondria (18; 21) or no change between the two fractions (19; 22).

Several inner-membrane enzyme activities have been examined and suggest that IMF mitochondria are more oxidative than SS mitochondria. The activities of matrix enzymes isocitrate dehydrogenase and malate dehydrogenase have both been shown to be higher in IMF than in SS mitochondria. More ambiguous results have been found with other enzymes. Krieger et al. (21) reported a 65% greater succinate dehydrogenase

(SDH) activity in IMF vs. SS mitochondria, while Cogswell et al. (19) found a 40% greater SDH activity in SS mitochondria. Cogswell and Lombardi (19; 24) independently reported higher cytochrome oxidase (COX) activity in IMF mitochondria, but Jimenez et al. (25) reported higher COX activity in SS mitochondria of RG (43%) and no difference in the soleus and tibialis anterior muscles. No differences have been found in cytochrome *b*, *c*₁, *c*, and *a* protein content, citrate synthase (CS) and F1-ATPase activity between IMF and SS mitochondria (18; 19; 25). Combined with the increased state 3 and 4 respiration in IMF mitochondria, although ambiguous, these findings suggest that IMF mitochondria are more oxidative than SS mitochondria.

An important property of mitochondria is its ability to adapt to changes in chronic level of contractile activity. This capability has also been examined in IMF and SS mitochondrial subfractions. Muller (26) reported a 53% increase in the cross-sectional area occupied by SS mitochondria in the soleus of rats following training. Hoppeler (15) found a greater increase in volume density of SS vs. IMF mitochondria of the vastus lateralis of well-trained orienteers where as Kiessling (27) observed a greater increase of mitochondrial space in IMF over SS mitochondria in human skeletal muscle following 28 wks of training. Despite controversial results in regards to which mitochondrial fraction is more dynamic in response to training, both fractions have clearly shown the capacity to adapt.

1.2.3 Hypothesized Roles of Mitochondrial Subfractions

The interpretation of the findings described above is still under debate. Although progress has been made, only a few hypotheses have been put forward to explain the

rationale for IMF and SS mitochondrial subfractions. Some have suggested that the IMF and SS mitochondria are at different stages of biogenesis (28) while others have suggested that they have different functions related to metabolic compartmentalization. For example, SS mitochondria, which are nearer the capillaries, may be energetically supporting the transport of oxygen from the erythrocyte to the muscle cell (24). They could also be responsible for generating energy for the phosphorylation of sarcolemmal proteins and transport of ions/metabolites across the sarcolemma. Another hypothesis is that the lower respiration rate of SS mitochondria may preserve oxygen for IMF mitochondria (24). The uncoupled respiration of SS mitochondria could also be a useful mechanism for preventing the accumulation of reactive oxygen species as described by Skulachev (29). Since IMF mitochondria have been shown to be more efficient in ATP production, they have been proposed to support the high ATP demand of muscle contraction and the regulation of Ca^{2+} -ATPase activity (19; 21; 24).

Altogether, these findings demonstrate that research is warranted in the field of IMF and SS mitochondrial subfractions to understand their respective roles in muscle metabolism. The study of mitochondrial subfractions has been focused on rodent skeletal muscle and has been virtually unstudied in human skeletal muscle.

1.2.4 Isolation of Mitochondrial Subfractions

Isolating mitochondria from skeletal muscle offers several advantages over working with a muscle homogenate preparation. Among others, a more robust assessment of mitochondrial enzymatic activities is feasible. Measurements such as mitochondrial respiration, proton leak and transport across the mitochondrial membranes

can also be performed. In addition, working with isolated mitochondria allows for *in vitro* experiments, which offers more control over experimental conditions and the bypass of cellular uptake and metabolism. However, isolating mitochondria may obscure experimental findings, firstly, by having mitochondria outside of their natural environment, and secondly, by damaging membrane proteins of interest while homogenizing the tissue.

In order to isolate IMF and SS mitochondria, homogenization, differential centrifugation and the use of a proteolytic enzyme (nagarse) have been used in the past. SS mitochondria can easily be released by gentle homogenization due to their superficial localization. IMF mitochondria, on the other hand, are located deeper within the cell and require enzymatic digestion of the connective tissue surrounding the myofibrils to be released (22). Because nagarse facilitates the release of IMF mitochondria, its use can double mitochondrial recovery to approximately 30-40% while maintaining high integrity (80-95%) of mitochondria. However, nagarse has been shown to degrade proteins like UCP3 and to reduce CPTI - malonyl-CoA (M-CoA) sensitivity by digesting a sequence key to allosteric inhibition, but not catalytic activity (25; 30-33), (personal unpublished observations). Work by Muzzin et al. (25) has demonstrated an alternative to the use of nagarse. They used a Teflon pestle in a glass Potter-Elvehjem homogenizer with a large and small clearance, to liberate the SS and IMF fractions, respectively. Homogenizing with a smaller clearance was shown to be harsh enough to release the IMF mitochondria without damaging them (25). It must be noted that regardless of nagarse use or not, no specific marker protein for IMF or SS mitochondria has been identified to date, thus some inter-subfraction contamination must be assumed.

In summary, mitochondrial isolation is a delicate procedure, which allows for powerful *in vitro* measurements. Evidence of IMF and SS mitochondrial subfractions with different oxidative characteristics may add another level of complexity to the regulation of skeletal muscle metabolism. More research is warranted to elucidate the respective functions of IMF and SS mitochondria.

1.3 Carnitine Palmitoyltransferase I (CPTI)

1.3.1 Overview

The CPTI enzyme is part of a 3-protein complex (CPT complex), which includes CPTI, CPTII and carnitine-acyltransferase (CAT). Together, they span the inner and outer mitochondrial membranes. In 1987, it was established that CPTI was located in the outer membrane while CPTII and CAT are on the inner membrane (34). By spanning both mitochondrial membranes, the CPT complex acts as a LCFA transport system from the cytosol to the mitochondria. LCFA must be activated in the cytosol by an acyl-CoA synthetase (ACS) to form LCFA-CoA in order to become a substrate for CPTI. In this form, the fatty acyl units bind to the CPTI LCFA binding domain on the outer leaflet of the outer membrane. The CoA is then cleaved off and replaced by a carnitine molecule through the action of CPTI. LCFA-carnitine is handed over to CPTII, where carnitine is cleaved off and recycled in the intermembrane space. The LCFA anion is now facing the matrix where it can bind CoA. CoA pools in the cytosol and the matrix as well as carnitine are required for proper functioning of this system.

CPTI is known as the rate-limiting step of LCFA transport whereas CAT and CPTII are near-equilibrium enzyme. The use of molecular biology techniques in the late

1980s was necessary to elucidate the structure and function of the CPT system. Although significant advancements have been made, the regulation of CPTI in human skeletal muscle is still not fully understood.

1.3.2 Tissue Expression of CPTI Isoforms

Two different isoforms of CPTI have been identified. They are designated as L-CPTI and M-CPTI based on the tissues in which they were both first identified, liver and muscle, respectively. However, both isoforms are expressed in other tissues as well. L-CPTI is expressed predominantly in the liver, kidneys, lungs, spleen, intestines, pancreas, ovaries and human fibroblasts. M-CPTI, on the other hand, is found largely in skeletal muscle, heart, brown adipose tissue, white adipocytes and testis (35; 36). The isoforms differ in their sensitivity to known substrates and inhibitors. They exhibit different sensitivity to M-CoA (IC_{50} of $\sim 2.7 \mu\text{M}$ in liver vs. $\sim 0.03 \mu\text{M}$ in muscle) as well as different K_m values for the substrate carnitine ($\sim 30 \mu\text{M}$ and $500 \mu\text{M}$, respectively) (37).

1.3.3 Identification

Molecular characterization of the CPT proteins started in the late 1980s and was predominantly completed by McGarry and colleagues (see McGarry and Brown 1997 for review) (38). Not surprisingly, characterization of the CPT proteins was first performed using rodent mitochondria but isolation of the human counterpart of CPT proteins soon followed. Liver was the tissue of choice for the pioneering studies.

Rat L-CPTII was the initial focus of research since it was detergent soluble, thus easier to isolate when compared to L-CPTI. Rat L-CPTII was isolated, purified and

antibodies were quickly raised against it (39). CPTII was found to be formed of 658 amino acids containing a 25 amino acid NH₂-terminal leader sequence which is cleaved upon mitochondrial import and results in a functionally mature protein of 71 kDa (39). Human L-CPTII was cloned based on the rat L-CPTII protein and it was quickly determined that rat and human L-CPTII proteins were 82% identical at the amino acid level, although the rat mature protein has a molecular mass 100 Da greater than that of the human L-CPTII (40; 41).

Characterization of L-CPTI was also performed in rat prior to human mitochondria. Difficulties were encountered due to its tight membrane association and loss of catalytic activity when removed from its natural environment (42). Five years later, it was concluded that the rat L-CPTI molecule consisted of a single polypeptide containing both the inhibitor and catalytic domains (43). The human L-CPTI was then isolated from a human liver cDNA library and found to be 88% identical to the rat L-CPTI (35). Cloning of the human muscle isoform of CPTI and CPTII was completed a year later (44). The nucleotide sequences and primary structures of the rat and human proteins are very similar (45; 46) but as will be discussed in a later section, regulation of rat and human CPTI differ greatly. From this point onwards, only the M-CPTI isoform will be discussed and for simplicity purposes, will be referred to as 'CPTI'.

1.3.4 Structure of CPT Components

As mentioned above, CPTI is located on the outer mitochondrial membrane. It is almost entirely located on the cytosolic side of the outer membrane. CPTI contains two transmembrane domains (TM), separated by a 27-residue loop, and both amino and

carboxy terminals (composed of ~46 and 651 residues, respectively) are exposed on the cytosolic surface of the outer membrane (Figure 1.2) (30; 47; 48).

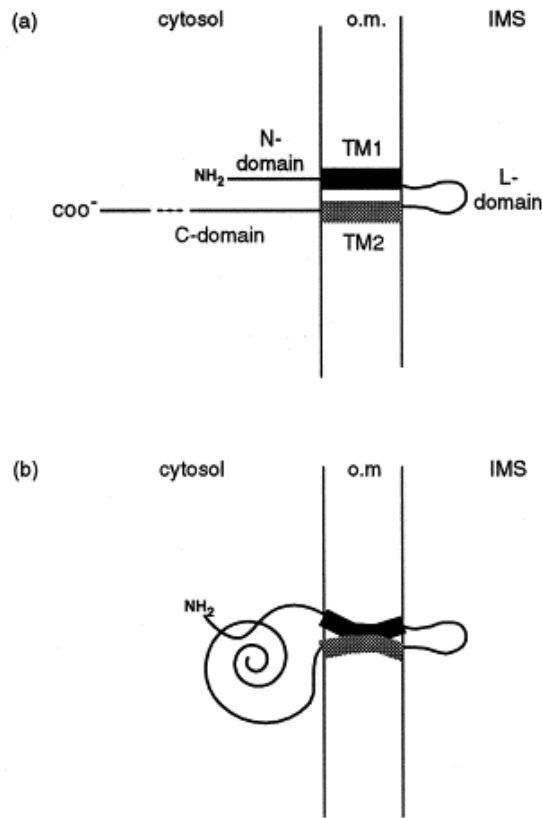


Figure 1.2. Topology of CPTI. A) Polytopic (hair-pin) topology of CPTI. B) Tertiary structure of CPTI. IMS, intermembrane space; TM, transmembrane domain; o.m., outer membrane. From Zammit et al. (49).

Strong evidence for this topology comes from a study by Fraser et al (30) in which octanoyl-CoA and M-CoA were rendered impermeable to the outer membrane by coupling to agarose beads. Despite this, octanoyl-CoA and M-CoA were still capable of acting as a CPTI substrate and inhibitor, respectively, indicating that domains necessary for regulation of CPTI are accessible from the cytosolic side. The specific residues

forming the carnitine and acyl-CoA pockets are still under investigation. However, A'Bhaird and colleagues (50) have demonstrated that binding of CoA (or CoA derivative) must precede that of carnitine (or carnitine derivative) for CPTII and it is believed that the same order is required for CPTI substrate binding.

CPTII is only loosely associated with the inside of the inner mitochondrial membrane. It lacks a hydrophobic amino acid sequence indicative of a membrane-spanning domain and is easily solubilized by treatment with mild detergents (51). Its catalytic centre has been shown to be located in the matrix since intact mitochondria are insensitive to protease treatment while when the matrix is exposed by freeze/thaw cycles, CPTII is readily proteolysed (52).

The CAT is a 32.5 kDa protein containing three homologous tandem repeats which are common among mitochondrial transporters (53; 54). It is located on the outer leaflet of the inner mitochondrial membrane and appears to function as a ping-pong type carrier. This mechanism of action has been studied by reconstitution of the carrier in liposomes loaded with carnitine and fatty acylcarnitine of various chain lengths (53).

1.3.5 Molecular Mechanisms of Action

The general structure of the CPT complex is fairly well understood but the key residues allowing substrate and inhibitor binding are still under debate. The interaction of M-CoA and effect of pH have been studied the most. Inhibition of CPTI activity is produced by the presence of two binding sites. It has been hypothesized that a low affinity binding site is located near the substrate binding site (carboxy terminal) and allows M-CoA and other smaller CoA moeity to bind and physically interfere with

substrate binding (55; 56). The high affinity M-CoA binding site is located on the amino terminal of CPTI, a sequence that is not present on M-CoA insensitive CPTII (40; 41; 45; 46). Chimeric studies demonstrated that deletion of the first 18 N-terminal residues and specifically substitution of glutamate-3 to alanine abolished M-CoA induced CPTI inhibition and binding but not catalysis (57). Substitution of histidine-5 to alanine also causes a partial loss of M-CoA inhibition (58). It is not known at this point whether these residues form directly the M-CoA binding site or whether they are required for amino-carboxy terminal interaction, which together, allow M-CoA to bind CPTI. A lowering in pH has also been shown to decrease the affinity of CPTI for carnitine and increase that of M-CoA (59; 60). The pH change has been associated with the protonation of histidine residue imidazole groups involved in the CPTI reaction.

1.3.6 Regulation of CPTI

When LCFA oxidation is too great, A-CoA units accumulate and lead to the production of M-CoA, the main inhibitor of CPTI. The enzyme acetyl-CoA carboxylase (ACC) is responsible for the synthesis of M-CoA (61). In rat skeletal muscle, M-CoA is elevated at rest and partially inhibits CPTI activity and fat oxidation (62). During muscle contraction, M-CoA levels decrease, relieving CPTI inhibition and allowing greater rates of fat oxidation (62) (Figure 1.3). In human skeletal muscle however, the situation appears to be more complex. Firstly, the resting M-CoA concentrations are greater than the IC_{50} , which would lead one to believe that CPTI is always inhibited (63). An explanation for this paradox could be that M-CoA is stored as a pool or is bound to a protein and cannot be seen by CPTI such that the effective concentration of M-CoA is

below the IC_{50} (38). Also, mitochondrial damage during the isolation process could result in decreased M-CoA sensitivity *in vitro*. As well, Kim et al. (64) have demonstrated the presence of a M-CoA insensitive isoform of CPTI in rodent skeletal muscle. The controversy persists during exercise since the majority of studies found that M-CoA levels remain elevated during exercise in humans despite increased fat oxidation rates (65-67). Only recently has a group been successful in showing decreased M-CoA levels with moderate intensity exercise (68). Again, it is important to note that the magnitude of M-CoA decrease with exercise is in the same order of magnitude in all the studies, regardless of statistical significance. This inconsistency suggests that the regulation of CPTI is more complex or that M-CoA inhibition is overridden during exercise.

Starritt et al. (69) have previously examined the effects of other muscle metabolites on CPTI activity in an isolated mitochondrial preparation from human skeletal muscle. It was determined that exercising levels of A-CoA, CoA, and acetylcarnitine had no effect on CPTI activity, but that a decrease in pH from 7.1 to 6.8 reduced CPTI activity by 40%. This decrease in pH could partially explain the decreased reliance on fat during very high intensity exercise when pH is lower. However, it does not provide an explanation for the up-regulation of CPTI during moderate intensity exercise where changes in pH are minimal (70). The regulation of CPTI activity is also affected by aerobic training (69). Starritt et al found that CPTI activity was close to two-fold greater in aerobically trained subjects when compared to untrained subjects, but were more sensitive to M-CoA inhibition *in vitro*. However, this paradox can be explained by

the fact that trained subjects had greater CPTI activity than untrained subjects at any given M-CoA concentration.

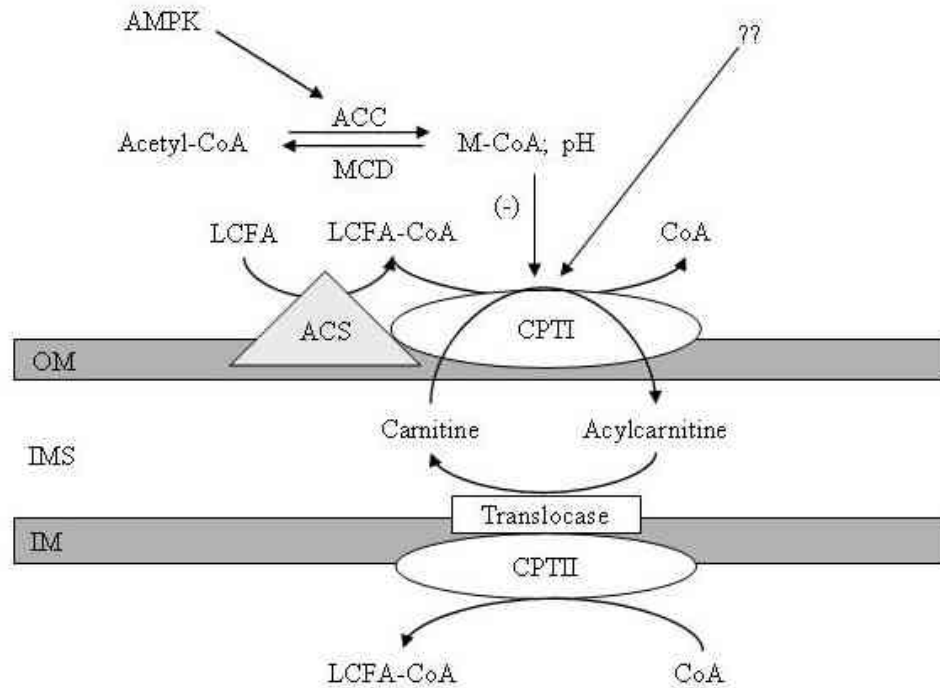


Figure 1.3. Regulation of CPTI activity in skeletal muscle. OM, outer membrane; IMS, intermembrane space; IM, inner membrane; ACC, acetyl-CoA carboxylase; MCD, malonyl-CoA decarboxylase; ACS, acyl-CoA synthetase; LCFA-CoA, long chain fatty acid-CoA.

In summary, the CPT complex is a major player in the regulation of LCFA metabolism by providing means for mitochondrial uptake of LCFA. Surprisingly, the regulation of such an imperative step remains ambiguous. Whether an unknown

regulator of CPTI or another transport protein is involved in LCFA transport across the mitochondrial membrane remains to be proven.

1.4 Fatty Acid Translocase (FAT/CD36)

1.4.1 Overview

FAT/CD36 is a multi-ligand scavenger protein. Its wide-ranging functions include roles in angiogenesis, atherosclerosis, inflammation and lipid metabolism. Its original role is related to innate immunity but lately, it is the advancements on the lipid metabolism front that have been the source of many publications. Transgenic studies and the use of giant vesicles have demonstrated a role for FAT/CD36 in cellular LCFA uptake in rat heart and skeletal myocytes. Specifically, it has been shown that FAT/CD36 is a transmembrane protein with LCFA saturation kinetics. It can also be inhibited by sulfo-*N*-succinimidyl-oleate (SSO), a reactive oleate ester. Some controversy revolves around the idea of an intracellular pool and its translocation to both the mitochondrial and plasma membranes but evidence supporting this is growing. According to this theory, insulin and muscle contraction appear to be the main regulators of LCFA translocation and uptake.

1.4.2 Tissue Expression

FAT is the rat homologue of human CD36, a member of the class B scavenger receptor family. CD36 takes its name from its original antigenic properties (71). FAT has 85% homology at the amino acid level to human CD36 (72). As a multi-ligand scavenger protein, it is expressed in a variety of tissues. For simplicity, rat FAT and

human CD36 homologues will from now on be referred to as FAT/CD36. FAT/CD36 was first identified in human platelets, where it was known as glycoprotein IV, a receptor for thrombospondin-1 (TSP-1) (73). As a TSP-1 receptor, FAT/CD36 mediated antiangiogenesis (74). It has also been found in hematopoietic cells where it has been shown to bind oxidized low-density lipoprotein (LDL) and participate in foam cell formation and the pathogenesis of atherosclerosis (75; 76). FAT/CD36 is widely expressed in epithelial cells (77), endothelial cells (78), dendritic cells (79), epithelia of the retina (80), and several other tissues with a high capacity for LCFA such as adipose tissue (72), heart muscle (81) and skeletal muscle cells (82). It is not present in liver, brain and kidney (72; 83; 84). The wide-ranging expression of FAT/CD36 is concomitant to its wide-ranging functions described above.

1.4.3 Structure

FAT/CD36 is an 88 kDa protein transmembrane glycoprotein. Until recently, two structural models for FAT/CD36 were accepted. The first model proposed a short carboxy cytoplasmic tail followed by a lone transmembrane domain near the same terminal while the remainder of the protein was extracellular. A stretch of 27 hydrophobic residues representative of a transmembrane domain near its carboxy terminal along with 6 amino acids, thought to be an intracellular domain responsible for signal transduction and internalization of bound ligands have both been confirmed (85). Greenwalt et al (77) proposed another model, this one with a second transmembrane domain near the amino terminal, and its own amino terminal cytosolic tail (Figure 1.4). The bulk of the protein, which is highly N-linked glycosylated, is believed to be

extracellular. Tao et al have (86) provided evidence for Greenwalt's two transmembrane domain model using carboxy-terminal mutant FAT/CD36. Tao also followed up on Jochen and Hays' (87) work showing that rat adipocyte FAT/CD36 could be palmitoylated (addition of palmitate molecule) when incubated with $^3\text{[H]}$ -palmitate and that this process was amplified in the presence of insulin and during energy depletion. They showed specifically by expressing human CD36 vector in embryonic kidney cells that FAT/CD36 can be palmitoylated on cysteine residues 3, 7, 464 and 466, located at the interface of the cytoplasm and the cytoplasmic leaflet of the membrane. These findings are of great importance for the proposed roles of FAT/CD36 in lipid metabolism. Other structure-function information of importance include a TPS-1 binding site at amino acids 93-120 (88), oxidized LDL binding domains at amino acids 28-93 and 120-155, and an apoptotic cell binding site between amino acids 155 and 183 (89).

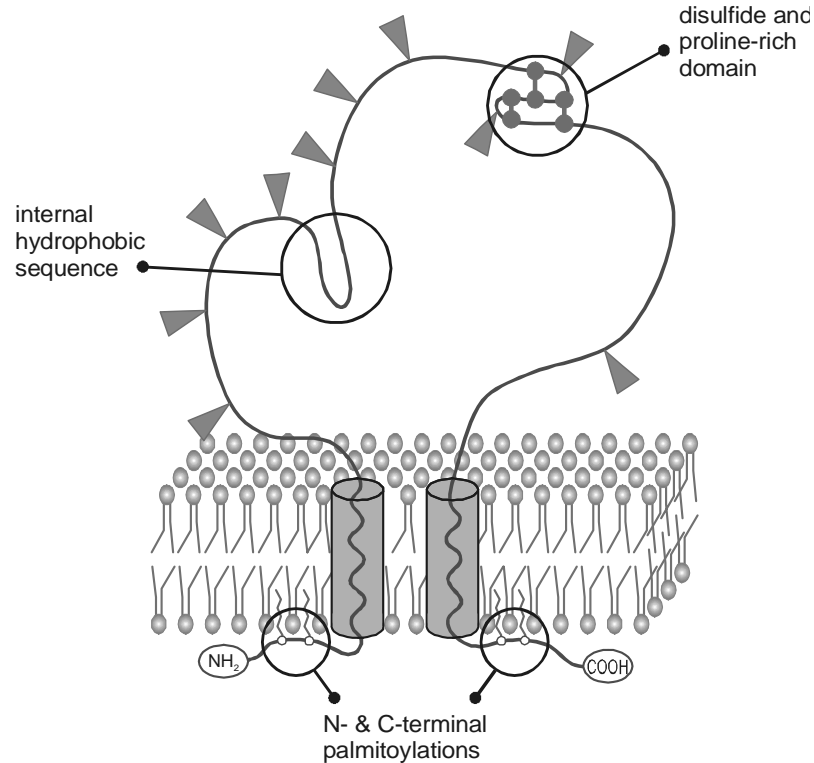


Figure 1.4. Structure of FAT/CD36 its key features. Triangles indicate N-linked glycosylations. From Duttaroy et al 2003 (90).

1.4.4 Role in lipid metabolism

Cellular LCFA uptake has been a controversial issue for fifteen years and fuelling the fire has been the question of passive diffusion versus protein-mediated uptake of LCFA. In the late 1980s, studies showed kinetic evidence of protein-mediated uptake of LCFA (91-93). But to unequivocally demonstrate protein-mediated LCFA uptake, transport across the membrane needed to be dissociated from subsequent metabolism. Luiken et al (94) achieved this by preparing giant membrane vesicles isolated by collagenase treatment. The vesicles were fully right side out, contained cytosolic LCFA

binding protein (FABPc) which acted as a LCFA sink, and were larger than traditional vesicles, allowing for greater uptake. Using this model, it was shown that LCFA uptake in heart, red and white skeletal muscle vesicles is protein mediated and involves FAT/CD36 and FABPpm. Saturation kinetics and inhibition of FAT/CD36 and LCFA uptake using SSO provided evidence for this protein-mediated system.

Transgenic studies provided more information relating to the role of FAT/CD36 in LCFA metabolism. In 1998, Van Nieuwenhoven et al (95) expressed FAT/CD36 in a rat heart cell line not normally expressing the protein. They found LCFA uptake to be mainly the result of passive diffusion but with a small uptake component, which was subject to substrate saturation. They found no correlation between FAT/CD36 expression levels and the rate of palmitate uptake. Ibrahimi et al (96) took a more relevant approach and overexpressed the muscle-specific FAT/CD36 in mice skeletal muscle. They found that FAT/CD36 overexpression lead to lower body weights, decreased blood triglycerides, and enhanced ability to oxidize LCFA in response to stimulation. With only two overexpression studies in the literature yielding opposing outcomes, it is difficult to draw a firm conclusion.

Only one group has ventured in the FAT/CD36 ablated mice field but with convincing results. Febbraio et al (97) found that the FAT/CD36 null mice had decreased binding and uptake of oxidized LDL and increased fasting cholesterol, LCFA and triglycerides, decreased fasting serum glucose and decreased oleate uptake in adipocytes, thus clearly supporting a role for FAT/CD36 in lipid metabolism.

1.4.5 Regulation of FAT/CD36

If FAT/CD36 is indeed a LCFA transport protein, one would expect it to be subject to regulation by LCFA-related signals. Bonen et al (98) investigated the effects of muscle contraction on FAT/CD36. Using their giant vesicle preparation, they showed that following muscle contraction, palmitate uptake was increased compared to vesicles prepared from non-contracted muscle. With the aid of a fractionation technique, they also demonstrated that FAT/CD36 was found both in plasma membrane and cytosolic fragments. Similarly to glucose transport protein 4 (GLUT4), they showed that a greater fraction of total FAT/CD36 was located at the plasma membrane following muscle contraction, suggesting the translocation of FAT/CD36 from a cytosolic pool upon muscle contraction. They later demonstrated that insulin had a similar effect in rat hindlimb muscle and cardiac myocytes (5; 99). These findings are particularly interesting given the palmitoylation of FAT/CD36 previously discussed. Palmitoylation of enzymes is usually associated with a change in subcellular localization by reversible membrane association (81; 100). Recently, the same group has demonstrated the presence of FAT/CD36 in rat skeletal muscle mitochondria (Figure 1.5) (3). They demonstrated the importance of mitochondrial FAT/CD36 in palmitate oxidation by inhibiting FAT/CD36 with SSO and thereby abolishing oxidation. Similarly to plasma membrane FAT/CD36, they showed that acute and chronic electrical stimulation increased mitochondrial FAT/CD36 content. Lastly, they found that FAT/CD36 co-precipitated with CPTI suggesting a physical link between the two proteins. How

FAT/CD36 would translocate from an intracellular pool to the mitochondria and sarcolemma where it would play different roles was not discussed.

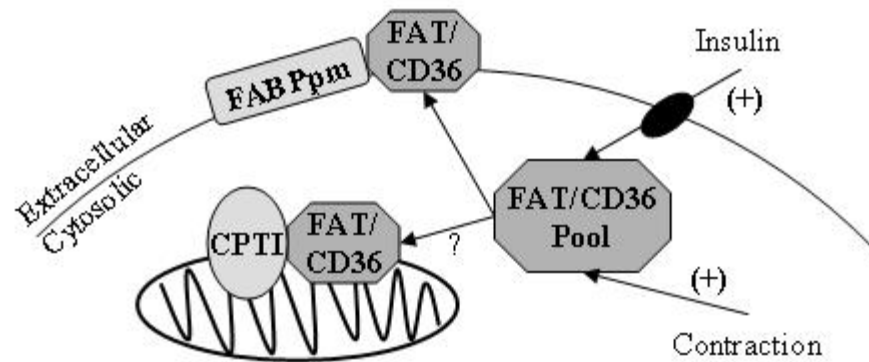


Figure 1.5. Regulation of FAT/CD36 by insulin and muscle contraction. FAT/CD36 migrates to the sarcolemma and mitochondrial membrane to possibly work in conjunction with FABPpm and CPTI, respectively.

The majority of the work in the field of FAT/CD36 and lipid metabolism has been conducted by one group only, which limits an objective assessment. However, Vistisen et al (101) recently examined FAT/CD36 in human skeletal muscle but using a different approach, electron microscopy. Their results differed significantly from Bonen and colleagues. Firstly, they found that FAT/CD36 was expressed strongly in endothelial cells and only weakly in sarcolemma. Importantly, they found no evidence of an intracellular or mitochondrial pool of FAT/CD36 despite being able to detect intracellular GLUT4. They acknowledge that the resolution of the electron microscope could possibly prevent detection of a small (when compared to GLUT4) cytosolic pool of FAT/CD36.

Interestingly, FAT/CD36 colocalized with caveolin-3, a muscle-specific marker protein for plasma membrane invaginations. These findings extend on previous findings indicating colocalization of endothelial cell CD36 with the ubiquitous caveolin-1 (102). From these findings, they proposed that caveolae may regulate the function of FAT/CD36 as LCFA transporter. However, while FAT/CD36 was expressed to greater extent in red muscle, caveolin-3 was found preferentially in white muscle. The authors argue that this discrepancy is the result of other fiber type specific functions of caveolin-3.

In summary, FAT/CD36 is a multi-ligand protein with functions as diverse as its ligands. Its role in LCFA uptake at the plasma and mitochondrial membranes is rapidly making headway and could suggest major changes to the traditional mitochondrial LCFA uptake system.

1.5 Uncoupling Protein 3 (UCP3)

1.5.1 Overview

UCP3 belongs to the mitochondrial carrier protein superfamily. UCP3 is part of the ‘uncoupling protein’ subfamily along with UCP1, UCP2, and bird UCPs. These proteins have been termed ‘uncoupling’ based on their high homology to the original uncoupling protein, UCP1, also known as thermogenin. UCP1 is located on the outer leaflet of the inner mitochondrial membrane of brown adipose tissue and uncouples oxygen consumption from oxidative phosphorylation by dissipating the proton motive force. The novel UCP3 is thought to play a similar role in skeletal muscle but its true function remains under investigation. The hypothesized functions of UCP3 range from

true uncoupler, to protection against reactive oxygen species and exporter of LCFA anion. Therefore, it is very likely that it is incorrectly named.

1.5.2 Uncoupling and UCP1

The ETC, located on the mitochondrial inner membrane (IM), is the site of oxidative phosphorylation. It is in the ETC that reducing equivalents from the pyruvate dehydrogenase (PDH) reaction, the TCA cycle, glycolytic activity (via the shuttle systems) and β -oxidation are oxidized in exchange for electrons. This process creates a net proton gradient across the inter membrane space (IMS) generating a given membrane potential. When the gradient is high enough, protons flow back to the matrix via the ATP synthase, releasing the energy needed to phosphorylate ADP and generate ATP (state 3 respiration) (See Brand et al for review (103)). In perfectly coupled mitochondria, no protons leak across the IMS and all the energy from the electron transport chain is used for ATP synthesis. However it has repeatedly been shown that mitochondria do show respiration in the absence of ADP (state 4 respiration). This indicates that protons are escaping the inner membrane without generating ATP. This process, referred to as ‘proton leak’ or ‘mitochondrial uncoupling’ accounts for a major part of normal metabolism in several tissues (Figure 1.6).

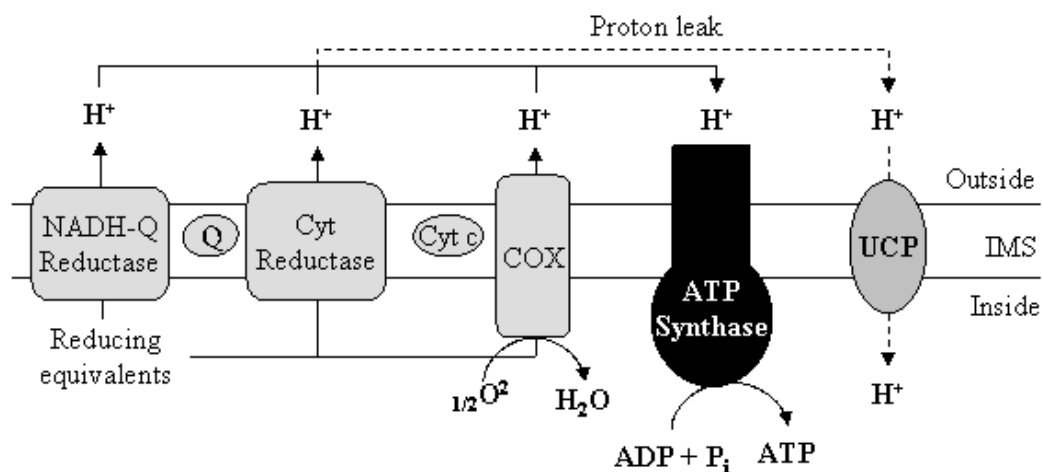


Figure 1.6. Electron transport chain and the proton leak process through UCP. Q, succinate-Q reductase; Cyt reductase: cytochrome reductase; Cyt c: cytochrome c; COX: cytochrome oxidase; IMS, inner membrane space.

Mitochondrial uncoupling has been calculated to account for up to 20% of basal metabolic rate (104). Mitochondrial uncoupling causes a decrease in membrane potential, but this decrease is not sufficient to qualify a process as ‘uncoupling’. Any type of work conducted by the mitochondria will result in decreased membrane potential, whether the energy is used for ATP synthesis or not. Proton leak curves in isolated mitochondria must be performed to assess mitochondrial uncoupling (for review see Brand MD 1997, (105)).

The brown adipose tissue (BAT) protein UCP1 is known as the original uncoupler. Its gene was cloned in 1988 (106; 107). It plays the well recognized role of adaptive thermogenesis in BAT (108). This signifies that the energy generated from the ETC is released as heat as opposed to being used for ATP synthesis following adaptation

to cold. This process is activated by LCFA and inhibited by purine nucleotides. Adaptive thermogenesis is of great importance for energy balance in rodents. Adult humans have very little BAT thus the discovery in the late 1990s of UCP1 homologues expressed in non-BAT tissues, has been exciting to researchers in mitochondrial energetics.

1.5.3 Location/Structure of UCP3

The UCP3 protein spans the IMS. Its gene contains seven exons spread over 8.5 kb and includes six transmembrane domains. Adjacent to UCP2, it is found on chromosome 11 (11q13), a loci which has been associated with obesity (109-111). The UCP3 gene generates two mRNA transcripts, UCP3_L and UCP3_S. The UCP3_S form is generated by a polyadenylation signal in exon 6 which terminates elongation early (ie: before exon 7) in 50% of the time. UCP3_S differs from UCP3_L by lacking the last 37 carboxy residues. Whether the shorter UCP3 transcript yields a functional protein is still under investigation.

1.5.4 Tissue Expression of Novel Uncoupling Proteins

Unlike UCP1, the novel uncoupling proteins were identified by ‘reversed cloning’: they were identified in databases due to their high homology to UCP1 but their proteins possessed no known functions (112-116). The first step in identifying the function(s) of the novel uncoupling proteins was a complete examination of tissue expression, at the mRNA and protein level. However, this revealed few hints as to what their role may be. UCP3 is expressed at the mRNA level in brown adipose tissue and

muscle but the UCP3 protein is found in muscle only (25; 117-119). UCP2 mRNA expression is widespread but its protein is mainly found in mitochondria isolated from spleen, stomach, lung, intestine and white adipose tissue (120-123). Although important information, tissue expression of the novel uncoupling proteins was of little benefit to the search for their potential functions.

1.5.5 UCP3 as an Uncoupler

Given the high homology between UCP3 and UCP1, the investigation of the role of UCP3 as an uncoupler is not unexpected. Early studies in yeast, cell cultures or tissues where UCP3 was entopically or ectopically overexpressed support a role in uncoupling (115; 124-127). However, Matthias et al (128) demonstrated that neither UCP2 nor UCP3 were thermogenically active in BAT of UCP1 ablated mice eliminating the possibility that the novel uncoupling proteins are ‘thermogenic uncouplers’. Moreover, they demonstrated that the uncoupled action observed following supraphysiological ectopic expression or entopic overexpression of uncoupling proteins is not physiologically relevant. Specifically, they demonstrated that entopic UCP1 in BAT uncouples only when physiologically activated whereas ectopic UCP1 constitutively uncouples and is not subject to regulation (128). The explanation behind these findings appears to be related to the degree of overexpression. When carrier proteins are ectopically expressed or entopically overexpressed to supraphysiological levels, the functional protein is not correctly inserted in the membrane, causing artifactual uncoupling (129; 130). This being said, studies demonstrating uncoupling following overexpression of UCP3 should be interpreted carefully. To circumvent this problem, it

has been suggested that researchers attempt to demonstrate that the function of UCP3 as a result of the overexpression can not be mimicked by an artificial uncoupler.

Artifactual uncoupling aside, could UCP3 still be responsible for a significant fraction of proton leak in mitochondria? Reports appear to support this hypothesis but with a degree of inconsistency. Vidal-Puig et al. (119) showed a decreased state 4 respiration in UCP3 ablated mice and a trend for an increased ATP/ADP ratio. Gong et al (118) and Bezaire et al (131) showed increased membrane potential in UCP3 ablated mice while Cadenas et al (117) saw no change in respiration rates, respiratory exchange ratios or proton conductance. Importantly, Cadenas et al were the only group to conduct their experiments in wild-type and UCP3 ablated mice of congenic background.

The uncoupling-related hypothesized functions of UCP3 do not end here. It has also been suggested that through its uncoupling action, UCP3 could lead to protection against obesity. Evidence supporting this line of thought comes from the important contribution of skeletal muscle to basal metabolic rate. It is thought that UCP3 expression levels could be responsible for differences in basal metabolic rate between humans. Indeed, the overexpression of UCP3 in mouse skeletal muscle proved to be a cure for obesity (132). However, evidence against this function is quite strong. Firstly, fasting, which is an energy-preserving state increases UCP3 expression (115; 133; 134). If uncoupling renders oxidative phosphorylation less efficient, it is counter intuitive to believe that the uncoupling process should be augmented during fasting. Furthermore, physiological increases in UCP3 expression do not lead to increased proton leak. Cadenas et al. (135) and Bezaire et al. (131) independently showed that fasting increases

UCP3 expression 4-fold (protein 2-fold) without increasing proton leak arguing against a primary role for UCP3 in proton leak.

1.5.6 Role in Protecting Against Reactive Oxygen Species

UCP3, along with UCP1 and UCP2, has been proposed to play a role in reducing reactive oxygen species (ROS). ROS are produced in the mitochondria when flux through the ETC is high and oxidation is limited (ie, intense exercise, elevated LCFA oxidation). This creates an accumulation of electrons in the ETC, which reacts with oxygen to form ROS. ROS have deleterious effects on metabolism and mitochondria are a large contributor to cellular ROS production. Although protective mechanisms like glutathione peroxidase, catalase and superoxide dismutase already exist (136), UCP3 (and UCP2) has been proposed to relieve ROS formation by uncoupling related processes and decreasing mitochondrial membrane potential.

Evidence suggesting a role for UCP2/UCP3 in reducing ROS production comes from the observation that fasting, a state of elevated oxygen stress, increases UCP2 and UCP3 expression. Other highly oxygen stressed conditions such as fever, or lipopolysaccharide injection, increase UCP2 expression in lungs (122). Increased ROS production has also been found in macrophages of UCP2 ablated mice, and skeletal muscle of UCP3 ablated mice (119; 137; 138). Evidence supporting this hypothesis comes primarily from Brand and colleagues. They have shown, in isolated mitochondria from a variety of tissues that superoxide, a ROS byproduct, interacts with UCP1, UCP2 and UCP3 to cause proton conductance. The interaction is activated by LCFA and inhibited by purine nucleotides, which is in accordance with UCP characteristics. A

more detailed positive feedback loop was proposed by Echtay et al 2003 (139) (Figure 1.7). Briefly, it suggests that mitochondrial ROS production leads to lipid peroxidation and hydroxynonenal (HNE) production. HNE induces mild uncoupling through the UCPs and the adenine nucleotide translocase (ANT) to decrease membrane potential and ROS production.

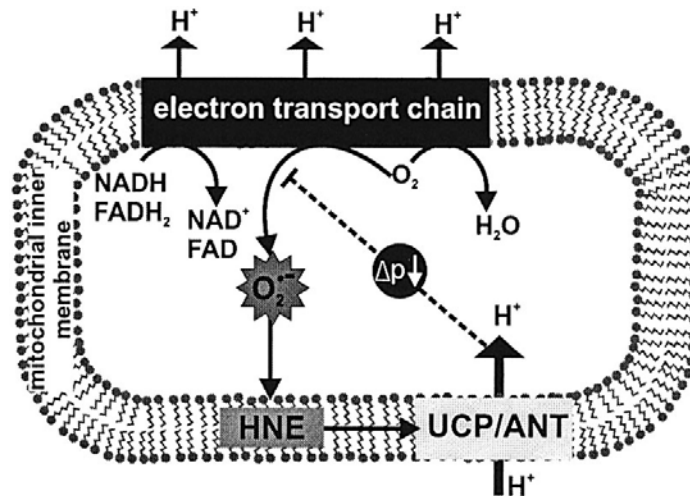


Figure 1.7. HNE stimulates proton conductance through UCP/ANT. O₂⁻, superoxide, Δp, membrane potential. From Echtay et al 2003 (139).

It is reasonable to expect uncoupling action to provide assistance in ROS management by increasing flux through ETC and thereby lowering ROS formation. But for this to take place, UCP3 must have innate uncoupling properties and based on the evidence presented above, those properties have yet to be demonstrated unequivocally. As well, the lack of UCP homologue in liver and kidney, organs with steep ROS production rates may suggest that the presence of UCP is not imperative to control oxygen damage. Arguing more specifically, Brand's hypothesis is not unique to UCP but includes other mitochondrial carrier proteins like ANT. Moreover, UCP3

overexpressing mice do not benefit from additional protection against ROS when compared to wild-type mice (138). Lastly, Couplan et al. (140) were unable to reproduce results from Brand et al. in wild-type and UCP2 ablated mice. Mainly, they saw no change in basal proton leak, no effect of superoxide on proton leak and no change in ATP/ADP ratio between wild-type and UCP2 ablated mice.

1.5.7 Role as LCFA anion exporter

UCP3 was first thought to be involved in LCFA metabolism in 1998, one year after it was discovered (141). Its expression patterns in response to acute exercise, high fat diets, endurance training and weight reduction supported this idea. Samec et al. (140) hypothesized a role for UCP3 in the regulation of lipid as a fuel substrate based on the observation that UCP2/UCP3 expression increased during food restriction in rats. Since then, several groups have shown similar increases in response to fasting in both rodent and human skeletal muscle (131; 133; 135; 142; 143). Weigle et al (134) provided an explanation for the ‘fasting paradox’. They showed that an intralipid injection in fed rats had the same effect on UCP3 expression as a 24 hour fast, suggesting that UCP3 expression is regulated by LCFA levels. It has also been shown that UCP3 gen and protein expression increases following an exercise bout in rodent and human skeletal muscle (144-147). Schrauwen and colleagues (148) demonstrated that the increase in UCP3 expression during exercise was not caused by exercise per se, but rather by the increased circulating LCFA induced by exercise. Endurance training and weight reduction have the opposite effect on UCP3 expression (149; 150). Both have been shown to reduce its expression, suggesting an adaptation to lower levels of LCFA. It was

also demonstrated that UCP3 contains a peroxisome proliferators activated receptor (PPAR)-response element, confirming its regulation by LCFA (151).

From a genetic standpoint, it has been shown that genetic variations in the UCP3 gene is associated with decreased fat oxidation rates and increased body mass index (152; 153). More recently, studies with transgenic mice have demonstrated that UCP3 overexpression (albeit, non physiological) leads to a leaner phenotype, improved fat oxidation capacity, and resistance to diet-induced obesity (132; 154; 155). Altogether, these findings pointed in the direction of a role for UCP3 in lipid metabolism and urged for the proposal of a specific hypothesis for UCP3 in LCFA handling.

Two slightly different hypotheses were put forward in an attempt to elucidate the above-mentioned mechanism. Both describe a role in LCFA anion export from the matrix (Figure 1.8). Firstly, Schrauwen and Saris (149) hypothesized that when LCFA flux is elevated, an increased amount of LCFA enters the mitochondria by passive diffusion (or flip-flop) resulting in an accumulation of non-esterified LCFA units in the matrix. They propose that UCP3 is required for the outward translocation of the non-esterified LCFA units. Although this hypothesis does not link UCP3 to improved fat oxidation, it links UCP3 expression to LCFA levels and reduced membrane potential (export anion = import proton). A second hypothesis goes one step further and links UCP3 expression to improved fat oxidation capacity (156). It suggests that UCP3 acts in conjunction with a mitochondrial thioesterase (MTE-1) to release CoA from LCFA-CoA units accumulating in the matrix and export LCFA anions from the matrix to the cytosol. This is based on previous findings by Alexson et al (157) suggesting that LCFA-CoA accumulation in the matrix inhibits beta-oxidation by sequestering CoA as seen during

erucic acid (very LCFA - $C_{22}H_{42}O_2$) metabolism. Supporting evidence also comes from correlation studies between UCP3 expression and MTE-1 expression (158; 159) and activity (160). This hypothesis therefore links UCP3 expression to improved fat oxidation capacity and reduced ROS production by maintaining a lower membrane potential.

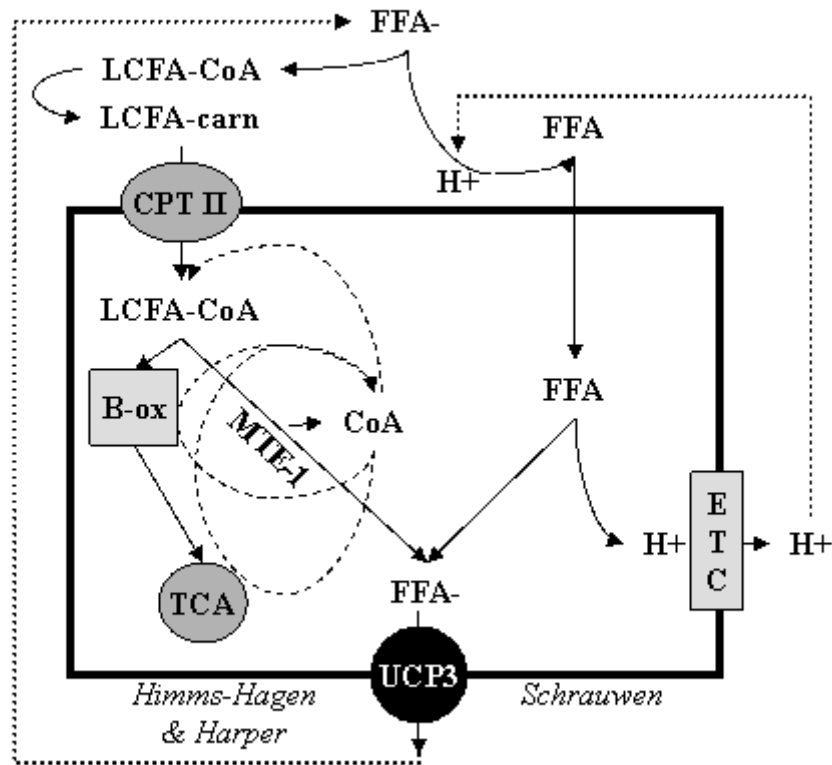


Figure 1.8. Hypotheses of UCP3 as a LCFA anion exporter. Based on proposed hypotheses of Schrauwen et al. (149) and Himms-Hagen & Harper (156). Modified from Nedergaard and Cannon 2003 (161).

The strongest argument against these hypotheses is the lack of direct evidence of LCFA export in isolated systems. Studies of the type are greatly warranted. Also, despite

evidence for leaner phenotypes and diet-resistant obesity in UCP3 overexpressing mice, UCP ablated mice lack an obese phenotype (118; 119; 131). Nonetheless, since the proposal of these hypotheses in 2001, a plethora of studies have been added to the literature, either in support or arguing against a role for UCP3 in LCFA anion export.

In summary, the advancements on UCP3 function have progressed tremendously since its discovery in 1997. The main proposed functions for UCP3 are related to uncoupling of oxidative phosphorylation, reducing reactive oxygen species and LCFA metabolism but much more research is required to pinpoint its function in skeletal muscle metabolism.

CHAPTER TWO
AIMS OF THESIS

2.1 Aims of thesis

The aim of this thesis was to examine, in human and rodent skeletal muscle, key proteins involved in LCFA transport across the mitochondrial membrane. Given the irreversible nature of mitochondrial LCFA uptake, it is imperative to better understand the complex interplay and impact of CPTI, FAT/CD36, and UCP3 on skeletal muscle fat oxidation.

Upon undertaking this thesis, the regulation of CPTI activity, the traditional textbook mode of entry of LCFA inside the mitochondria, was extremely controversial. No studies had yet demonstrated a decrease in M-CoA, the CPTI inhibitor, during moderate intensity exercise in human skeletal muscle despite known increases in fat oxidation rates. Our aim for this first study (Chapter three) was to examine the effects of exercise-related metabolites, known to activate other regulated enzymes in the important metabolic pathways, on CPTI activity in isolated mitochondria from human and rat skeletal muscle. We hypothesized that AMP, ADP, Pi and calcium would override M-CoA inhibition *in vitro*. Given the recent emphasis on IMF and SS mitochondrial subfractions and the superior oxidative capacity of IMF mitochondria, we measured maximal CPTI activity, sensitivity to M-CoA, citrate synthase activity and the effects of adenylate or energy charge metabolites and calcium on CPTI activity in both mitochondrial subfractions.

From our first study, we concluded that our understanding of the regulation of CPTI activity was still incomplete. This opened the door to the possibility that mitochondrial FA uptake involves another transport protein or additional level of regulation. Thus given the recent identification of FAT/CD36 on the mitochondrial

membranes in rat skeletal muscle, we examined the presence of FAT/CD36 on human skeletal muscle mitochondria in Chapter four. We hypothesized that FAT/CD36 would be present on pure isolated mitochondria from human skeletal muscle and would play a crucial role in FA oxidation such that inhibiting FAT/CD36 with a specific inhibitor would abolish mitochondrial FA oxidation. We also hypothesized that FAT/CD36 content would correlate with other mitochondrial oxidative markers in human skeletal muscle.

A strong link between UCP3 content and levels of LCFA has been established for years. Skeletal muscle UCP3 overexpression has led to leaner phenotypes and increased fat oxidation rates in mice but the mechanisms involved have not been examined. Our aim for the final study (Chapter five) was to investigate how UCP3 overexpression and ablation would affect LCFA uptake, CPTI activity and subsequent oxidation capacity and potential phenotypical changes that may occur. To do so, we examined the effects of UCP3 overexpression and ablation on the multiple steps and metabolites involved in fat oxidation. We hypothesized that cellular and mitochondrial LCFA uptake capacity, as well as cofactor abundance would be increased with UCP3 overexpression and decreased with UCP3 ablation.

Taken together, these studies examine three mitochondrial proteins involved in mitochondrial LCFA transport and their respective roles and impact on LCFA metabolism and oxidation.

CHAPTER THREE

**REGULATION OF CPTI ACTIVITY IN INTERMYOFIBRILLAR AND
SUBSARCOLEMMAL MITOCHONDRIA FROM HUMAN AND RAT
SKELETAL MUSCLE**

3.1 Abstract

CPTI is considered the rate-limiting enzyme in the transfer of LCFA into the mitochondria and is reversibly inhibited by M-CoA (M-CoA) *in vitro*. In rat skeletal muscle, M-CoA levels decrease during exercise releasing the inhibition of CPTI and increasing LCFA oxidation. However, in human skeletal muscle, M-CoA levels do not change during moderate intensity exercise despite large increases in fat oxidation, suggesting that M-CoA is not the sole regulator of increased CPTI activity during exercise. In the present study, we measured CPTI activity in intermyofibrillar (IMF) and subsarcolemmal (SS) mitochondria isolated from human vastus lateralis (VL), and rat soleus (Sol) and red gastrocnemius (RG) muscles. We tested whether exercise-related levels (~65% peak O₂ uptake) of calcium and adenylate charge metabolites (free AMP, ADP, and P_i) could override the M-CoA-induced inhibition of CPTI activity and explain the increased CPTI flux during exercise. Protein content was ~25-40% higher in IMF than SS mitochondria in all muscles. Maximal CPTI activity was similar in IMF and SS mitochondria in all muscles (VL: 282 ± 46 vs. 280 ± 51, Sol: 390 ± 81 vs. 368 ± 82, RG: 252 ± 71 vs. 278 ± 44 nmol·min⁻¹·mg protein⁻¹). Sensitivity to M-CoA did not differ between the IMF and SS mitochondria in all muscles (25-31% inhibition in VL and 52-70% in Sol and RG). Calcium and the adenylate charge metabolites did not override the M-CoA-induced inhibition of CPTI activity in mitochondria isolated from VL, Sol and RG muscles. Decreasing pH from 7.1 to 6.8 reduced CPTI activity by ~34-40% in both VL mitochondrial fractions. In summary, this study reports no differences in CPTI activity or sensitivity to M-CoA between IMF and SS mitochondria isolated from human and rat skeletal muscles. Exercise-induced increases in calcium and adenylate charge

metabolites do not appear responsible for upregulating CPTI activity in human or rat skeletal muscle during moderate aerobic exercise.

3.2 Introduction

The carnitine palmitoyltransferase (CPT) complex consists of CPTI, acylcarnitine translocase, and CPTII. This complex facilitates the entry of LCFA from the cytosol to the mitochondrial matrix, where LCFA undergo beta-oxidation (38). CPTI, which spans the outer mitochondrial membrane, catalyzes the transfer of a variety of LC fatty acyl groups from free coenzyme A (CoASH) to carnitine. The generated acylcarnitine can then permeate the inner membrane via the acylcarnitine/carnitine translocase system. The acyl-CoA moiety is then reformed in the matrix of the mitochondria via CPTII.

CPTI is considered the rate-limiting step in the transfer of LCFA into the mitochondria and is reversibly inhibited by M-CoA, the first committed intermediate of *de novo* LCFA synthesis (37; 162). Some have speculated that M-CoA could be the key regulator of fat oxidation selection in skeletal muscle and early work in rodent skeletal muscle supported this hypothesis (62). It has been shown that M-CoA levels are highest at rest, inhibiting CPTI activity and maintaining low rates of fat transport. During exercise, M-CoA levels decrease releasing the inhibition of CPTI and allowing LCFA oxidation to increase (62; 163). In human skeletal muscle, the situation is more complex, as M-CoA levels do not decrease during moderate intensity exercise despite large increases in LCFA oxidation rates (65; 66; 164). A possible explanation is that CPTI regulation is independent of M-CoA as Kim et al. (64) have shown the presence of a M-CoA-resistant CPTI subfraction in rodent skeletal muscle. In either case, the biological mechanisms to explain how LCFA oxidation is increased in human muscle during exercise are not presently known. Taken together, these results suggest that M-CoA is

not the sole regulator of CPTI activity and/or that M-CoA inhibition is overridden during exercise.

In searching for regulators of CPTI activity during exercise, we focused on calcium, the adenylate charge metabolites (free ADP, AMP and P_i) and pH. Important enzymes in the pathways that provide ATP, such as the carbohydrate metabolizing enzymes, glycogen phosphorylase and pyruvate dehydrogenase (PDH) and the tricarboxylic (TCA) cycle enzymes, isocitrate dehydrogenase and 2-oxoglutarate dehydrogenase are regulated by calcium, the adenylate charge metabolites and pH. This mechanism of action leads to low activities at rest and high activities during exercise and led us to investigate the effects of calcium, the adenylate charge metabolites and pH on CPTI activity.

An additional level of complexity regarding LCFA transport and CPTI activity relates to the existence of mitochondria in two locations, intermyofibrillar (IMF) and subsarcolemmal (SS). Morphological and functional differences in IMF and SS mitochondria have been reported in rodent skeletal muscle (165). It has been suggested that the IMF and SS mitochondria have different functions related to metabolic compartmentalization (26; 166; 167). Some have also suggested that these two populations are at different stages of biogenesis (28). IMF mitochondria have been shown to be more efficient in ATP production, possibly to support the high ATP demand of muscle contraction and the regulation of Ca^{2+} -ATPase (19; 21; 24). SS mitochondria, which are nearer the capillaries, may also be involved in the transport of oxygen from the erythrocyte to the mitochondria (24). In rodent skeletal muscle, inner membrane and matrix enzymes of IMF mitochondria appear to have higher oxidative capacity than the SS mitochondria (18; 19). CPTI activity has yet to be examined in IMF and SS

mitochondria in both human and rodent skeletal muscle. Moreover, most studies examining the characteristics of IMF and SS mitochondria were simply conducted in rat hindlimb muscle dominated by the fast-glycolytic fiber type, disregarding possible fiber type differences.

Thus in this study, we compared CPTI activity and CPTI sensitivity to M-CoA in both IMF and SS mitochondria from human skeletal muscle and rat soleus and RG muscles. We also investigated the effects of physiological concentrations of calcium, free AMP, ADP, and P_i , and pH in the presence of M-CoA on CPTI activity. We hypothesized that IMF mitochondria would have greater CPTI activity than SS mitochondria and that physiological concentrations of calcium and energy charge metabolites representative of 65% VO_{2peak} would override M-CoA inhibition in all muscles.

3.3 Methods

3.3.1 Subjects

Twelve healthy males volunteered for this study. Nine subjects were recreationally active, participating in moderate intensity aerobic exercise 3-5 times a week, and three subjects were well trained with more frequent and longer training sessions (Table 3.1). Subjects were fully informed of the purpose of the experiments and of the possible risks before giving written consent to participate. The study was approved by the University of Guelph Ethics Committee.

3.3.2 Experimental protocol

Subjects visited the laboratory on two occasions. On the first occasion, peak pulmonary O₂ uptake (VO₂ peak) was measured with a metabolic cart (SensorMedics model) during incremental exercise on a cycle ergometer (LODE Instrument, Groningen, The Netherlands). On the second occasion, a resting muscle sample was obtained from the vastus lateralis under local anesthesia (2% lidocaine without epinephrine) using the percutaneous needle biopsy technique described by Bergstrom (168). Visible fat and connective tissue were dissected free from the muscle and the muscle was blotted to remove excess blood. The sample (~ 170 mg) was divided into two portions: the first (~160 mg) was used for immediate mitochondrial isolation for the determination of CPTI activity, and the second (~10 mg) was frozen in liquid N₂ for later analysis of citrate synthase (CS) activity as an index of mitochondrial volume in recreationally and well-trained subjects.

3.3.3 Animals and tissue extraction

Female Sprague-Dawley rats ($n = 13$) weighing on average 200 ± 9 g were used in the experiments. The animals were housed in a controlled environment with a 12:12-h light-dark cycle and fed Purina rat chow *ad libitum*. Rats were anesthetized with an intraperitoneal injection of pentobarbital sodium (6 mg/100 g body wt) and the soleus and RG muscle were excised as quickly as possible. This study was approved by the University of Guelph Animal Care Committee.

3.3.4 Isolation of mitochondria

The procedure for the isolation of IMF and SS mitochondria was adapted from Jimenez et al (25). The entire procedure was performed at 0-4°C. The buffer solutions used contained the following: *solution I*: 100 mM KCl, 5mM MgSO₄·7H₂O, 5 mM EDTA, and 50 mM Tris HCl, pH 7.4; *solution II*: solution 1 and 1mM ATP, pH 7.4; *solution III*: 220 mM sucrose, 70 mM mannitol, 10 mM Tris HCl and 1 mM EDTA, pH 7.4. Muscle was immediately placed in ice-cold solution I and then blotted and weighed. Muscle was minced with scissors in 1 ml of solution II and transferred to an ice-cold glass Potter-Elvehjem homogenizer (Tri-R Stir-R model S63C – Fisher Scientific, Toronto, ON Canada). Tissue was homogenized in 5 ml of solution II with a loose fitting Teflon pestle (10 up and down strokes, 1500 rpm). The homogenate was centrifuged at 700 g for 10 min at 4°C. The pellet was kept at 4°C for the extraction of IMF mitochondria. The supernatant was filtered through two layers of surgical gauze and then centrifuged at 12,000 g for 10 min at 4°C. The resulting SS mitochondrial pellet was resuspended in 1 µl/mg of tissue of solution III. The pellet from the initial spin was resuspended in 5 ml of solution II and homogenized with a tight-fitting homogenizer (1 min at 1500 rpm + 1 min at 2000 rpm). The strong mechanical disruption resulted in the release of the IMF mitochondria from the myofibrils. The resulting homogenate was centrifuged at 700 g for 10 min at 4°C. After filtration through two layers of surgical gauze, the supernatant was centrifuged at 12,000 g for 20 min at 4°C. The resulting IMF pellet was resuspend in 1 µl/mg of tissue of solution III.

The quality of the mitochondrial preparations (intact mitochondria) was determined by first measuring the CS activity of the extramitochondrial fraction in the suspension (1:20 dilution) and then measuring the total CS activity of the suspension (1:20 dilution) after lysing the mitochondria with 0.04% Triton X-100 and repeated freeze thawing. The difference in these activities equals the intramitochondrial fraction. CS activity was measured spectrophotometrically at 25°C as previously described (169).

3.3.5 Determination of CPTI (EC 2.3.1.21) activity

The forward radioisotope assay for the determination of CPTI activity from needle biopsy samples has been previously described (37; 69). Briefly, the reaction was run at a temperature of 37°C and started by the addition of 10 µl of mitochondrial suspension (1:3 dilution) to 90 µl of the following standard reaction medium: 117 mM Tris-HCl (pH 7.4), 0.28 mM reduced glutathione, 4.4 mM ATP, 4.4 mM MgCl₂, 16.7 mM KCl, 2.2 mM KCN, 40 mg/l rotenone, 0.5% BSA, 300 µM palmitoyl-CoA, and 5 mM L-carnitine with 1 µCi of L-[³H]carnitine. The reaction was stopped after 6 min with the addition of 60 µl of ice-cold HCl. Palmitoyl-[³H]carnitine formed during the reaction was extracted in 400 µl of water saturated butanol in a process involving three washes with distilled water and subsequent recentrifugation to separate the butanol phase. Finally, radioactivity was assayed in 100 µl of the butanol phase in 5 ml of scintillation cocktail. Assays were performed in duplicate, and blanks were subtracted. IMF and SS measurements of CPT1 activity were expressed relative to their mitochondrial protein contents. Protein concentration was measured using the BCA protein kit (Pierce, Rockford, IL).

When the effects of M-CoA and metabolites were tested in human skeletal muscle, the reaction mixture was modified to contain the following final concentrations of metabolites, representative of exercise at 65% VO_2 peak: 100 μM CaCl_2 , 0.65 μM AMP, 65 μM ADP, and 15 mM Pi (170). These metabolites were added individually and combined with 0.7 μM M-CoA, the physiological concentration of M-CoA in human skeletal muscle (67). A M-CoA sensitivity curve was also determined with the addition of M-CoA alone in concentrations of 0.2, 0.7, and 2.0 μM . The pH of the CPTI reaction mixture was adjusted to 7.1. When examining the effects of altered pH on CPTI activity, the pH of the reaction mixture was adjusted to 6.8

In rat soleus and RG, the M-CoA concentrations used for the sensitivity curve were the same as in human muscle. Final concentrations of M-CoA in rat soleus and RG during simulated contractions were 0.43 μM and 0.29 μM M-CoA, respectively. Final concentrations of AMP_f , ADP_f and Pi_f were 0.8 μM , 70 μM , and 6.2 mM in rat soleus and 2 μM , 116 μM , and 14.6 mM in RG, respectively (171; 172).

3.3.6 Statistics

All data are presented as the mean \pm SEM. The effect of metabolites and sensitivity to M-CoA were analyzed by a one-way ANOVA. When a significant F-ratio was obtained, post hoc analysis was completed using a Tukey's test. Paired-t tests were used to determine significance between all other treatments. Statistical significance was accepted at $P < 0.05$.

3.4 Results

3.4.1 Human skeletal muscle

Characteristics of the recreationally active group and three well-trained individuals appear in Table 3.1.

Table 3.1. Subject characteristics

Variables	Recreationally active	Well-trained
Age, yrs	19.3 ± 1.1	22.7 ± 2.0
Weight, kg	74.9 ± 5.4	72.9 ± 0.7
Height, cm	177.1 ± 5.5	181.3 ± 3.3
VO ₂ peak, ml·min ⁻¹ ·kg ⁻¹	46.1 ± 2.2	64.0 ± 1.2*

Values are mean ± SEM, $n = 9$ for recreationally active and $n = 3$ for well-trained.

*Significantly different from recreationally active. $P < 0.05$

Protein content was ~1.6 fold higher in the IMF compared to SS mitochondrial fractions of both the recreationally active group (1.68 ± 0.32 vs. 1.06 ± 0.21 mg/g wet muscle (wm) and trained individuals (2.61 ± 0.44 vs. 1.65 ± 0.18 mg/g wm). CS activity was measured in all fractions to assess the quality of both mitochondrial preparations. The fraction of the CS activity inside the intact mitochondria was 85.2 ± 1.2 and 83.4 ± 1.1 % in IMF and SS mitochondria, respectively.

Maximal CPTI activity normalized for mitochondrial protein content was not significantly different between IMF and SS mitochondria (282 ± 46 vs. 280 ± 51 nmol/min/mg protein, respectively, Table 3.2). CS activity was significantly lower in

IMF than SS mitochondria (0.073 ± 0.004 vs. 0.132 ± 0.016 mmol/min/mg protein, Table 3.2).

Table 3.2. Enzymatic activities and response to $0.7 \mu\text{M}$ M-CoA in IMF and SS mitochondria isolated from human vastus lateralis muscles of recreationally active subjects.

	IMF	SS
CPTI, $\text{nmol}\cdot\text{min}^{-1}\cdot\text{mg protein}^{-1}$	282 ± 46	280 ± 51
CS, $\text{mmol}\cdot\text{min}^{-1}\cdot\text{mg protein}^{-1}$	0.073 ± 0.004	$0.132 \pm 0.016^*$
Inhibition, %	31.2 ± 4.8	25.3 ± 4.5

Values are mean \pm SEM, $n = 9$. *Significantly different from IMF mitochondria. $P < 0.05$.

Inhibition with physiological levels of M-CoA ($0.7 \mu\text{M}$) was similar between the IMF and SS fractions of human muscle (31.2 ± 4.8 and 25.3 ± 4.5 % inhibition, Table 3.2). Inhibition of CPTI activity with a range of M-CoA concentrations was also similar between the fractions (Fig. 3.1).

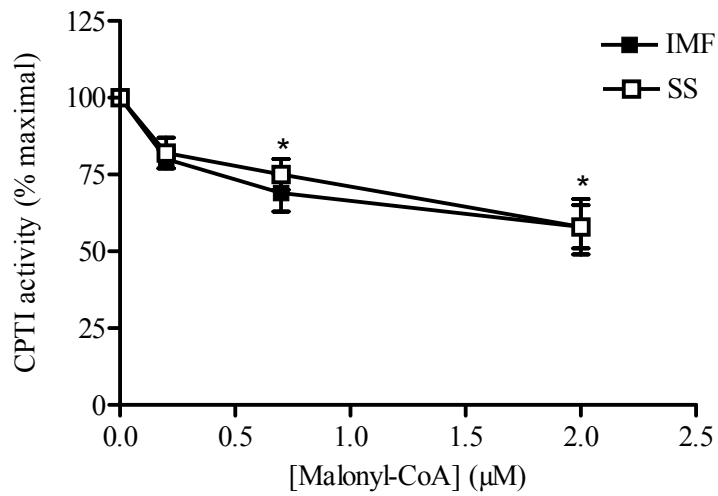


Figure 3.1. Effects of M-CoA on CPTI activity of IMF (filled) and SS (open) mitochondria isolated from human vastus lateralis of recreationally active males. [M-CoA] = 0.2 μM, 0.7 μM, and 2.0 μM. Values are mean ± SEM, $n = 9$. *Significantly different from own control (no M-CoA).

There was no effect of adding exercising levels of calcium (100 μM), free AMP (0.65 μM), ADP (65 μM) and P_i (15 mM) in the presence of 0.7 μM M-CoA, on CPTI activity in either the IMF or SS mitochondria (Fig. 3.2).

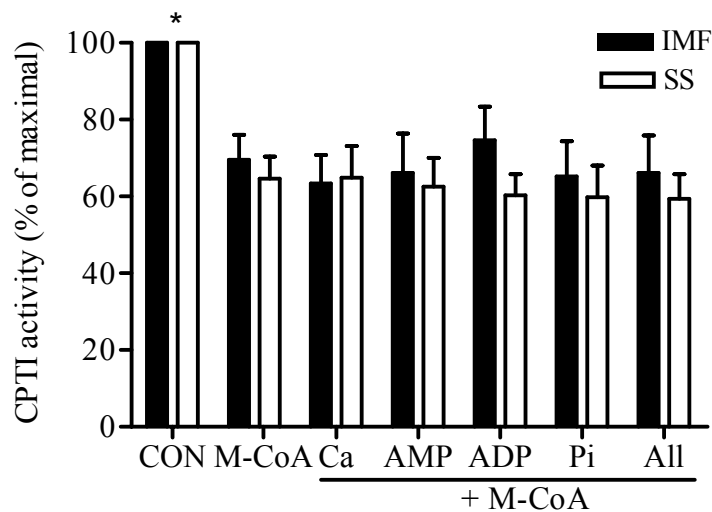


Figure 3.2. CPTI activity of IMF (filled) and SS (open) mitochondria isolated from human vastus lateralis of recreationally active males in the presence of physiological concentrations (65% VO₂peak) of calcium, free AMP, ADP, and Pi, with 0.7 μM M-CoA. Values are mean ± SEM, *n* = 9. *Significantly different from own M-CoA (0.7 μM).

Lowering the pH of the assay medium from 7.1 to 6.8 reduced CPTI activity in both the IMF and SS mitochondrial fractions of human skeletal muscle to the same level (33.8 and 40.4%, respectively; Fig. 3.3). The presence or absence of physiological concentration of M-CoA had no effect on the pH-induced reduction of CPTI activity.

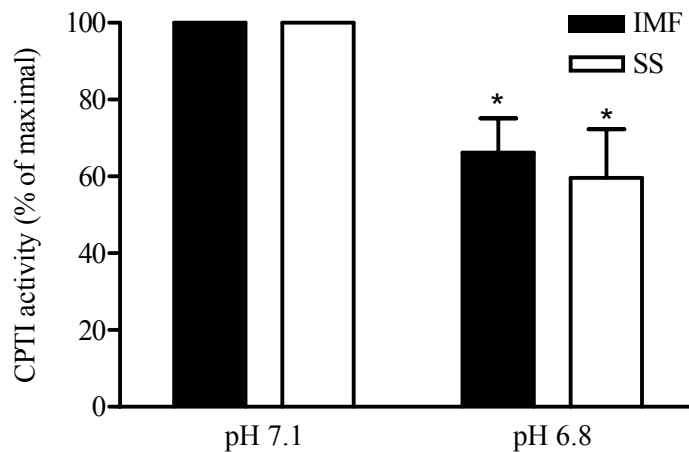


Figure 3.3. Effect of pH on CPTI activity of IMF (filled) and SS (open) mitochondria isolated from human vastus lateralis of recreationally active males. Values are mean \pm SEM, $n = 9$. *Significantly different from pH 7.1.

The addition of exercising levels of ADP ($65 \mu\text{M}$) using a submaximal concentration of palmitoyl-CoA ($150 \mu\text{M}$) in the presence of $0.7 \mu\text{M}$ M-CoA did not alter CPTI activity when compared to P-CoA and M-CoA alone in both the IMF and SS mitochondria (data not shown).

Similar to the results with the recreationally active individuals, the addition of exercising levels of calcium and the adenylate charge metabolites had no effect on muscle CTPI activity in well-trained individuals (data not shown).

3.4.2 Rat soleus and RG muscles

Protein content was 25% higher in the IMF vs. SS mitochondria (2.75 ± 0.31 vs. 2.19 ± 0.40 mg/g wm) in soleus muscle and 40% greater in the IMF than SS mitochondria of RG (3.15 ± 0.35 vs. 1.91 ± 0.19 mg/g wm, $P = 0.034$). Quality of the

mitochondrial preparation was good as the fraction of CS activity that was inside the intact mitochondria was 82.0 ± 4.0 and 84.2 ± 2.5 % in IMF and SS mitochondria of rat soleus muscle and 83.4 ± 3.2 and 80.4 ± 5.1 % in RG.

CS activity was lower in IMF than SS mitochondria in soleus, but no significant difference was observed between the fractions in RG (Table 3.3). Maximal CPTI activity was similar between IMF and SS mitochondrial populations in both rat muscle groups.

Table 3.3. Enzymatic activities and response to 2 μ M M-CoA in IMF and SS mitochondria of rat soleus and RG muscle

	Tissue	IMF	SS
CPTI, $\text{nmol}\cdot\text{min}^{-1}\cdot\text{mg protein}^{-1}$	Sol	390 ± 81	368 ± 82
	RG	252 ± 71	278 ± 44
CS, $\text{mmol}\cdot\text{min}^{-1}\cdot\text{mg protein}^{-1}$	Sol	0.044 ± 0.008	$0.095 \pm 0.012^*$
	RG	0.086 ± 0.003	0.093 ± 0.015
Inhibition, %	Sol	70.0 ± 10.7	55.1 ± 9.3
	RG	52.8 ± 10.3	57.9 ± 12.9

Values are mean \pm SEM, $n = 5$. *Significantly different from IMF mitochondria. $P < 0.05$

In soleus and RG muscles, IMF and SS mitochondria were inhibited to the same degree with the addition of various concentrations of M-CoA (Fig. 3.4a, b). In soleus, M-CoA inhibition (2 μ M) resulted in a 70.0 ± 10.7 and $55.1 \pm 9.3\%$ reduction in CPTI

activity in IMF and SS mitochondria. The M-CoA inhibition was similar in RG for IMF vs. SS (52.8 ± 10.3 vs. 57.9 ± 12.9 %, Table 3.3).

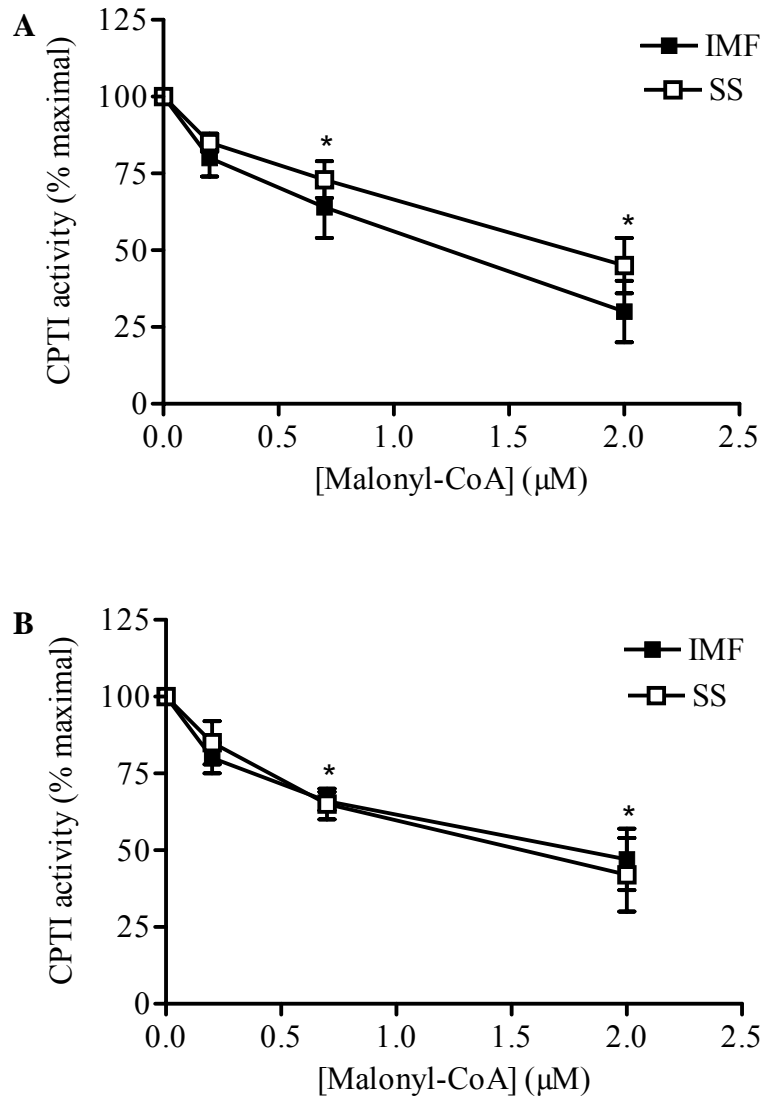


Figure 3.4. Effects of M-CoA on CPTI activity of IMF (filled) and SS (open) mitochondria isolated from rat soleus (A) and RG (B). [M-CoA] = 0.2 μM, 0.7 μM, and 2.0 μM. Values are mean ± SEM, n=8 in A, n = 5 in B; *Both mitochondria significantly different from own control (no M-CoA).

No effect was observed when metabolites representative of moderate intensity exercise were added to IMF and SS mitochondrial fractions of rat soleus and RG in the presence of 0.7 μ M M-CoA (Fig. 3.5a, b). The metabolites were also added to 2.0 μ M M-CoA but no effect was noted (data not shown).

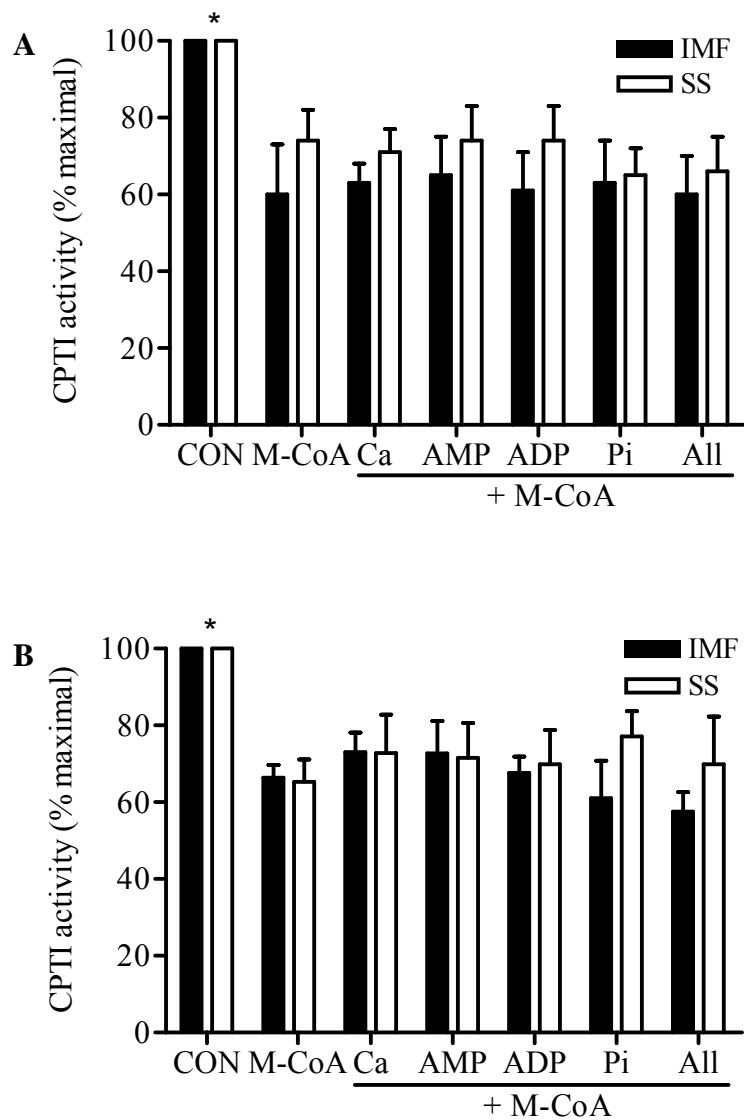


Figure 3.5. CPTI activity of IMF (filled) and SS (open) mitochondria isolated from rat soleus (A) and RG (B) skeletal muscle with physiological concentrations (65% VO₂peak) of calcium, free AMP, ADP, and Pi, with M-CoA. A. [M-CoA] = 0.43 μ M,. B. [M-CoA] = 0.23 μ M. *n* = 5 *Significantly different from control.

3.5 Discussion

To our knowledge, this is the first report to isolate IMF and SS mitochondria in human skeletal muscle and measure maximal CPTI activity and sensitivity to M-CoA in both fractions of human and rat skeletal muscle. Both fractions had similar CPTI activities and responses to the inhibitor M-CoA. Physiological concentrations of calcium and adenylate charge metabolites had no effect on *in vitro* CPTI activity in human or rat muscles in the presence of M-CoA. Decreasing pH from 7.1 to 6.8 reduced CPTI activity by ~34-40% in both mitochondrial fractions of human skeletal muscle.

3.5.1 IMF and SS mitochondria extraction

We adapted a mitochondrial extraction protocol (25) to maximize mitochondrial IMF and SS yield when using ~160 mg of muscle obtained from human needle biopsies. Our mitochondrial protein yield with recreationally active and well trained subjects (~2.7 and ~4.8 mg prot/g wet muscle (wm), SS and IMF total) were similar to the results of Wibom et al. (173) who also extracted mitochondria from human skeletal muscle (~2.2 for sedentary, ~2.8 for moderately active and ~5.5 mg/g wm for trained subjects). However, the mitochondrial protein yield from another human study was higher at ~8-13 mg/kg wm (174). This may have been due to the proteinase treatment used to isolate the mitochondria, which was not used in our study or by Wibom et al. (173).

Our protein yield in rat muscles was similar to previously reported for rat muscle. The quality of the preparations was good as ~82-85% of the mitochondria extracted from all muscles were intact.

3.5.2 CPTI activity in human muscle IMF and SS mitochondria

Our results revealed no differences in CPTI activity or M-CoA sensitivity between IMF and SS fractions of human skeletal muscle. We measured a 25-31% inhibition of CPTI activity using physiological concentrations of M-CoA. These data are consistent with previous findings from our laboratory and suggest that only ~30% of CPTI could be regulated by M-CoA under normal conditions (69). Similar *in vitro* CPTI activities and sensitivity to M-CoA in the IMF and SS mitochondria suggest that CPTI activity between the two fractions would be similar *in vivo*, unless M-CoA levels differed in IMF and SS populations. However, there is no indication to date of such differences. Calcium and adenylate charge metabolites are powerful activators of several enzymes in the pathways that metabolize carbohydrate, including the TCA cycle. Calcium is released upon muscle contraction and increases in free AMP, ADP, and P_i occur at the onset of exercise and during prolonged moderate intensity exercise. We tested the possibility that these metabolites could override M-CoA inhibition of CPTI or directly increase CPTI activity. The results demonstrated that this was not the case in human skeletal muscle, as CPTI activity remained at ~70% of maximal in the presence of M-CoA, with and without these potential regulators. The results were similar in muscles from well-trained subjects in spite of trained muscles having tighter metabolic control and greater sensitivity to small changes in the cell energy status (175; 176). Our *in vitro* conditions result in maximal CPTI activity. In an attempt to better simulate *in vivo* conditions, we tested the effect of free ADP and M-CoA using submaximal concentrations of palmitoyl-CoA, again, with no stimulatory effects on CPTI activity.

We previously determined that exercising levels of acetyl-CoA, CoASH, and acetylcarnitine had no effect on CPTI activity (69). However, Starritt et al. (69) reported a 40% inhibition of CPTI activity when pH was reduced from 7 to 6.8 in a mixture of IMF and SS mitochondria. We extended this finding by demonstrating that the IMF and SS fractions responded in a similar fashion to a change in pH. A change in pH could be the link between increasing carbohydrate and decreasing fat oxidation when exercise intensity increases from moderate to high. Muscle pH values have been estimated at ~6.9 and ~6.6 during cycle exercise at 65% and 90% VO_2peak , respectively (70).

In the course of assessing the quality of the mitochondrial extractions, we also determined that CS activity was significantly lower in IMF vs. SS mitochondria. CS is a key TCA cycle enzyme, which serves both the carbohydrate and fat metabolic pathways. Since CPTI activity did not differ between the mitochondrial fractions, it is possible that the higher CS activity in the SS fraction is needed for higher carbohydrate flux through PDH and the TCA cycle. However, to our knowledge these data are unavailable and future measurements of maximal activities and regulation of key regulatory enzymes in the two populations of mitochondria are needed to answer these questions.

3.5.3 CPTI activity in rat muscle IMF and SS mitochondria

CPTI activity was similar between the two fractions in rat soleus and RG muscles, but was higher in the soleus due to the greater proportion of oxidative fibers. The similar CPTI activities is puzzling as IMF mitochondria have higher inner membrane oxidative capacity, higher state III and IV respiration, and are more coupled (24; 25). Thus, they are more efficient at generating ATP, possibly to support muscle contraction. However, it

is possible that CPTI differences on the outer mitochondrial membrane are not necessary since the IMF protein content is significantly greater than SS protein. This may imply that the differential regulation of oxidative metabolism lies distal to the transport of LCFA into the mitochondria.

While few outer membrane enzymes have been measured in IMF and SS mitochondria, several inner membrane enzyme activities have been examined with ambiguous results. Kreiger et al. (21) reported a 65% greater succinate dehydrogenase (SDH) activity in IMF vs. SS mitochondria, while Cogswell et al. (19) found a 40% greater SDH activity in SS mitochondria. Cogswell et al. (19) also reported slightly higher cytochrome oxidase (COX) activity (13%) in IMF mitochondria of mixed rat hindlimb muscle, while Jimenez et al. (25) reported higher COX activity in SS mitochondria of RG (43%) and no difference in the soleus and tibialis anterior muscles. Cogswell et al. (19) also found no difference in cytochrome *b*, *c*₁, *c*, and *a* protein content of IMF and SS mitochondria. The matrix enzyme isocitrate dehydrogenase activity was 70% higher in IMF vs. SS mitochondria while CS activity did not differ (18; 19). We also found similar CS activities between SS and IMF fractions in RG muscle. However, it should be noted that both mixed rat hindlimb muscle and RG contain ~33% slow- and fast-oxidative fibers and ~67% fast-glycolytic fibers. We did observe higher CS activity in SS mitochondria of rat soleus muscle, which may be related to the presence of more oxidative fibers. The lack of consistency in these findings makes it difficult to draw firm conclusions regarding the potential for oxidative metabolism in the two mitochondrial fractions. Specific measurements from the mitochondrial fractions of the predominant fibre types in rodent skeletal muscle are needed.

3.5.4 Regulation of CPTI activity

M-CoA is thought to be the main regulator of CPTI activity in rodent skeletal muscle since a decrease in M-CoA correlates with increased fat oxidation during contractions. Because no difference was observed in M-CoA sensitivity between the IMF and SS fractions, we combined the results for the purpose of this discussion. CPTI activity was inhibited by ~53-58% in soleus and ~55-70% in RG muscles using only 2 μ M M-CoA. Kim et al. (64) recently suggested the presence of a M-CoA insensitive CPTI isoform that correlated with the proportion of type IIA fibers in rat skeletal muscle. Using 10 μ M M-CoA, they reported only 39% and 29% inhibition in soleus and RG muscles. The two data sets differ as we reported a broader range and more powerful inhibition of CPTI activity in the RG vs. soleus, which argues against the type IIA - M-CoA insensitivity correlation (64). We also report a 1.4 to 2-fold greater inhibition in CPTI activity in both muscles using only 20% of the M-CoA concentration used by Kim et al. (64). The magnitude of the inhibition may depend on the different protocols as we isolated mitochondria and measured CPTI activity directly, whereas Kim et al. (64) used whole muscle homogenates and measured palmitate oxidation to estimate CPTI activity. It may be that M-CoA does not fully interact with CPTI in a whole muscle homogenate, as it may in isolated mitochondria. A similar theory may explain the lack of response to M-CoA *in vivo*, as it may be bound to a protein or compartmentalized making it less accessible to CPTI (38). Future experiments using intact soleus strips and isolated mitochondria may answer these questions.

3.5.5 Summary

This study is the first to measure CPTI activity in IMF and SS mitochondria extracted from needle biopsy samples of human skeletal muscle. CPTI activity and inhibition by M-CoA were similar between fractions in human muscle and also in rat soleus and RG IMF and SS fractions. Physiological concentrations of calcium and adenylate charge metabolites had no effect on CPTI activity in the presence of M-CoA in all muscles. CS activity was lower in IMF vs. SS mitochondria of human and rat soleus muscle, but not in RG muscle. The present findings suggest a similarity in the maximal ability to transport LCFA into the mitochondrial fractions in human skeletal muscle. Decreasing pH from 7.1 to 6.8 reduced CPTI activity by ~34-40% in both mitochondrial fractions of human skeletal muscle. Additional measurements of IMF and SS oxidative enzymes and their regulation are needed to understand their roles in the oxidative production of energy in skeletal muscle.

CHAPTER FOUR

**IDENTIFICATION OF FATTY ACID TRANSLOCASE ON HUMAN SKELETAL
MUSCLE MITOCHONDRIAL MEMBRANES: ESSENTIAL ROLE IN FATTY
ACID TRANSPORT**

4.1 Abstract

Fatty acid translocase (FAT/CD36) is an 88 kDa transporter protein with a strong affinity for long chain fatty acids (LCFA). Its role in LCFA uptake has been established in the plasma membranes of adipocytes, and cardiac and skeletal muscle cells in normal conditions as well as in the altered LCFA handling in insulin resistance and type-2 diabetes. Recently, FAT/CD36 was also identified on rat skeletal muscle mitochondrial membranes and found to be required for palmitate uptake and oxidation. Our aim was to identify the presence and elucidate the role of FAT/CD36 on human skeletal muscle mitochondrial membranes. We provide evidence that FAT/CD36 is indeed present in highly purified human skeletal mitochondria. Blocking of human muscle mitochondrial FAT/CD36 with sulfo-N-succimidyl-oleate (SSO) (0-200 μM) decreased palmitate oxidation in a dose-dependent manner. At maximal SSO concentrations (200 μM) palmitate oxidation was decreased by 95% ($P < 0.01$), suggesting an important role for FAT/CD36 in LCFA transport across the mitochondrial membranes. SSO treatment of mitochondria did not affect mitochondrial octanoate oxidation and had no effect on maximal and submaximal CPTI activity. However, SSO treatment did inhibit palmitoylcarnitine oxidation by 92% ($P < 0.001$), suggesting that FAT/CD36 may be playing a role downstream of CPTI activity. Therefore, we hypothesize that FAT/CD36 is important for LCFA transfer into the mitochondria, possibly playing a role in the transfer of palmitoylcarnitine from CPTI to CPTII in the intermembrane space. These data provide new insight regarding the LCFA transport system across the mitochondrial membranes in human skeletal muscle, and could be involved in the etiology of insulin resistance.

4.2 Introduction

Circulating LCFA are an important source of energy for muscle cells. Following cellular uptake and activation of LCFA to their coenzyme derivative (LCFA-CoA), the two major fates of LCFAs are storage in cytosolic lipid droplets or oxidation in the mitochondria. LCFA-CoA transport across the mitochondrial membranes is a key step in LCFA oxidation but its regulation is poorly understood. Therefore, it is important to decipher the regulation of LCFA oxidation in skeletal muscle, since its impairment has been linked to insulin resistance (177; 178).

Aside from diffusion, the carnitine palmitoyltransferase (CPT) system has long been viewed as the only mode of LCFA-CoA transport across the mitochondrial membranes. The CPT complex is comprised of the regulated enzyme CPTI, the carnitine:acylcarnitine transferase (CAT), and the latent CPTII (38). CPTI spans the outer mitochondrial membrane, while CAT and CPTII are located on the outer and inner leaflets of the inner mitochondrial membrane, respectively (see McGarry and Brown 1997 for review (38)). CPTI catalyzes the trans-esterification of LCFA-CoA to LCFA-carnitine, and CAT translocates LCFA-carnitine to the inner membrane where it is reconverted to LCFA-CoA by CPTII. Taken altogether, this system translocates LCFA-CoA from the cytosol into the mitochondria matrix.

Evidence for regulation of the CPT system has been identified in rat skeletal muscle (62; 163). Briefly, M-CoA, a product of the acetyl-CoA carboxylase (ACC) reaction is formed at rest and inhibits CPTI activity, which reduces the rate of LCFA entry into the mitochondrion and hence lowers the rate of LCFA oxidation. During exercise, M-CoA levels decrease due to AMP-activated protein kinase phosphorylation

and subsequent inactivation of ACC, as well as through M-CoA degradation catalyzed by M-CoA decarboxylase (179). However, the regulation of CPTI activity appears to differ in human skeletal muscle. A large portion of CPTI activity in human muscle appears to be insensitive to M-CoA inhibition (69; 180; 181). Moreover, the majority of studies have shown that unlike M-CoA levels in rodent muscles, M-CoA levels in human muscle do not decrease during moderate exercise, despite a marked increase in LCFA oxidation (65-67). The search for other regulators of CPTI activity has not been successful (69; 181).

Fatty acid translocase (FAT/CD36) is a multi-ligand scavenger receptor involved in LCFA transport in adipocytes, heart and skeletal muscle. Binding of sulfo-*N*-succinimidyl-oleate (SSO), a reactive oleate ester, to a cell surface protein led to the identification of the LCFA transporter FAT/CD36 (72; 182). Since then, SSO has been a valuable tool in examining the role of FAT/CD36 on cell membranes, since it binds specifically and covalently to FAT/CD36 and prevents transport of LCFA into adipocytes, heart, and skeletal muscle (94; 98; 183; 184). Recently, FAT/CD36 was identified as having a role in regulating LCFA oxidation in rat skeletal muscle mitochondria (3). Mitochondrial FAT/CD36 protein content correlated with oxidative capacity of different muscle tissues, and FAT/CD36 coprecipitated with CPTI. Moreover, in isolated mitochondria, blocking FAT/CD36 with SSO inhibited LCFA oxidation by 86%. With acute muscle electrical stimulation (30 min) LCFA oxidation increased and was associated with the translocation of FAT/CD36 to the mitochondria. Blocking the increased mitochondrial FAT/CD36 inhibited the contraction-induced

increase in LCFA oxidation. These studies indicated that FAT/CD36 may act in concert with CPTI to regulate LCFA oxidation in rodent muscle (3).

Since the regulation of CPTI in rodent and human muscle appears to differ (65-67), the aim of the present study was to investigate the presence and potential role of FAT/CD36 in LCFA oxidation in human skeletal muscle mitochondria. Our studies indicate that FAT/CD36 associates with CPTI to regulate LCFA oxidation in human muscle. Since it has been shown that the plasmalemmal content of FAT/CD36 is increased in insulin resistant muscles in rodents (185) and humans (186), it may be that alterations in mitochondrial FAT/CD36 contribute to reducing the rates of LCFA oxidation in insulin resistant human skeletal muscle (177).

4.3 Methods

4.3.1 Subjects

Twenty-three healthy individuals volunteered for this study (n = 15 males; n = 8 females; age: 23 ± 1 yr, weight: 78 ± 5 kg, BMI: 25 ± 1 kg/m² and VO₂peak: 42 ± 2 mL/min/kg body weight (mean \pm SEM). Activity and aerobic fitness level varied among these individuals, which enabled us to obtain muscle samples over a wide range of aerobic capacities. A subset of fourteen subjects (11 males and 3 females) was used for the correlation studies; age: 23 ± 1 yr, weight: 84 ± 7 kg, BMI: 26 ± 2 kg/m² and VO₂peak: 41 ± 3 mL/min/kg body weight (mean \pm SEM). Female subjects were in the early follicular phase of their menstrual cycle phase at time of muscle biopsies. Subjects were fully informed of the purpose of the experiments and of any possible risk before

giving written consent to participate. The study was approved by the University of Guelph Ethics Committee.

4.3.2 Experimental protocols

Subjects visited the laboratory on two occasions and were asked to refrain from exercise in the 48 hrs prior to each visit. On the first occasion, peak pulmonary O₂ uptake (VO₂ peak) was measured with a metabolic cart (SensorMedics model) during an incremental exercise test on a cycle ergometer (LODE Instrument, Groningen, The Netherlands). On the second occasion, three resting muscle samples were obtained from the vastus lateralis under local anesthesia (2% lidocaine without epinephrine) using the percutaneous needle biopsy technique described by Bergstrom (168). Visible fat and connective tissue were dissected free from the muscle and the sample was blotted to remove excess blood. The muscle sample (~ 600 mg) was divided into two portions: the first (~590 mg) was used for the immediate isolation of mitochondria for the determination of CPTI activity and palmitate oxidation rates. A portion of the mitochondria were frozen until analyzed for selected proteins with Western blotting. A small section of the muscle biopsy sample (~10 mg) was frozen in liquid N₂ for the subsequent analysis of citrate synthase (CS) and 3-Hydroxyacyl-CoA dehydrogenase activities (β -HAD).

4.3.3 Isolation of mitochondria from skeletal muscle

Differential centrifugation was used to obtain pure and intact mitochondria containing both intermyofibrillar (IMF) and subsarcelommal (SS) subfractions (3). IMF

and SS mitochondria were pooled due to the limited amount of muscle. All procedures were performed at 0-4°C. Media used were as follows: *Medium I*: 100 mM KCl, 5 mM MgSO₄·7H₂O, 5 mM EDTA, and 50 mM Tris HCl, pH 7.4; *Medium II*: solution I supplemented with 1 mM ATP, pH 7.4; *Medium III*: 220 mM sucrose, 70 mM mannitol, 10 mM Tris HCl and 1 mM EDTA, pH 7.4. Muscle was immediately placed in ice-cold medium I and then blotted and weighed. Muscle was minced with scissors in 1 ml of medium II and transferred to an ice-cold glass Potter-Elvehjem homogenizer (Tri-R Stir-R model S63C; Fisher, Toronto, ON). Tissue was homogenized in 20 volumes of medium II with a tight fitting Teflon pestle (10 up and down strokes, 30% of maximal speed). The homogenate was centrifuged at 800 g for 10 min at 4°C. SS mitochondria remained in the supernatant, which was removed and kept on ice. The IMF mitochondria found in the pellet, were resuspended in 5 volumes of medium II and treated with a protease (Sigma P5380, 0.025 ml/g) for exactly 5 minutes to digest the myofibrils. Addition of 15 ml of ice-cold medium II was used to diminish the action of the protease. Samples were centrifuged at 5 000 g for 5 min and the excess medium (supernatant) was removed. The pellet was resuspended in 10 volumes of medium II and centrifuged at 800 g for 10 min. The IMF mitochondria found in the supernatant fraction were combined with the SS supernatant fraction to increase the mitochondrial yield. The samples were centrifuged at 10 000 g for 10 min. The pellet was washed twice in medium II and centrifuged at 10 000 g for 10 min at 4°C. The pellet was resuspended in 1µl of medium III per mg of tissue and used for CPTI activity measurements. The remaining mitochondria were further diluted for palmitate oxidation measurements.

Mitochondria were further purified using a Percoll gradient (Sigma-Aldrich) for Western blotting analysis. Samples were centrifuged at 20 000 g for 1 hour and the mitochondrial layer was removed. The Percoll was removed from the sample by further centrifuging at 21 000 g for 5 hours. At this point the mitochondria are no longer metabolically viable, but are suitable for Western blotting (3).

4.3.4 Mitochondrial lipid oxidation measurements

Labeled CO₂ production and acid soluble trapped ¹⁴C from palmitate oxidation were measured following a 30 min incubation of viable mitochondria in a sealed system. A 900 µl aliquot of pre-gassed (37°C for 15 min - 5% CO₂ : 95% O₂ and constantly shaking) Modified Krebs Ringer buffer (MKR: 115 mM NaCl, 2.6 mM KCl, 1.2 mM KH₂PO₄, 10 mM NaHCO₃, 10 mM HEPES; pH 7.4) supplemented with 5 mM ATP, 1 mM NAD⁺, 0.5 mM DL-carnitine, 0.1 mM coenzyme A, 25 µM cytochrome C, and 0.5 mM malate was added to a 20 ml vial. The 20 ml glass scintillation vial contained a microcentrifuge tube with 300 µl of 1 M of benzethonium hydroxide inserted in a 1.5 ml centrifuge tube to capture ¹⁴CO₂ produced during the oxidation reaction. Viable mitochondria (100 µl) were added to the system, which was then sealed with a rubber cap and further sealed with parafilm. The reaction was initiated by the addition of a 6:1 palmitate:BSA complex (containing 10 µCi of [1-¹⁴C] palmitate) administered by syringe through the rubber cap. The reaction ran for 30 min at 37°C and was terminated with the addition of ice-cold 12 N perchloric acid by syringe through the rubber cap.

A fraction of the reaction medium was removed through the cap and analyzed for isotopic fixation. Briefly, 500 µl of reaction medium was transferred to a 14 ml

centrifuge tube and combined to 3 ml of 2:1 chloroform:methanol mixture (vol:vol), shaken for 15 min before the addition of 1.2 ml of 2 M KCl:HCl. Samples were shaken again and centrifuged at 5000 g for 15 min. A 1 ml aliquot of the aqueous phase was removed and quantified by liquid scintillation determination.

Gaseous CO₂ produced from oxidation of [1-¹⁴C] palmitate was measured by acidifying the remaining reaction mixture in the 20 ml glass scintillation vial with 1.0 ml of 1M H₂SO₄. Liberated ¹⁴CO₂ was trapped by benzethonium hydroxide over a 90 min incubation period at room temperature. The microcentrifuge tube containing the ¹⁴CO₂ was put in a scintillation vial and radioactivity was counted.

Final palmitate concentration was 77 μM (15 nCi ¹⁴[1-C] palmitic acid, Amersham Biosciences). By substituting palmitate with the equivalent concentration of palmitoylcarnitine and the short chain FA, octanoate, we were able to measure the rate of palmitoylcarnitine (15 nCi [1-¹⁴C] palmitoylcarnitine, Perkin Elmer) and octanotate (15 nCi [1-¹⁴C] octanoic acid, MP Biomedicals) oxidation.

Inhibition studies with SSO were performed by pre-incubating mitochondria with SSO dissolved in dimethylsulfoxide (DMSO) in supplemented MKR (gift from Dr. Jan Glatz, CARIM) for 30 minutes. Following the pre-incubation, mitochondria were centrifuged at 10 000 g for 10 min and washed twice in medium III to remove traces of SSO/DMSO before being resuspended in their original volume of supplemented MKR. Vials were sealed and the reaction was initiated with the addition of 6:1 palmitate:BSA complex (containing 10 μCi of [1-¹⁴C] palmitate) by syringe through the rubber cap. Based on dose-response experiments the final SSO concentration was set at 200 μM. For

control purposes, the same volume (1 μ l) of DMSO was added to vials that were not supplemented with SSO.

4.3.5 Enzymatic activities

Carnitine palmitoyltransferase-I (CPTI; EC 2.3.1.21) activity

The forward radioisotope assay was used for the determination of CPTI activity as described by McGarry et al (37) with minor modifications (180). Briefly, the assay was conducted at 37°C and initiated by the addition of 10 μ l of mitochondrial suspension (1:3 dilution) to 90 μ l of the following standard reaction medium: 117 mM Tris-HCl (pH 7.4), 0.28 mM reduced glutathione, 4.4 mM ATP, 4.4 mM MgCl₂, 16.7 mM KCl, 2.2 mM KCN, 40 mg/l rotenone, 0.5% BSA, 300 μ M palmitoyl-CoA, and 5 mM L-carnitine with 1 μ Ci of L-[³H]carnitine and a final pH of 7.1. The reaction was stopped after 6 min with the addition of ice-cold HCl. Palmitoyl-[³H]carnitine was extracted in water-saturated butanol in a process involving three washes with distilled water and subsequent re-centrifugation steps to separate the butanol phase, in which the radioactivity was counted.

Inhibition studies were performed by the addition of SSO to the reaction mixture prior to initiation of the reaction with mitochondria. The final concentration of SSO was set at 200 μ M. As a control, the same volume of DMSO was added to the control tubes. CPTI activity was expressed in terms of the whole muscle (nmol·min⁻¹·kg wet muscle⁻¹), and was normalized to the ratio of CS activity in intact mitochondrial suspensions to total muscle CS activity to account for the quality of the mitochondrial preparation (see below).

Citrate Synthase (CS; EC 4.1.3.7) and 3-hydroxyacyl-CoA dehydrogenase activity (β – HAD; EC 1.1.1.3) activity.

Activity was determined in isolated mitochondria as well as in aliquots of homogenized whole muscle. Total muscle CS activity was assayed in a portion of quadriceps muscle (~10 mg) that was homogenized in 100 vol/wt of a 100 mM potassium phosphate buffer solution (169). CS activity in intact mitochondria was determined by first assaying the extramitochondrial fraction in the suspension (1:20 dilution) and then assaying the total CS activity of the suspension (1:20 dilution) after lysing the mitochondria with 0.04% Triton X-100 and repeated freeze-thawing. The net difference provided a measure of activity in the intramitochondrial fraction. β -HAD activity was assayed spectrophotometrically at 37°C by measuring the disappearance of NADH using the whole muscle homogenate as for citrate synthase (187).

4.3.6 Western Blotting

Purified isolated mitochondrial fractions were analyzed for total protein (BCA protein assay) and 25 μ g of denatured protein from each sample were separated by electrophoresis on 8 % SDS-polyacrylamide gel and transferred to a polyvinylidene difluoride (PVDF) membrane. The monoclonal antibody MO25 (188) was used to detect FAT/CD36. Commercially available antibodies were used to detect cytochrome c oxidase IV (COXIV – Molecular Probes, city, State), Na⁺/K⁺ ATPase_1 (Upstate Biotechnology, USA), and sarcoplasmic reticulum (SERCA1) ATPase (Affinity Bioreagents Inc, USA). An internal control of previously extracted human muscle crude membrane was used in each gel to normalize for variation in signal observed across the

membranes. Blots were quantified using chemiluminescence and the ChemiGenius 2 Bioimaging system (SynGene, UK).

4.3.7 Statistics

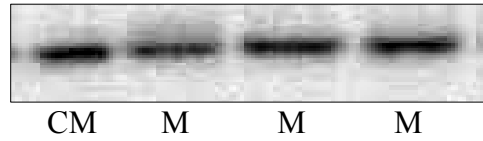
All data are presented as the mean \pm SEM. Differences between CON and SSO treatments were analyzed with paired t-tests. One-way analysis of variance was used to determine significance between all other treatments. When a significant F-ratio was obtained, a Dunnett's post hoc analysis was completed 100% activity as control. Associations between variables were investigated using simple or multiple regression analyses, as appropriate. Statistical significance was accepted at $P < 0.05$.

4.4 Results

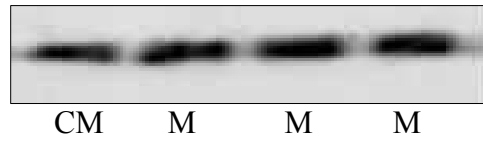
4.4.1 Identification of FAT/CD36 in pure human skeletal muscle mitochondria

FAT/CD36 was identified in isolated mitochondria from human skeletal muscle (Figure 4.1A). Figure 4.1B shows the presence of mitochondrial marker cytochrome c oxidase (COXIV) in our preparation demonstrating its mitochondrial origin. To eliminate the possibility of non-mitochondrial membrane contamination, we probed our purified mitochondrial preparations for plasma (Na^+/K^+ ATPase) and sarcoplasmic reticulum (SERCA1) membrane markers. Figure 4.1C and D demonstrate the absence of Na^+/K^+ ATPase and SERCA1 in our mitochondrial preparations compared to a crude membrane (CM) positive control, suggesting that the detected FAT/CD36 was located at the mitochondria.

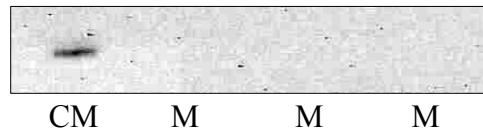
A. FAT/CD36



B. COXIV



C. Na⁺/K⁺ ATPase



D. SERCA1

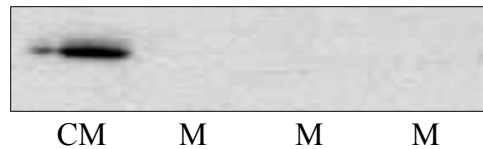


Figure 4.1. Representative Western blot of FAT/CD36 (A), COXIV (B), Na⁺/K⁺ ATPase (C), and SERCA1 (D). Performed on highly purified mitochondrial fractions (M) obtained from human skeletal muscle of trained and untrained subjects. Standards consisted of crude membranes (CM) obtained from vastus lateralis.

4.4.2 Assessment of FAT/CD36 function in LCFA mitochondrial transport

To perform the following *in vitro* assessments, a strong yield of intact functional mitochondrial preparations was required. Across all experiments, mitochondrial recovery from skeletal muscle was $32 \pm 2\%$, while quality of the preparation was $90 \pm 1\%$ (see Methods). Average mitochondrial protein content from muscle biopsies was 10.32 ± 1.28 mg/g wet muscle.

Average mitochondrial palmitate oxidation was 22.6 ± 3.5 nmol/min/mg protein. We used increasing concentrations of SSO, a specific inhibitor of FAT/CD36 to examine the relationship between FAT/CD36 and palmitate oxidation (Figure 4.2). We demonstrate a strong inverse relationship between FAT/CD36 inhibition and palmitate oxidation rates. Half maximal inhibition of LCFA oxidation occurred at 49.2 ± 1.3 μ M SSO, while at 200 μ M SSO palmitate oxidation was reduced by 95% ($P < 0.001$).

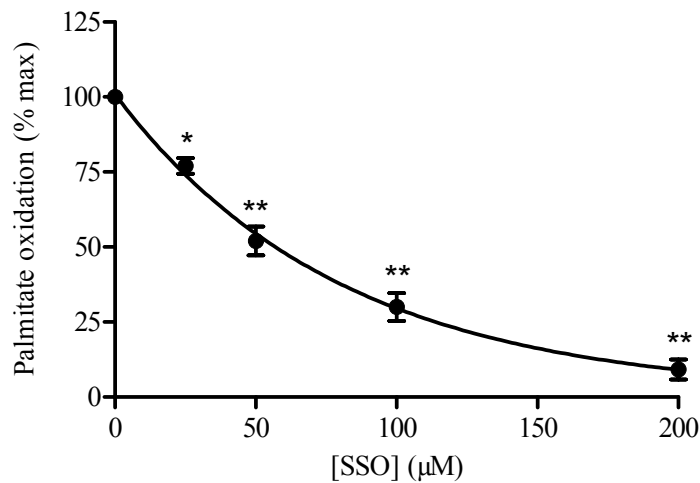


Figure 4.2. Effect of SSO on palmitate oxidation. Activity is expressed as a percentage of maximal palmitate oxidation. Values expressed as mean \pm SEM; $n = 5$. *Significantly different from 0 μ M SSO.

SSO specificity to inhibit FAT/CD36 mediated LCFA oxidation was demonstrated by the failure of SSO to inhibit short chain FA (octanoate) oxidation. (Figure 4.3).

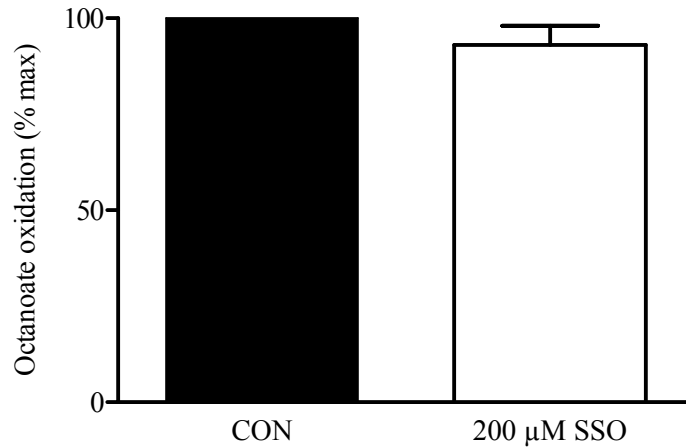


Figure 4.3. Effect of 200 μM SSO on octanoate oxidation. Activity is expressed as a percentage of maximal octanoate oxidation. Values expressed as mean \pm SEM; n = 2.

To ascertain the possible interaction of FAT/CD36 with CPTI, and its product in the mitochondria, we examined the effects of SSO on CPTI activity and palmitoylcarnitine oxidation. Maximal and submaximal CPTI activities were unchanged in the presence of SSO (Figure 4.4A). Average mitochondrial palmitoylcarnitine oxidation was (68.0 ± 9.5 nmol/min/mg protein) was inhibited by 92% ($P < 0.001$) in the presence of 200 μM SSO (Figure 4.4B). These experiments indicate a relationship between palmitoylcarnitine and FAT/CD36.

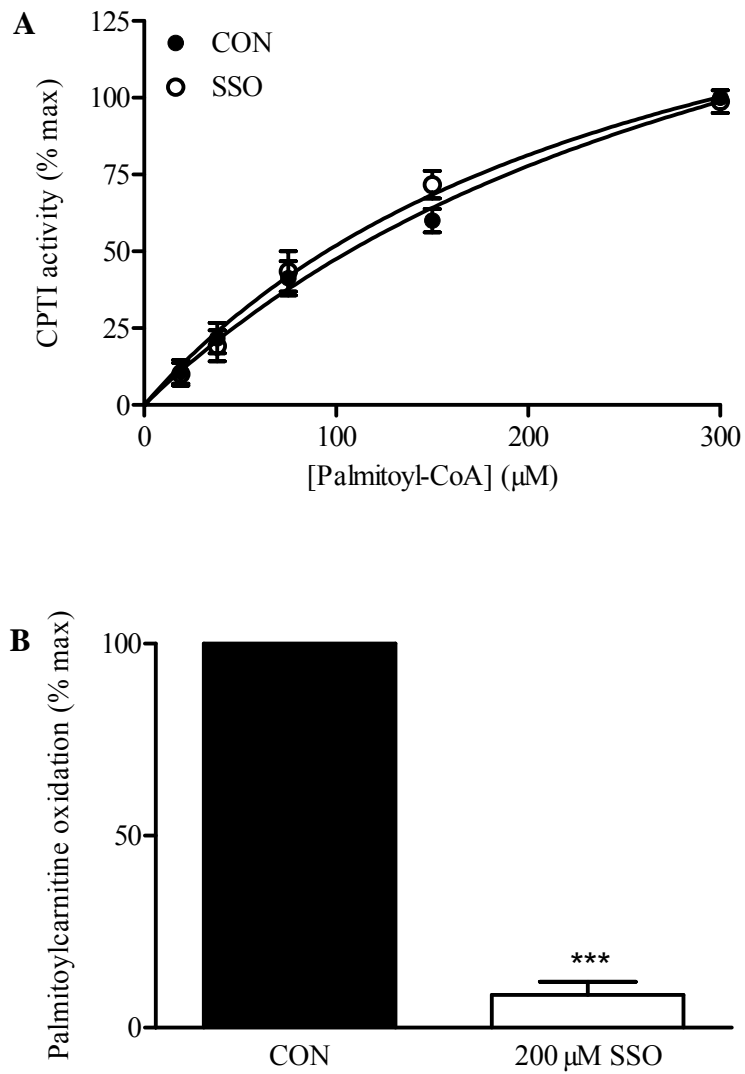
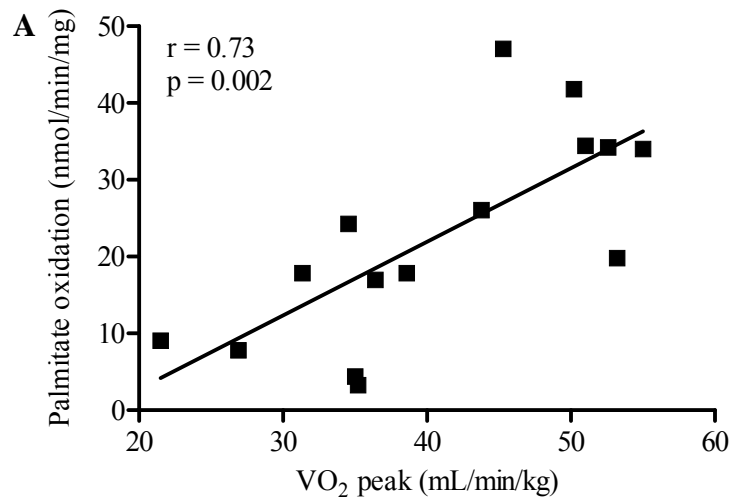
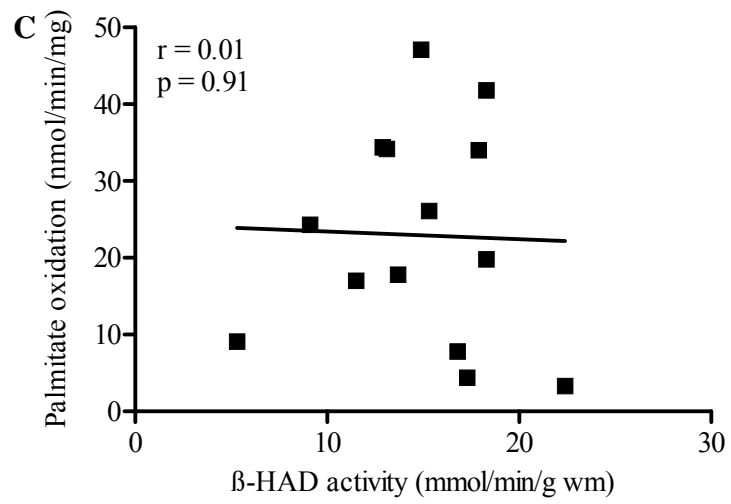
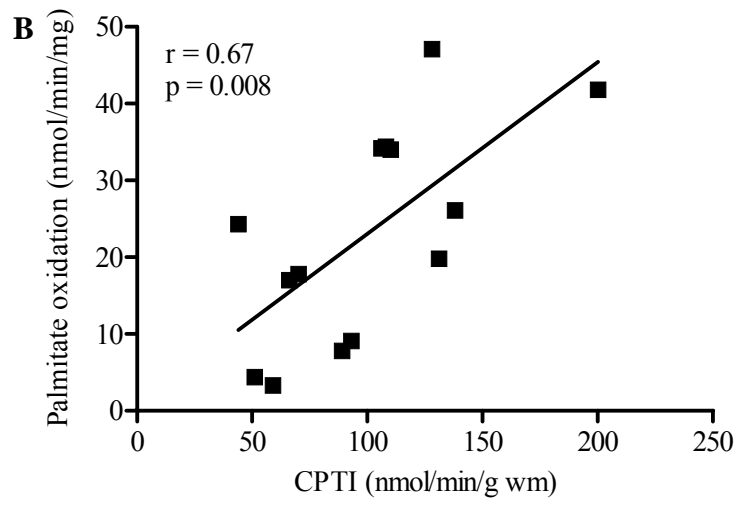


Figure 4.4. Effect of SSO on maximal and submaximal CPTI activity (A) and palmitoylcarnitine oxidation (B). Activity expressed as a percentage of maximal control CPTI activity or palmitoylcarnitine oxidation. Values expressed as mean \pm SEM; n = 4. *Significantly different from SSO.

4.4.3 Relationships between palmitate oxidation, FAT/CD36 content and markers of oxidative capacity

We performed simple linear regression analysis between mitochondrial palmitate oxidation, VO_2peak and mitochondrial enzyme activities. Rates of mitochondrial palmitate oxidation were correlated with VO_2peak (Figure 4.5A) and CPTI activity (Figure 4.5B). β -HAD activity was not associated with rates of palmitate oxidation (Figure 4.5C), but there was a significant correlation between palmitate oxidation and CS activity (Figure 4.5D).





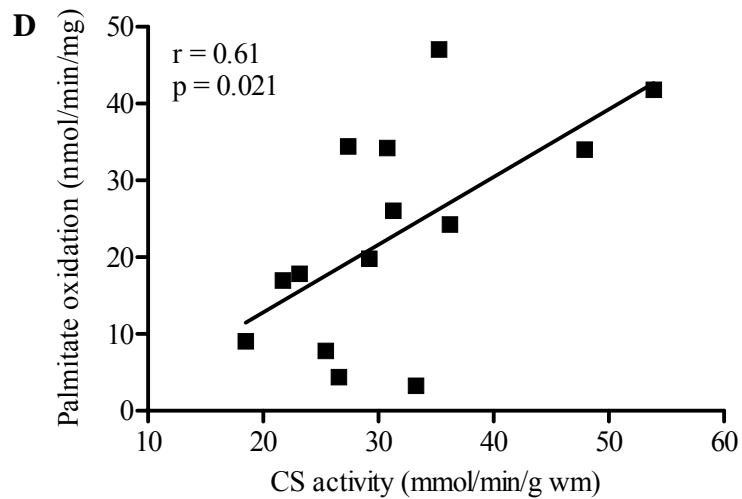


Figure 4.5. Simple linear regression analysis between palmitate oxidation and VO_2 peak (A), CPTI (B), β -HAD (C) and CS (D); $N = 14$.

Correlations between palmitate oxidation and FAT/CD36 could only be performed in a smaller subset of subjects ($n = 8$) where no correlation was found. However, to further assess the relationship between CPTI and FAT/CD36 and their impact on mitochondrial palmitate oxidation, a multiple regression analysis was performed on this smaller subset of subjects. The interaction between CPTI and FAT/CD36 strongly predicted mitochondrial palmitate oxidation ($R = 0.90$; $p = 0.017$). To illustrate the strength of the relationship between CPTI and FAT/CD36 and its impact on mitochondrial oxidation, the calculated rate of mitochondrial oxidation was plotted against the predicted rate of mitochondrial oxidation (Figure 4.6).

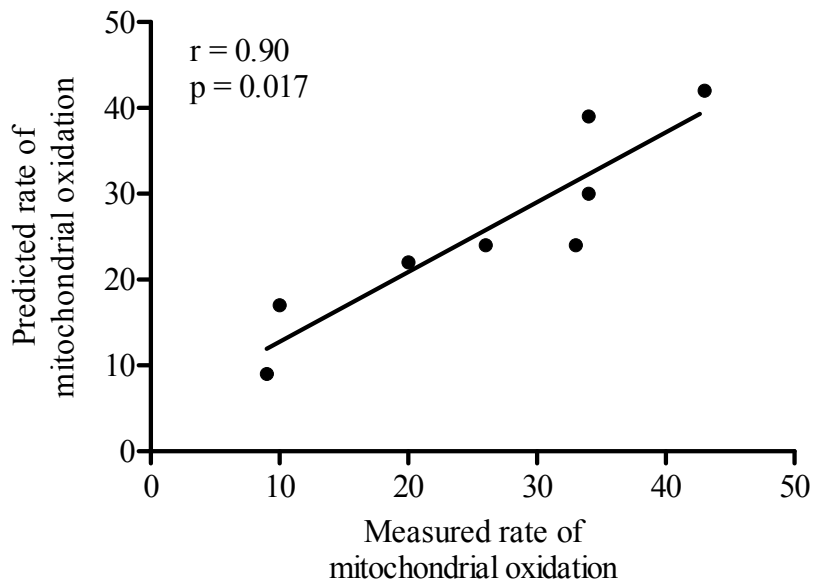


Figure 4.6. Multiple regression analysis of CPTI and FAT/CD36 on predicted mitochondrial palmitate oxidation. N = 8.

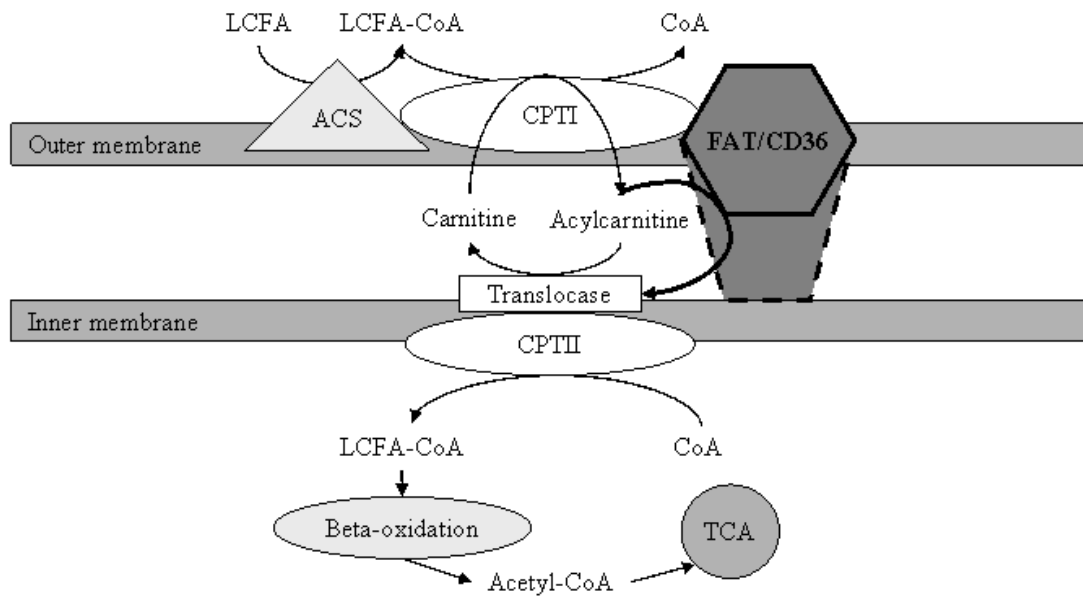


Figure 4.7. Schematic representation of FAT/CD36 facilitating palmitoylcarnitine from CPTI to CPTII.

4.5 Discussion

Identifying the mechanisms controlling LCFA transport across the mitochondrial membranes is of key importance in understanding the regulation of skeletal muscle fat oxidation at rest and during exercise. The upregulation of human skeletal muscle CPT activity and increased fat oxidation during moderate intensity exercise cannot exclusively be explained by M-CoA control. Thus, the mechanism by which LCFA oxidation is increased during exercise remains unanswered. In this study, we provide the first report of the presence of the LCFA transporter protein, FAT/CD36 in the membranes of human skeletal muscle mitochondria. Functional assessment of FAT/CD36 using a specific inhibitor demonstrated that this LCFA transporter protein is required for palmitate oxidation. Blocking of FAT/CD36 had no effect on CPTI activity but did inhibit palmitoylcarnitine oxidation suggesting that FAT/CD36 is playing a role downstream of CPTI activity.

4.5.1 Mitochondrial LCFA transport: roles for the CPTI complex and FAT/CD36

These studies are the first to identify the presence of FAT/CD36 in highly purified human skeletal muscle mitochondria. This is of considerable importance given the uncertainty regarding the regulation of the CPTI complex in human skeletal muscle (64; 66-69; 181). In both human and rodent skeletal muscle, M-CoA levels are elevated at rest inhibiting CPTI activity and minimizing fat oxidation. During moderate intensity exercise in rodent skeletal muscle, M-CoA levels decrease, relieving CPTI inhibition (62; 163). However, the majority of studies in human skeletal muscle show no change in M-CoA levels during moderate intensity exercise (65-67). Despite this, there was a large

increase in LCFA oxidation rates as determined by open circuit calorimetry (65). Only one group has been successful in showing a significant but very modest (-13%) decrease in M-CoA levels following 60 min of moderate intensity exercise (68), which the authors also concluded could not explain the increase in FA oxidation during exercise. These results suggest that the regulation of CPTI activity is more complex than regulation by only one modulator. Thus, the following points should be considered: First, there is a possibility that there are other as yet unknown regulator(s) of CPTI. In this regard, the search for potential modulators, including factors known to upregulate metabolism in many other metabolic pathways, has been unsuccessful (69; 181). However, a CPTI regulator other than M-CoA would support data reported by Kim et al. who have demonstrated the presence of a M-CoA insensitive CPTI isoform (64). In addition, several reports have been unable to account for the 50-70% residual CPTI activity that remains following the M-CoA inhibition *in vitro* (36; 37; 64; 69; 181). Secondly, it is possible that another LCFA transport/binding protein is associated with the mitochondrial membranes of human skeletal muscle, providing another level of regulation to mitochondrial LCFA uptake. This hypothesis is supported by the recent identification and characterization of the well-known LCFA transport protein FAT/CD36 in rat skeletal mitochondria membranes (3). Our present work confirms those findings to human skeletal muscle mitochondria, and we extend the work of Campbell et al (3) by showing that FAT/CD36 appears to interact with LCFA transport downstream of CPTI.

4.5.2 FAT/CD36 and mitochondrial LCFA transport

Our functional assessment studies demonstrated that mitochondrial FAT/CD36 plays an essential role in the transport of LCFA into the mitochondria for oxidation in human skeletal muscle. Inhibition studies with SSO which blocks FAT/CD36, suggest that FAT/CD36 must participate in the shuttling of LCFA into the mitochondria, as otherwise a significant residual palmitate oxidation would have been observed following SSO pre-incubation. Indeed, we demonstrated a strong causal relationship between FAT/CD36 inhibition and palmitate oxidation using increasing concentrations of SSO and almost complete inhibition of palmitate oxidation when using 200 μ M SSO (Figure 2). Importantly, the maximal SSO concentration had no effect on octanoate oxidation. This short chain FA is known to enter the mitochondrion by passive diffusion (189). These observations confirm the specificity of SSO to inhibit FAT/CD36 and the proper functioning of mitochondrial LCFA oxidation, as previously demonstrated (Figure 4.3) (3).

A major difference between our results and those reported by Campbell et al. (3) in rat skeletal muscle was that CPTI activity was not reduced by pre-incubating mitochondria with SSO. This finding changes the interpretation of the role of mitochondrial FAT/CD36, suggesting that FAT/CD36 may be located downstream of CPTI activity, rather than upstream, as previously hypothesized. This interpretation is supported by the results showing that LCFA oxidation was inhibited by SSO when the product of CPTI activity, palmitoylcarnitine was the substrate. It has previously been established that FAT/CD36 is a multi-ligand scavenger protein. It binds to a variety of ligands which structurally can vary significantly from each other (73-76). Thus, these

findings do not allow us to necessarily conclude that palmitoylcarnitine is the *bona fide* substrate of FAT/CD36, but our results do point strongly towards a functional interaction between FAT/CD36 and palmitoylcarnitine. To this end, we have modified our initial hypothesis (3) regarding the functioning of mitochondrial FAT/CD36 (Figure 4.7). We suggest, based on our present data, that FAT/CD36 facilitates the transport of LCFA-carnitine from CPTI to CPTII in the intermembrane space.

4.5.3 CPT and FAT/CD36 cooperation: structural feasibility

The structure of the CPT complex has been studied extensively (see McGarry and Brown 1997 for review (38)). It is widely accepted that CPTI is tightly inserted in the outer mitochondrial membrane, while CAT and CPTII are loosely attached to the outer and inner leaflet of the inner mitochondrial membrane, respectively. Studies examining the structure of FAT/CD36 are more recent and rely on the amino acid sequence of FAT/CD36 and a mere handful of chimeric experiments (77; 85; 90). The consensus, at the sarcolemma, is that FAT/CD36 has two transmembrane domains and is largely extracellular (77; 90). Four palmitoylation sites near the cytosolic interface of FAT/CD36 have been identified (86; 87) and associated with a change in subcellular localization (81; 100). These findings support the recent demonstration that FAT/CD36 translocates from a cytosolic pool to mitochondrial and plasma membranes in response to either muscle contraction (98) and insulin (5). Assuming an identical structure and translocation process as seen at the sarcolemma, mitochondrial FAT/CD36 could be located on the outer mitochondrial membrane with both terminals in the intermembrane space, and the bulk of the protein facing the cytosol. In this arrangement, mitochondrial

FAT/CD36 could become an intermembrane space receptor for palmitoylcarnitine and facilitate its translocation to CAT and CPTII. However, despite evidence of mitochondrial LCFA uptake by FAT/CD36 (3), the specific location of a LCFA binding site on this protein has yet to be established. SSO, the reactive oleate ester that inhibits FAT/CD36 is too large to cross the outer mitochondrial membrane and inhibit from the cytosol, suggesting a cytosolic LCFA binding site. However, palmitoylation sites on the intermembrane space support the possibility of an intermembrane space LCFA binding site.

4.5.4 Correlation studies of FAT/CD36 and oxidative capacity

Few studies have performed complete correlations between markers of oxidative capacity in human skeletal muscle due to the large amount of tissue required for analysis. We have examined several markers of oxidative capacity at the whole body, muscle homogenate, and mitochondrial level in both the carbohydrate and fat oxidation pathways. We demonstrate that rates of mitochondrial palmitate oxidation are correlated with maximal aerobic power, CS and CPTI activity, which corroborate previous findings (180; 190). The exception appeared to be β -HAD, which did not correlate with palmitate oxidation, but did correlate with CS activity. Despite being a marker of β -oxidation, β -HAD activity has not consistently been shown to increase in response to long-term aerobic training (191-193).

We found that mitochondrial FAT/CD36 protein content did not correlate with palmitate oxidation on its own. Campbell et al. (3) have previously demonstrated that FAT/CD36 levels from various rat tissues followed oxidative potential hierarchy.

However, the variations in oxidative potential between rat heart, and red and white gastrocnemius muscles far exceeds the differences that would be expected in recreationally active human vastus lateralis muscle. Thus not being able to detect differences in FAT/CD36 content across our relatively homogenous sample population is not startling. Importantly, the interaction between FAT/CD36 and CPTI proved to be a strong predictor of mitochondrial palmitate oxidation, and this, on a limited sample size. This finding supports our current hypothesis that FAT/CD36 may be working in conjunction with CPTI to allow proper transport of LCFA-CoA to the matrix.

4.5.5 Summary

In summary, we provide the first evidence of the presence of FAT/CD36 in the membranes of mitochondria isolated from human skeletal muscle. Our *in vitro* functional studies demonstrate that FAT/CD36 is necessary for mitochondrial LCFA transport and subsequent palmitate oxidation. We hypothesize that FAT/CD36 is functioning downstream of CPTI activity, possibly playing a role in the transfer of palmitoylcarnitine from CPTI to CPTII in the intermembrane space. These data provide new insight regarding the LCFA transport system across the mitochondrial membranes in human skeletal muscle, and could be involved in the etiology of insulin resistance.

CHAPTER FIVE

CONSTITUTIVE UCP3 OVEREXPRESSION AT PHYSIOLOGICAL LEVELS

INCREASES MOUSE SKELETAL MUSCLE CAPACITY FOR FATTY ACID

TRANSPORT AND OXIDATION

5.1 Abstract

Uncoupling protein 3 (UCP3) expression is directly correlated to LCFA oxidation in skeletal muscle. UCP3 has been hypothesized to facilitate high rates of LCFA oxidation, but evidence thus far is lacking. Our aim was to investigate the effects of Ucp3 overexpression and ablation on LCFA uptake and metabolism in muscle of mice having congenic backgrounds. In mice constitutively expressing the UCP3 protein (human form) at levels just over 2-fold higher than normal (Ucp3tg), indirect calorimetry demonstrated no differences in total energy expenditure (VO_2), but a shift towards increased fat oxidation compared to wild-type (WT) wild-type mice. Metabolic efficiency (g weight gain/kcal ingested) was similar between Ucp3 overexpressors, WT and Ucp3 (-/-) mice. In muscle of Ucp3-tg mice, plasma membrane LCFA binding protein (FABPpm) content was increased compared to WT mice. While hormone sensitive lipase activity was unchanged across the genotypes, there were increases in carnitine palmitoyltransferase I, β -hydroxyacylCoA dehydrogenase and citrate synthase activities and decreases in intramuscular triacylglycerol in muscle of Ucp3-tg mice. There were no differences in muscle mitochondrial content. High energy phosphates and total muscle carnitine and coenzyme A (CoA) were also greater in Ucp3-tg compared to WT mice. Taken together, the findings demonstrate an increased capacity for fat oxidation in the absence of significant increases in thermogenesis in Ucp3-tg mice. Findings from Ucp3 (-/-) mice revealed few differences compared to WT mice, consistent with the possibility of compensatory mechanisms. In conjunction with our observed increases in CoA and carnitine in muscle of Ucp3 overexpressors, the findings support the hypothesized role for Ucp3 in facilitating LCFA oxidation in muscle.

5.2 Introduction

The physiological role of uncoupling protein 3 (UCP3) in skeletal muscle where it is selectively expressed is unknown. Upon its identification in 1997, UCP3 was hypothesized to uncouple ATP synthesis from mitochondrial respiration by causing a proton leak (115; 125; 194). Early studies in which UCP3 was ectopically expressed or entopically overexpressed in cell culture or yeast systems supported the proposed uncoupling function (115; 125; 194). Indeed, it was shown that overexpression of human recombinant UCP3 in yeast lowered mitochondrial membrane potential (115), and increased basal oxygen consumption and state 4 respiration (194). However, the fact that the proton leak resulting from ectopic expression of UCP3 in yeast could not be fully inhibited by purine nucleotides led to concerns about artifactual proton leaks (129; 130). Moreover, we and others have demonstrated that while a 24-hour fast increases UCP3 expression and protein levels, it does not lead to increased mitochondrial proton leak in muscle mitochondria (131; 135).

Rather than supporting a role in the uncoupling of oxidative phosphorylation, the literature describing the effects of physiological interventions consistently supports a role for UCP3 in LCFA handling (141; 152; 195). For example, UCP3 expression increases with food restriction (196), acute bouts of exercise (144; 197) and with high fat feeding (198), all conditions in which circulating LCFA levels are elevated. UCP3 is also a target gene of the PPAR δ transcription factor, which is modulated by LCFA and thereby regulates the expression of several key genes in the regulation of fat oxidation in skeletal muscle (151).

A hypothesis was recently advanced to explain the role of UCP3 in facilitating LCFA oxidation and the seemingly paradoxical effects of fasting on UCP3 expression in muscle. It holds that UCP3 acts in conjunction with mitochondrial thioesterase-1 (MTE-1) to enable high rates of beta-oxidation by liberating free coenzyme A (CoA) and exporting the LCFA anions (156). CoA is thought to be a rate-limiting cofactor during high rates of LCFA oxidation (199). This hypothesis is bolstered by correlations between UCP3 and MTE-1 expression (158; 159), and MTE-1 activity (160). What has been lacking is direct evidence for UCP3-mediated enhanced LCFA oxidation.

Our specific objective was to examine the importance of UCP3 in LCFA metabolism in muscle. Here we report on a range of phenotypic alterations and adaptations caused by UCP3 overexpression (at physiological levels) and its ablation on the potential for LCFA handling in muscle at the levels of the plasma membrane, cytosol, and mitochondria. Our findings clearly demonstrate that skeletal muscle of UCP3-tg mice has an augmented capacity for LCFA import and oxidation resulting in decreased intramuscular triglyceride when compared to wild-type (WT) and UCP3 (-/-) mice.

5.3 Methods

5.3.1 Treatment of animals

Female WT, UCP3 (-/-), and UCP3-tg C57BL/6J mice ($n = 48$) were housed individually from weaning, and were given free access to rodent chow (4.5% fat by weight; Charles River-5075) and water. UCP3-tg mice were provided originally by Dr. John Clapham at Glaxo-Smith-Kline (UK). UCP3 (-/-) mice, UCP3-tg mice have been previously described (118; 132); however these previous reports describe mice having

mixed genetic backgrounds. Here we examine unique aspects of LCFA metabolism in UCP3 (-/-) mice, UCP3-tg mice and WT controls that have been backcrossed ten generations into the C57Bl6 background to minimize any effects of genetic background. As demonstrated in the Western blot presented in Figure 1, the levels of UCP3 overexpression in F10 mice is much lower than the estimated 15-20-fold overexpression reported for the F1 generation. In F10 UCP3-tg mice the level of overexpression is just over two-fold (on average, 230% of wildtype control levels). Mice were kept at 23°C with light at 0700-1900 and were studied at seven to ten weeks of age. Animals were cared for in accordance with the principles and guidelines of the Canadian Council on Animal Care and the Institute of Laboratory Animal Resources (National Research Council), and the study was approved by the Animal Care Committee of the University of Ottawa.

5.3.2 Indirect Calorimetry

Oxygen consumption (VO_2) and carbon dioxide production (VCO_2) of mice were measured using a four-chamber Oxymax system with automatic temperature and light controls (Columbus Instruments, Columbus, OH). Temperature was maintained at 23°C, and lights were on from 0700 to 1900. System settings included a flow rate of 0.5 L/min, a sample line-purge time of 2 min, and a measurement period of 60 s every twelve minutes. Twenty-four hours before the collection of tissues and starting at 0900, mice were placed in separate calorimetry chambers (each with a volume of 2.5 litres). Mice had *ad libitum* access to chow and water. 24-hour energy expenditure was calculated as the mean of all points collected throughout a 24-hour period. The respiratory exchange ratio

(RER) was calculated as the ratio of carbon dioxide produced (VCO_2) divided by oxygen consumed (VO_2).

5.3.3 Collection of Tissue Samples

Mice were anesthetized with an intraperitoneal injection of pentobarbital sodium (30 μ g/kg body wt) prior to muscle collection. All muscle samples were excised and snap frozen before death. The left hindlimb of the first series of mice was used for mitochondrial isolation and measurement of carnitine palmitoyltransferase I (CPTI) activity. The entire quadriceps muscle of the right leg was frozen and used for citrate synthase (CS) and β -hydroxyacylCoA dehydrogenase (β -HAD) activity measurements. A second series of mice was used for muscle metabolite analyses and hormone sensitive lipase (HSL) activity measurement. The entire quadriceps was quickly excised, frozen in liquid nitrogen, freeze-dried and powdered. Total gastrocnemius muscle was removed and frozen in liquid nitrogen for Western blots and lipid quantification. Lipid quantification was performed on freeze-dried gastrocnemius muscle. Intrascapular brown adipose tissue (IBAT) and periovarian white adipose tissue (PWAT) were also collected and weighed.

5.3.4 Collection of Blood and Serum Analysis

Blood was collected following decapitation and was analyzed for serum glucose, LCFA and total ketones using commercially available kits from Wako (Richmond VA). These included: Autokit Glucose (994-90902), NEFA C (994-75409), and Autokit Total Ketone Bodies (415-73301).

5.3.5 Isolation of Mitochondria from Skeletal Muscle

All procedures were performed at 0-4°C. Media used were as follows: *Medium I*: 100 mM KCl, 5mM MgSO₄·7H₂O, 5 mM EDTA, and 50 mM Tris HCl, pH 7.4; *Medium II*: solution I and 1mM ATP, pH 7.4; *Medium III*: 220 mM sucrose, 70 mM mannitol, 10 mM Tris HCl and 1 mM EDTA, pH 7.4. Muscle was immediately placed in ice-cold medium I and then blotted and weighed. Muscle was minced with scissors in 1 ml of medium II and transferred to an ice-cold glass Potter-Elvehjem homogenizer (Tri-R Stir-R model S63C; Fisher, Toronto, ON). Tissue was homogenized in 20 volumes of medium II with a loose fitting Teflon pestle (2 up and down strokes, 30% of maximal speed) followed by 5 up and down strokes with a tighter fitting Teflon pestle. The homogenate was spun at 700 g for 10 min at 4°C. The supernatant was removed and then spun at 12,000 g for 10 min at 4°C. The mitochondrial pellet was washed in 10 volumes of medium II and spun again at 12,000g for 10 min at 4°C. The pellet was resuspended in 0.5 µl medium III /mg tissue.

5.3.6 Western blots of UCP3 protein

Equal amounts of hindlimb muscle mitochondrial protein (100 µg) were loaded into each lane of a BioRad minigel (16% polyacrylamide) system. Following transfer to nitrocellulose membranes, primary antibody (UCP3, AB-3046; Chemicon, Tecmecula, CA) was incubated at a 1:2000 dilution, overnight at 4°C. The secondary antibody was a peroxidase-conjugated goat anti-rabbit IgG (Santa Cruz Inc., Santa Cruz, CA) and was incubated at a 1:5000 dilution for one hour at room temperature. As a positive control,

recombinant murine UCP3 (prepared in our laboratory) was used. For detection, blots were processed using enhanced chemiluminescence kits (Amersham Pharmacia; Baie d'Urfe, QC, Canada).

5.3.7 Enzyme Activity measurements

Carnitine palmitoyltransferase-I (CPTI; EC 2.3.1.21) activity. The forward radioisotope assay for the determination of CPTI activity was as described by McGarry *et al.* (37) with minor modifications (180). Briefly, the assay was conducted at 37°C and started by the addition of 10 µl of mitochondrial suspension (1:3 dilution) to 90 µl of the following standard reaction medium: 117 mM Tris-HCl (pH 7.4), 0.28 mM reduced glutathione, 4.4 mM ATP, 4.4 mM MgCl₂, 16.7 mM KCl, 2.2 mM KCN, 40 mg/l rotenone, 0.5% BSA, 300 µM palmitoyl-CoA, and 5 mM L-carnitine with 1 µCi of L-[³H]carnitine and a final pH of 7.1. The reaction was stopped after 6 min with the addition of ice-cold HCl. Palmitoyl-[³H]carnitine was extracted in water-saturated butanol in a process involving three washes with distilled water and subsequent re-centrifugation steps to separate the butanol phase, in which the radioactivity was counted. Activity was expressed in terms of the whole muscle (nmol·min⁻¹·kg wet muscle⁻¹), and was normalized to the ratio of CS activity in intact mitochondrial suspensions to total muscle CS activity to account for the quality of the mitochondrial preparation as well as recovery (see below).

Citrate Synthase (CS; EC 4.1.3.7) activity. Activity was determined in isolated mitochondria as well as in aliquots of homogenized quadriceps muscle. Total muscle CS activity was assayed in a portion of quadriceps muscle (~10 mg) that was homogenized in

100 vol/wt of a 100 mM potassium phosphate buffer solution (169). Mitochondrial quality was assessed by measuring CS activity in intact mitochondria by first assaying the extramitochondrial fraction in the suspension (1:20 dilution) and then assaying the total CS activity of the suspension (1:20 dilution) after lysing the mitochondria with 0.04% Triton X-100 and repeated freeze-thawing. The net difference provides a measure of activity in the intramitochondrial fraction. Mitochondrial recovery was also assessed by calculating the ratio of intramitochondrial fraction to total muscle CS activity. Changes in muscle mitochondrial protein content were determined by performing a protein assay on the isolated mitochondrial fraction and normalized to wet muscle mass used (BCA Assay; Pierce, Rockford, IL).

3-Hydroxyacyl-CoA dehydrogenase activity (β -HAD; EC 1.1.1.3). Total muscle β -HAD activity was assayed in an aliquot of homogenized quadriceps muscle (~10 mg) in 100 vol/wt of a 100 mM potassium phosphate buffer (187). Activity was measured in Tris-HCl buffer (50 mM Tris-HCl, 2 mM EDTA, 250 μ M NADH, pH 7.0) and 0.04% Triton-X. The reaction was started by addition of 100 μ M acetoacetyl-CoA and absorbance was measured at 340 nm over a 2 min period (37°C).

Hormone Sensitive Lipase (HSL; EC 3.1.1.3) activity. Powdered frozen muscle was analyzed for HSLa activity as previously described, with minor modifications (7; 200). Muscle was homogenized on ice using a rotating Teflon pestle on glass in 20 volumes of homogenization buffer (0.25 M sucrose, 1 mM dithioerythritol, 40 mM β -glycerophosphate, 10 mM sodium pyrophosphate, 31 nM okadaic acid, 20 μ g/ml

leupeptin, 10 µg/ml antipain, and 1 µg/ml pepstatin, pH 7.0). Post-centrifugation supernatant was held on ice for subsequent HSL assays. The substrate suspension consisted of 5 mM triolein, 14×10^6 dpm [9,10-³H]triolein, 0.6 mg phospholipid (phosphatidylcholine-phosphatidylinositol, 3:1, wt/wt), 0.1 M potassium phosphate, and 20% BSA, and was emulsified by sonication. Muscle homogenate supernatant (14 µl) was incubated at 37°C with enzyme dilution buffer (86 µl) and 100 µl of triolein substrate. The reaction was stopped after 20 min by the addition of methanol-chloroform-heptane (10:9:7, vol/vol/vol); to facilitate the separation of the organic and aqueous phases 0.1 M potassium carbonate-0.1 M boric acid was added. Following mixing and centrifugation (1,100 g for 20 min) 1 ml of the upper phase was removed for scintillation counting. Activity was normalized to total protein (BCA Assay; Pierce, Rockford, IL).

5.3.8 Muscle metabolite and fuel determinations

A second aliquot of freeze-dried quadriceps muscle (~15 mg) was extracted in 0.5 M HClO₄ (1 mM EDTA) and neutralized with 2.2 M KHCO₃. The acid-insoluble pellet and supernatant fractions were stored at -80°C prior to metabolite assays. The supernatant was used for the determination of ATP, ADP, phosphocreatine (PCr), and creatine by spectrophotometric assays (187; 201) and acetyl-CoA, free CoA, acetylcarnitine, and free carnitine by radiometric methods (202). Lipid were extracted from freeze-dried gastrocnemius muscle (60-80 mg wet) using a chloroform-methanol solution (203) (2.5 ml of chloroform:methanol (2:1, vol/vol), and 0.5 ml of chloroform). Briefly, the intramuscular triglyceride (IMTG) was extracted and the chloroform phase evaporated

(203). After reconstitution, phospholipids were removed upon the addition of silicic acid. The IMTG was saponified and the free glycerol was assayed fluorometrically (187).

5.3.9 Western blot analyses of key proteins involved in LCFA uptake and metabolism

Muscle homogenates were analyzed for total protein (BCA protein assay) and aliquots of 100 µg protein were separated in a 7.5% SDS-polyacrylamide gel and transferred to nitrocellulose membrane. Commercially available antibodies were used to detect phosphorylated AMP-activated protein kinase (AMPK) (#2531; Cell Signaling; Beverly, MA) and total AMPK (#2532; Cell Signaling; Beverly, MA). The monoclonal antibody MO25 used to detect fatty acid translocase (FAT/CD36) was a gift from Dr. Narendra Nath Tandon, Otsuka Maryland Research Institute, USA. The plasma membrane LCFA binding protein (FABPpm) antibody was a gift from Dr. Jorge Calles-Escandon, Wake Forest University, USA. The cytosolic LCFA binding protein (FABPc) antibody was a gift from Dr. Jan Glatz, Maastricht University, The Netherlands. An internal standard of previously extracted rat muscle was used in each gel to normalize for interblot signal variations. Signals were quantified using chemiluminescence and the ChemiGenius2 bioimaging system.

5.3.10 Statistics

Results are from determinations conducted on 6-8 mice (except when indicated otherwise). Results are presented as the mean \pm SEM. Comparisons between genotypes were analyzed by one-way ANOVA with a Dunnett's post hoc test using results of the WT group as the control. Statistical significance was accepted at $P < 0.05$.

5.4 Results

5.4.1 Food intake, body and tissue weights

Food intake was monitored over a 14-day period during which all mice had free access to food and water. Food intake was similar across the genotypes (Table 5.1). Body weights were recorded immediately prior to sacrifice; results demonstrated no significant differences. Similarly there were no differences in IBAT and PWAT weights, indicating no differences in adiposity in the absence, normal presence and overexpression of UCP3.

Table 5.1. Food intake, body and fat pad weights of WT, UCP3-tg and UCP3 (-/-) mice.

	WT	UCP3-tg	UCP3 (-/-)
Food intake (g/day)	3.3 ± 0.2	3.1 ± 0.1	3.3 ± 0.1
Body wt (g)	18.3 ± 0.7	16.0 ± 0.7	16.6 ± 0.5
PWAT (mg/ g BW)	3.6 ± 0.5	3.9 ± 0.5	2.8 ± 0.3
IBAT (mg/g BW)	8.1 ± 1.6	7.1 ± 1.1	6.8 ± 0.8

PWAT, periovarian white adipose tissue; IBAT, interscapular brown adipose tissue.

5.4.2 In vivo studies of metabolic rate, and respiratory exchange ratio (RER)

Given the originally proposed function of UCP3 in uncoupling and metabolic inefficiency, we examined metabolic rate and RER across the genotypes. 24-hour energy expenditure was studied in an indirect calorimeter over the 24h-period preceding muscle collection. No changes were observed in VO_2 across the genotypes. The 24h mean RER

was significantly lower in UCP3-tg mice when compared with WT mice ($P < 0.05$; Table 5.2).

Table 5.2. 24h VO_2 and respiratory exchange ratio (RER) of WT, UCP3-tg and UCP3 (-/-) mice measured in the 24h period preceding sacrifice.

	WT	UCP3-tg	UCP3 (-/-)
VO_2 (ml/g/hour)	3.80 ± 0.14	3.95 ± 0.36	3.53 ± 0.21
RER	0.95 ± 0.02	$0.90 \pm 0.01^*$	0.97 ± 0.02

Values are means \pm SEM, for 5 mice in each group. Significant difference from WT, * = $P < 0.05$.

5.4.3 Blood analysis

Blood parameters related to muscle energy substrate uptake were examined. No significant differences were observed across the genotypes in serum glucose and ketones. LCFA were significantly lower in UCP3-tg mice when compared to WT ($P < 0.01$) but were unchanged in UCP3 (-/-) mice (Table 5.3).

Table 5.3. Serum analytes of WT, UCP3-tg, and UCP3 (-/-) mice measured immediately post-decapitation in the fed state.

	WT	UCP3-tg	UCP3 (-/-)
LCFA (μ M)	465 \pm 27	301 \pm 33**	427 \pm 29
Glucose (mM)	16.7 \pm 2.6	16.3 \pm 1.3	15.6 \pm 1.5
Ketones (μ M)	248 \pm 31	282 \pm 41	218 \pm 39

Significant difference from WT, ** = $P < 0.01$.

5.4.4 Western blots analyses

To confirm the presence, absence and overexpression of UCP3 protein in muscle of the wild-type, knockout and overexpressor mice, we conducted Western blot analyses of muscle mitochondria. The level of UCP3 overexpression in muscle of Ucp-tg mice in comparison to WT mice was also determined. Representative results are presented in Figure 5.1. Our findings demonstrate the absence of UCP3 protein in UCP3 (-/-) mice, and just over a two-fold increase in UCP3 protein expression in the UCP3-tg mice compared to WT levels. The latter finding indicates that our congenic mice provide a different mouse model from the F1 generation in which there was estimated to be a 20-fold increase in UCP3 protein (See discussion).

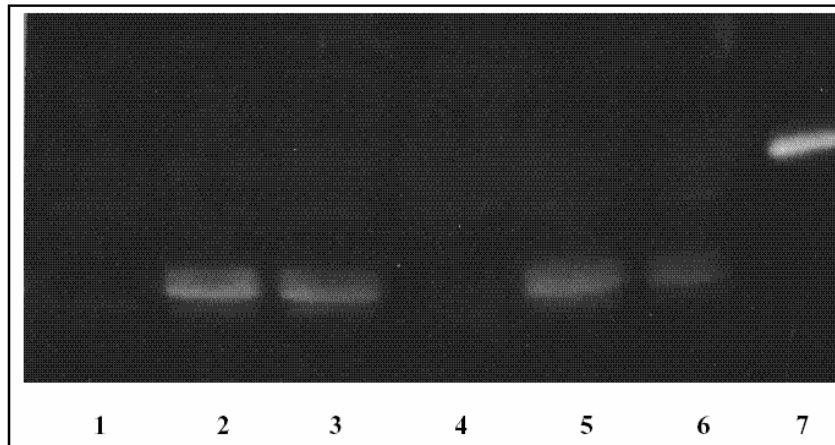


Figure 5.1. Western blot of skeletal muscle mitochondrial UCP3 protein. Lane 1: UCP3 (-/-) mitochondria, Lane 2: UCP3-tg mitochondria, Lane 3: Wildtype mitochondria, Lane 4: UCP3 (-/-) mitochondria, Lane 5: UCP3-tg mitochondria, Lane 6: Wildtype mitochondria, Lane 7: Recombinant murine UCP3, which migrates at a corresponding molecular weight of 39 kDa (rather than 34 kDa, due to a 5 kDa fusion peptide). Densitometric analyses indicated that UCP3 overexpression is just over two-fold higher in mitochondria of hUCP3tg mice than in wildtype controls.

Differences in LCFA transporter protein content were also examined by Western blotting. All analyses were performed on the same muscle homogenate prepared from gastrocnemius muscle (Table 5.4).

Table 5.4. Western blot analyses of LCFA transporter protein and AMPK in mixed gastrocnemius muscle of WT, UCP3-tg, and UCP3 (-/-) mice.

	WT	UCP3-tg	UCP3 (-/-)
FAT/CD36	1.00 ± 0.16	1.00 ± 0.08	1.17 ± 0.11
FABPpm	1.00 ± 0.08	1.57 ± 0.11*	1.05 ± 0.21
FABPc	1.00 ± 0.11	1.39 ± 0.13	1.12 ± 0.12
AMPKphos/total	1.00 ± 0.09	0.88 ± 0.11	0.86 ± 0.11

Data expressed as relative units using WT as reference. Significant difference from WT, * = P < 0.05.

Total muscle FAT/CD36 was similar across genotypes. FABPpm protein content was significantly greater in UCP3-tg when compared to WT levels, but was unchanged in UCP3 (-/-) mice. A similar pattern was generally observed for FABPc content, however differences did not reach statistical significance. These findings suggest an increased capacity for LCFA transport in UCP3-tg mice.

Given the published associations between AMPK and UCP3 expression (204), we assessed total AMPK protein content and levels of phosphorylated AMPK in skeletal muscle from each of the three mouse groups. Results show that the phosphorylated AMPK to total AMPK protein ratio of UCP3-tg and UCP3 (-/-) did not differ from WT levels, demonstrating no significant effect of altered UCP3 expression in our mouse models on phosphorylated and non-phosphorylated AMPK protein levels.

5.4.5 Enzymatic activities

To further examine the fate of LCFA inside the myocytes, we examined key cytosolic and mitochondrial enzymatic activities. Cytosolic HSL activity in muscle was similar across the genotypes (WT: 0.93 ± 0.05 , UCP3-tg: 0.91 ± 0.13 , UCP3 (-/-): 0.87 ± 0.10 nmol/min/mg protein; Figure 5.2a) suggesting comparable potential for TG lipolysis across the genotypes. However, in UCP3-tg mice CPTI activity was significantly increased compared to WT mice; no differences were observed between UCP3 (-/-) and WT mice (WT: 250 ± 34 , UCP3-tg: 422 ± 52 , UCP3 (-/-): 346 ± 46 vs. $\mu\text{mol}/\text{min}/\text{kg}$ wm; $P < 0.05$; Figure 5.2b).

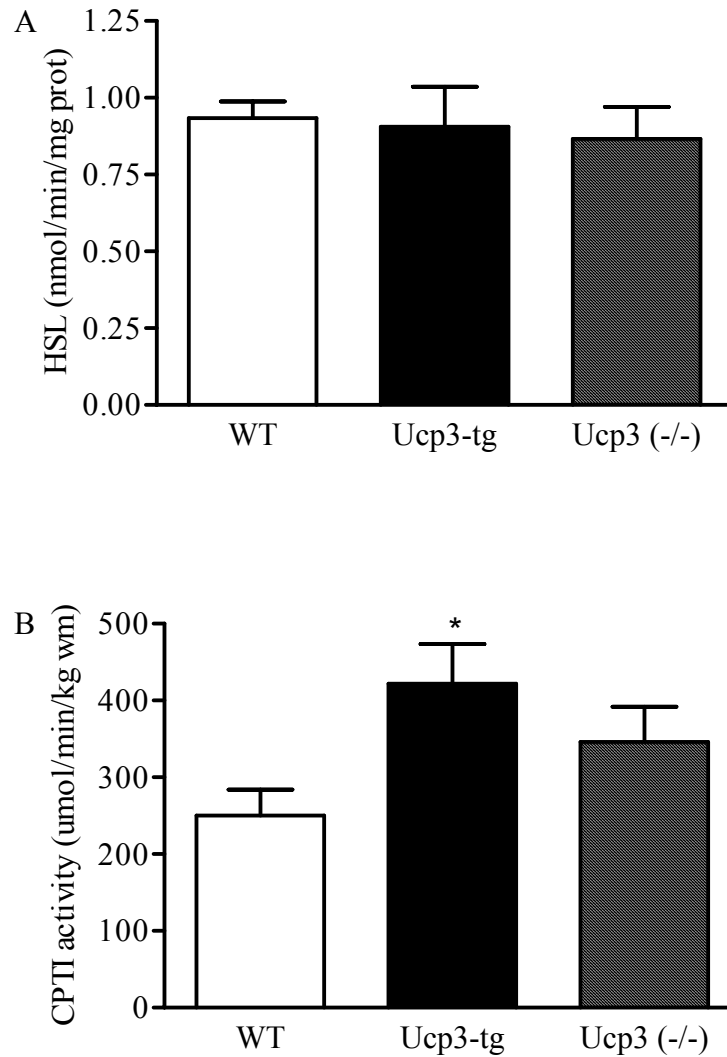


Figure 5.2. HSL (A) and CPTI (B) enzymatic activity measured in gastrocnemius muscle of WT, UCP3-tg, and UCP3 (-/-). Results are presented as the mean \pm SEM of 6-8 mice.

Moreover, mitochondrial β -HAD activity was greater in UCP3-tg mice when compared to WT mice, while UCP3 (-/-) did not differ (WT: 4.02 ± 0.56 , UCP3-tg: 6.49 ± 0.81 , UCP3 (-/-): 5.13 ± 0.74 mmol/kg wm; $P < 0.05$, Figure 5.3a). As a measure of Krebs

cycle activity, we assessed maximal CS activity and found that it was greater in UCP3-tg mice compared to WT; UCP3 (-/-) CS activity did not differ from WT (WT: 22.2 ± 1.4 , UCP3-tg: 29.0 ± 2.4 , UCP3 (-/-): 23.2 ± 2.1 mmol/kg wm; $P < 0.05$, Figure 5.3b). Importantly, these changes in maximal activity of enzymes occurred without a change in mitochondrial protein content of muscle (WT: 3.0 ± 0.2 , UCP3-tg: 3.0 ± 0.2 , UCP3 (-/-): 3.0 ± 0.3 mg protein/g wet muscle; NS). Differences in mitochondrial recovery were ruled out by expressing mitochondrial CS activity as a percent of total muscle CS activity (WT: 18.5 ± 3.1 , UCP3-tg: 16.1 ± 2.0 , UCP3 (-/-): 17.9 ± 3.8 %). These findings thereby dissociate mitochondrial volume from maximal activity.

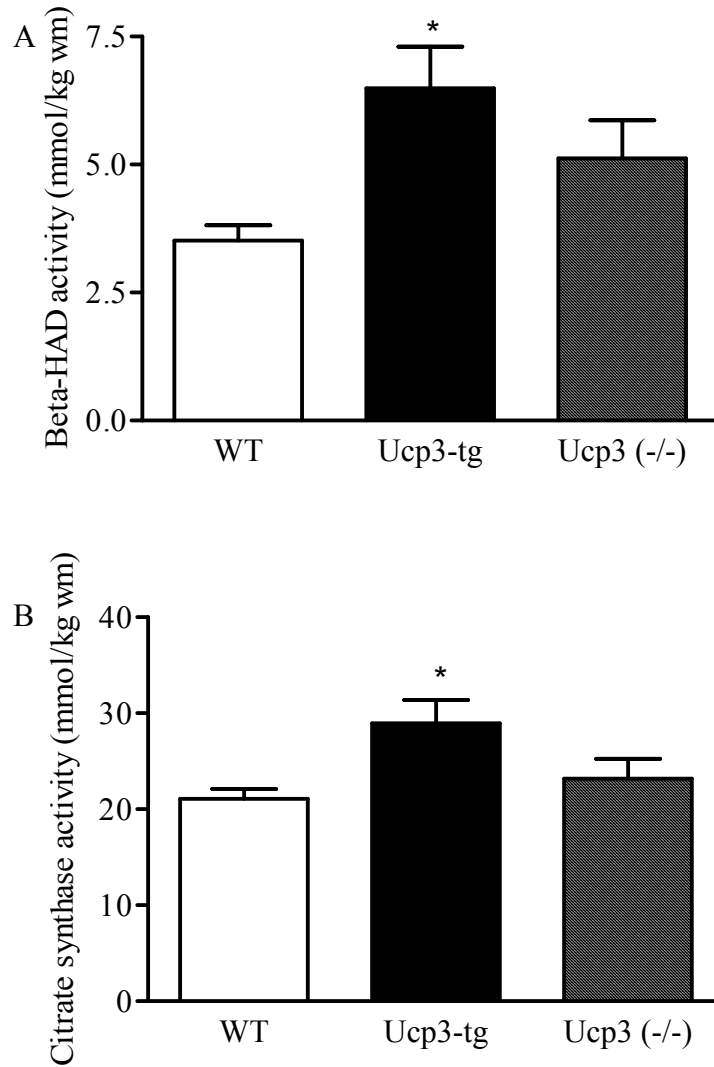


Figure 5.3. β -HAD (A) and citrate synthase (B) activity measured in red quadriceps homogenate of WT, UCP3-tg, and UCP3 (-/-). Results are presented as the mean \pm SEM of 6-8 mice.

Overall the findings demonstrate an increased potential for acyl-CoA transport across the mitochondrial membrane and increased capacity for LCFA oxidation in UCP3-tg mice.

5.4.6 Intramuscular triglyceride content (IMTG)

To confirm the increased oxidative capacity with UCP3 overexpression, we examined IMTG content across the genotypes. IMTG content was found to be lower in UCP3-tg mice when compared to WT and UCP3 (-/-) mice (WT: 45.0 ± 4.7 , UCP3-tg: 31.0 ± 3.5 , UCP3 (-/-): 46.4 ± 3.4 mmol/kg dm $P < 0.05$, Figure 5.4). These findings are consistent with increased muscle mitochondrial uptake and oxidation of LCFA with UCP3 overexpression.

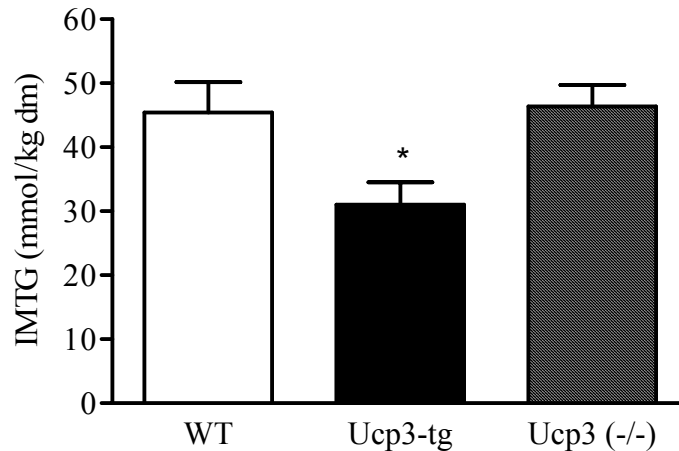


Figure 5.4. Intramuscular triglyceride content of gastrocnemius muscle from WT, UCP3-tg, and UCP3 (-/-) as measured by lipid extraction. Results are presented as the mean \pm SEM of 6-8 mice.

5.4.7 High energy phosphagens and related metabolites

To determine whether altered oxidative capacity for LCFA affected levels of high energy phosphagens, we then assayed muscle levels of phosphocreatine, creatine, ADP and ATP, carnitine, acetyl carnitine, acetyl CoA and total CoA. Contrary to what one might expect if UCP3 were fulfilling a role for mitochondrial uncoupling,

phosphocreatine levels were higher in UCP3-tg mice when compared to WT ($P < 0.05$); UCP3 (-/-) levels did not differ (Table 5.5). Free creatine levels were similar across the genotypes but total creatine levels were greater in UCP3-tg mice when compared to WT mice ($P < 0.01$). No differences in total creatine levels were observed between UCP3 (-/-) and WT mice.

Table 5.5. High energy phosphagen muscle content of WT, UCP3-tg, and UCP3 (-/-) mice measured in freeze-dried mixed quadriceps muscle following a perchloric acid extraction.

	WT	UCP3-tg	UCP3 (-/-)
PCr	30.6 ± 3.5	50.2 ± 5.2*	37.3 ± 5.0
Creatine	69 ± 5	68 ± 6	62 ± 6
Total creatine	99 ± 2	118 ± 2**	100 ± 2
ATP	20.8 ± 1.1	27.4 ± 0.7**	25.2 ± 0.8**
ADP	3.26 ± 0.13	3.82 ± 0.06*	3.22 ± 0.20
ATP/ADP	6.25 ± 0.21	7.19 ± 0.29	8.42 ± 0.68*

Data are expressed as mmol/kg dry muscle except for ADP, which is $\mu\text{mol/kg}$ dry muscle. Significant difference from WT, * = $P < 0.05$; ** = $P < 0.01$.

ATP levels were significantly higher in UCP3-tg and UCP3 (-/-) mice when compared to WT mice ($P < 0.01$). ADP levels were also significantly higher in UCP3-tg mice when compared to WT ($P < 0.05$) but UCP3 (-/-) ADP levels did not differ.

However, the ATP/ADP ratio was increased in the UCP3 (-/-) when compared to WT mice.

Related metabolites followed a similar pattern (Table 5.6). Free carnitine levels were significantly greater in UCP3-tg mice and UCP3 (-/-) mice when compared to WT ($P < 0.01$). No differences were observed in acetylcarnitine levels but total carnitine levels remained elevated in UCP3-tg mice when compared to WT mice ($P < 0.05$).

Table 5.6. Muscle metabolites of WT, UCP3-tg, and UCP3 (-/-) mice measured in freeze-dried mixed quadriceps muscle following a perchloric acid extraction.

	WT	UCP3-tg	UCP3 (-/-)
Free carnitine	4.26 ± 0.10	6.25 ± 0.18**	5.29 ± 0.16**
Acetylcarnitine	0.43 ± 0.06	0.35 ± 0.06	0.26 ± 0.07
Total carnitine	4.69 ± 0.07	6.60 ± 0.18**	5.55 ± 0.15
Free CoA	107 ± 8	161 ± 9**	123 ± 8
Acetyl-CoA	7.4 ± 0.5	8.7 ± 0.9	8.7 ± 1.2
Total CoA	114 ± 8	169 ± 10**	132 ± 8

Carnitine data expressed as mmol/kg dry muscle while CoA data are expressed as μ mol/kg dry muscle. Significant difference from WT, ** = $P < 0.01$.

Total carnitine levels of UCP3 (-/-) were not significantly different from WT mice. Free CoA levels were significantly greater in UCP3-tg mice when compared with WT mice ($P < 0.01$) whereas UCP3 (-/-) mice levels did not differ. No differences were observed in acetyl-CoA levels but total CoA levels remained elevated in UCP3-tg mice when

compared to WT mice ($P < 0.05$). Taken together these findings demonstrate a marked and consistent increase in high energy phosphagens and metabolites in UCP3-tg mice.

5.5 Discussion

The specific aim of this study was to explore the importance of UCP3 in LCFA metabolism by measuring key metabolites, fuels and protein levels in muscle of congenic mice overexpressing UCP3, expressing normal levels of UCP3 and those expressing no UCP3. A fundamental strength of this study resides in the fact that levels of UCP3 overexpression are in the physiological range. The level of overexpression is just over two-fold normal. While a previous report described increased palmitate oxidation with UCP3 overexpression in muscle (155), the present findings substantially extend the latter observation by identifying increased activity of key metabolic steps in LCFA transport and oxidation and decreases in intramuscular fat stores in the absence of any evidence of mitochondrial uncoupling. Our results also demonstrate increases in LCFA transporter proteins on the plasma and mitochondrial membranes as well as oxidation in the mitochondria. These findings, in conjunction with our documented increases in muscle CoA and carnitine levels, are consistent with a possible role for UCP3 as a mitochondrial LCFA anion exporter, responding to increased rates of LCFA oxidation (156). The lack of change in LCFA metabolism with UCP3 ablation suggests the presence of unknown compensatory mechanisms in this genotype.

Whole body VO_2 and RER were used to assess metabolic rate and fuel preference across the genotypes and our results demonstrate a shift toward fat oxidation for UCP3-tg mice when compared with WT and UCP3 (-/-) mice. The decreased RER occurred in the

absence of any detectable increase in VO_2 , and in the absence of any differences in *ad libitum* food intake or in adiposity. These results extend previous findings from our laboratory that documented a shift toward increased carbohydrate oxidation in UCP3 (-/-) mice (131). While a trend toward an increased RER in UCP3 (-/-) mice was noted in this study, it was not statistically significant (Table 4.2). This may be due to the fact that the mice used in the previous study were male and were five to twelve weeks older than those involved in the current study.

With regard to the effects of altered levels of UCP3 expression on VO_2 , the literature describes conflicting results. Similar to our findings, Vidal-Puig *et al.* (119) showed no change in VO_2 and RER between UCP3 (-/-) and WT mice. In UCP3-tg mice, Clapham and colleagues (132) found increased energy expenditure in UCP3-tg mice when compared to WT mice. The difference between the latter findings and our own may be related to the fact that the latter findings were obtained from F1 generation mice having mixed genetic backgrounds. In the present study, F10 generation mice were used to ensure an essentially identical genetic background amongst all mice studied. Contrary again to the original findings from the F1 generation hUCP3 mice, we found no decreases in body weight, fat pad weights and no increases in food intake compared to WT mice. Consistent with previous literature on the UCP3 (-/-) mice, there were no differences in body weight, adiposity and food intake between UCP3 (-/-) and WT mice (118; 132). There are several potential explanations for the differences between our findings with the hUCP3 overexpressors and those of Clapham *et al.* (132). These include the abovementioned differences in genetic background resulting in varying UCP3 overexpression levels, and differences in dietary composition. Using another

overexpression model (mRNA: 18-fold; protein: 15-fold), Son *et al.* (154) were not able to detect body weight differences in between UCP3-tg mice and WT mice on a control diet but showed attenuated weight gain by the UCP3-tg in response to a high fat diet. Thus, the increased fat oxidation capacity of UCP3-tg may not be sufficient to cause differences in weight loss on a low fat diet and may only be effective when LCFA supply is elevated. Indeed this is what has been observed in the other published mouse model of UCP3 overexpression (154) and may be of great importance in our physiological (protein: 2-fold) UCP3 overexpression model; our ongoing studies of the three groups of mice fed high and low fat defined diets (Costford et al submitted) also support this idea.

5.5.1 Serum analyses

Serum analyses were conducted in the fed state. UCP3 overexpression led to decreased LCFA levels when compared with WT and UCP3 (-/-) mice. This may suggest increased uptake of LCFA at the muscle cell level. The lack of change in LCFA levels with UCP3 ablation is consistent with findings from Vidal-Puig *et al.* and Gong *et al.* on a control diet (118; 119). No differences were found in serum glucose across the genotypes when measured in the fed state. These findings are consistent with results from Vidal-Puig *et al.* (119) and Son *et al.* (154) in UCP3 (-/-) and UCP3-tg mice, respectively. Clapham *et al.* (132) have shown lower fasting plasma glucose concentration and increased glucose clearance in mice overexpressing UCP3 by 66-fold at the mRNA level and 20-fold at the protein level but serum glucose levels in the fed state were not measured (132; 155). We observed no differences in ketone bodies, corroborating previous findings (118; 119).

5.5.2 Expression of fatty acid binding proteins and transporter

This study provides the first determinations of muscle LCFA transporter and binding proteins in UCP3-tg and UCP3 (-/-) mice. Our results demonstrate increased FABPm in the UCP3-tg mice when compared to WT and UCP3 (-/-). A similar trend was observed for the FABPc. FAT/CD36 protein content did not differ between WT controls and UCP3-tg and UCP3 (-/-) mice. Total muscle homogenates were used for all protein measurements due to limited muscle availability. Thus, FAT/CD36 results represent the sum of sarcolemmal, cytosolic and mitochondrial membrane pools. Previous results from Bonen et al. (205) showed translocation of FAT/CD36 from the cytosol to the sarcolemmal and mitochondrial membranes in response to muscle contraction and obesity to accommodate greater LCFA transport rates. Whether a similar translocation is occurring in the UCP3-tg mice could not be determined due to limited muscle availability. Increased FABP protein levels in UCP3-tg mice muscle indicate that myocytes of UCP3-tg are better equipped than WT control mice to handle increased LCFA entry into the cell. FABP and UCP3 have been previously examined together in FABP null mice in which UCP3 levels were shown to be increased (206). The authors interpreted their results by suggesting that there would be increased entry of non-esterified FA into mitochondria and subsequent export of LCFA anions. One could also speculate that the lack of FABP resulted in a PPAR-induced upregulation of UCP3 expression.

5.5.3 Intramuscular fuel handling and storage

To further examine the role of UCP3 in LCFA metabolism, we assessed characteristics of intramuscular lipid handling and storage. Measurements included assays of HSL activity and IMTG content, both of which represent the first measurements of this kind in UCP3-tg and UCP3 (-/-) mice. No differences were observed in HSL activity; however, IMTG content was significantly lower in UCP3-tg mice, consistent with either a shift towards increased oxidation, and/or decreased deposition. Given the increased capacity for transport of fat into the muscle, it seems likely that this finding is again supportive of an increased shift towards and an increased capacity for fat oxidation.

The role of AMPK in the context of UCP3 content in muscle has previously been investigated. Considered to be a ‘master switch’ of cell energy status, AMPK is activated by a decreased cellular ATP/AMP ratio (207). AMPK activity is thought to stimulate both glucose and fat metabolism through GLUT4 recruitment and acetyl-CoA carboxylase (ACC) phosphorylation, respectively (for review see (208)). Its role has been recently investigated in the context of UCP3 as a possible mechanism for improved glucose homeostasis in UCP3-tg mice (204). Schrauwen and colleagues (204) demonstrated a lowered ATP/AMP ratio in UCP3-tg mice and increased alpha-1 subunit AMPK activity, despite the lack of change in AMPK protein levels. Herein we evaluated AMPK (total and phosphorylated) at the protein level and detected no differences across the genotypes.

5.5.4 Mitochondrial adaptations

Previous findings showed increased palmitate and glucose oxidation in muscle of UCP3-tg mice (155). Our results significantly extend these findings by examining specific enzymatic steps and metabolic processes that are key players in LCFA transport and oxidation. Here we report on significant differences in the activities of enzymes involved in LCFA transport across the mitochondrial membrane (CPTI) and of key markers of the TCA cycle (CS) and β -oxidation (β -HAD) pathways. Maximal activities of all three enzymes were increased in the UCP3-tg and unaltered in UCP3 (-/-) mice when compared to WT controls. These changes were observed without a change in mitochondrial protein content, dissociating maximal mitochondrial activity from mitochondrial protein content. These adaptations are different from training-induced increases in enzymatic activity, which are largely supported by increased mitochondrial protein content (209). Results therefore demonstrate an increased capacity for LCFA transport and oxidation with UCP3 overexpression.

CPTI is considered as the rate-limiting step in LCFA transport across the mitochondrial membrane. In the absence of any other changes, one might hypothesize that an increased flux of LCFA into the matrix would lead to the accumulation of fatty acyl-CoA units in the matrix. However, we found that the maximal activities of the TCA cycle and beta-oxidation markers were also increased, reducing the likelihood of accumulation of fatty acyl-CoA within the matrix. Moreover, key muscle metabolites such as free carnitine and CoA were also increased in the UCP3-tg mice. The latter increased availability of CoA may be related to the increased expression of mitochondrial thioesterase-1 (MTE-1) in UCP3-tg mice (158). It has been suggested that LCFA

oxidation may be limited by CoA levels during elevated LCFA oxidation rates (210). Indeed, a correlation between CoA levels in peroxisomes and β -oxidation rates has been documented (211). CoA treatment has also been shown to decrease lipid accumulation and increase palmitate oxidation in mitochondria and peroxisomes (212). Together, these findings support the importance of not only substrates, but also of cofactors for increased fat oxidation.

5.5.5 High energy phosphate adaptations

The high energy phosphates ATP and ADP have been extensively examined in the context of UCP3 expression because of the originally proposed function of UCP3 in uncoupling oxidative phosphorylation. Here we report high energy phosphate values in UCP3-tg mice which clearly argue against a role for UCP3 in uncoupling. Phosphocreatine, ATP and ADP were all consistently higher with UCP3 overexpression (Table 5.5). In UCP3 (-/-) mice ATP levels were also elevated. These results support previous findings by Short et al. (213) who demonstrated enhanced ATP production despite thyroid hormone mediated elevations in UCP3 expression in oxidative skeletal muscle. In mice having mixed genetic backgrounds, others have reported no change in ATP levels between WT and UCP3 (-/-) mice and with UCP3 overexpression (119; 214). In regard to ADP levels, Vidal-Puig et al. (119) documented a trend for lower ADP levels in UCP3 (-/-) mice while Garcia-Martinez (214) found ADP levels to be decreased with UCP3 overexpression. These differences could be explained by several factors including the methods used in muscle sample collection, the level of UCP3 overexpression and the actual analytical methods.

We demonstrate increased total creatine content with UCP3 overexpression caused uniquely by increased phosphocreatine content in this genotype. To date, total creatine levels had not been measured with UCP3 overexpression. However, previous findings have shown phosphocreatine levels to be similar between WT and UCP3 (-/-) corroborating our current findings (119). Elevated concentrations of ATP argue against a role for UCP3 in uncoupling oxidative phosphorylation. Beyond this, the significance of these results is difficult to interpret.

Greater levels of high energy phosphates are a characteristic of glycolytic-type muscle fibers (215; 216). However, the improved LCFA transport and oxidation capacity of the UCP3-tg mice reported here would suggest that those fibers are also more oxidative. The answer may lie midway such that overexpression of UCP3 leads to increased glycolytic and oxidative capacity, resulting in fast-oxidative muscle fibers. A thorough examination of fiber type proportions in UCP3 overexpressing and ablated mice has not yet been completed and is warranted. On the other hand, UCP3 protein levels have been examined in various fibers types of human skeletal muscle (217). UCP3 was found to be expressed the least in oxidative type I, more in oxidative-glycolytic type IIa, and the most in glycolytic type IIx. These findings were interpreted as supporting evidence for decreased oxidative efficiency of type II fibers. One could also speculate that increased UCP3 levels in type II fibers demonstrates a situation of LCFA supply exceeding oxidation capacity, thus a need for LCFA anion export by UCP3.

5.5.6 Transgenic mouse models

Issues have been raised regarding the use of transgenic and gene-ablated mouse models and should be considered when analyzing the implications of the current findings. Two UCP3-tg mice models have been generated: the first one overexpressing human UCP3 by 66-fold at the mRNA level and 20-fold at the protein levels (132) and the second one overexpressing mouse UCP3 by 18-fold at the mRNA and 15-fold at the protein level (154). Differences in body weights, *ad libitum* food intake and fasting blood glucose have been found between the two groups and are reported as being associated with differences in the levels of overexpression. In WT mice, a five-fold increase in UCP3 protein levels has been seen following a fast or high fat diet (141; 160) but no condition has resulted in a 15 to 20-fold increase as seen with the UCP3-tg mouse model which indicates that results from overexpressing mice models should be interpreted cautiously. Concerns with proper folding and insertion of the UCP3 protein have been raised when the level of overexpression is too high (129; 130). The improper insertion of UCP3 has been found to cause proton leak. However, this does not appear to be the case in the UCP3 overexpressing mice studied herein as ATP levels are not decreased (in fact they are increased) and as whole animal VO_2 is normal. Moreover these previous findings were from studies of mice having mixed genetic backgrounds. A major strength of the present work is that it is based on congenic mice having just over a two-fold increase in UCP3 protein in muscle mitochondria. This increase is within the physiological range. A two-fold increase in protein level is observed with fasting (mRNA levels increase approximately four-fold) (131; 135).

Despite the use of congenic mice in this study, concerns with gene ablation continue as findings from UCP3 (-/-) did not demonstrate decreased LCFA transport and oxidation capacity in this genotype. Overall, the results from UCP3 (-/-) most closely resembled those of WT mice rather than opposing the UCP3-tg results. Compensation of other genes may be occurring as a result of gene ablation and thereby renders the examination of gene function more difficult to interpret. These results suggest that decreasing gene expression of the gene of interest may be a more appropriate approach than gene ablation to obtain relevant results.

5.5.7 Role of UCP3 in LCFA handling

The exact role of UCP3 in LCFA handling is unclear. Two hypotheses have been put forward proposing that UCP3 acts as a LCFA anion exporter (149; 156). Schrauwen and colleagues (149) proposed that when LCFA supply exceeds oxidation, a greater proportion of LCFA enter the mitochondria by flip-flop, resulting in an accumulation of non-esterified FA inside the matrix. They proposed that UCP3 is required for outward translocation of the non-esterified FA. This hypothesis does not link UCP3 with improved capacity for LCFA oxidation, but does propose a mechanism for efflux of LCFA anions that cannot be used in the matrix for fuel.

Another hypothesis that does associate UCP3 function with improved capacity for LCFA oxidation was put forward by Himms-Hagen and Harper (156). It was hypothesized that UCP3 functions in conjunction with a mitochondrial thioesterase to export LCFA anions when LCFA supply exceeds oxidation. MTE-1 functions to cleave CoA units from matrix fatty acyl-CoA and is thought to liberate CoA to support high

rates of Krebs cycle and β -oxidation pathway activities (218). Himms-Hagen and Harper (156) extended this line of thinking to propose that UCP3 would export the remaining LCFA anions, as the latter cannot be oxidized until they are reactivated outside of the matrix by acyl CoA synthetases (*e.g.*, ACS5, located on the mitochondrial outer membrane). This LCFA cycle would allow greater rates of fat oxidation by releasing sequestered CoA and minimize potentially deleterious effects of fatty acyl-CoA accumulation in the matrix. By lowering mitochondrial membrane potential (*e.g.*, an anion would be exported from the matrix), electron transport chain activity would be increased and complexes of the chain would be less reduced, which has repeatedly been shown to decrease reactive oxygen species production (for review see (29)). MTE-1 expression is significantly increased in UCP3-tg mice (158). The MTE1-UCP3 hypothesis is supported by a strong correlation between UCP3 and MTE-1 expression (158; 159) and activity levels (160). Other groups have indeed demonstrated increased palmitate oxidation with UCP3 overexpression (155). Our data extend those findings by showing an increased potential for LCFA uptake, transport into the mitochondria and flux through the TCA and β -oxidation pathways. That CoA and carnitine levels are also elevated in UCP3-tg mice is consistent with enhanced rates of fat oxidation. Although this study was not designed to test mechanistic aspects of this hypothesis, our results do support it.

5.5.8 Summary

In summary, the results of these studies provide novel integrative findings on the effects of UCP3 overexpression and ablation in congenic mice. Results demonstrate

increased LCFA transport at the plasma and mitochondrial membranes, decreased IMTG storage and increased mitochondrial LCFA oxidation with UCP3 overexpression. The observed high energy phosphates and muscle metabolites argue against a role for UCP3 as an uncoupler and support the proposed function of UCP3 as a LCFA anion exporter in a cycle to support high rates of LCFA oxidation.

CHAPTER SIX
DISCUSSION AND CONCLUSIONS

This thesis investigated the role and/or mechanisms by which CPTI, FAT/CD36 and UCP3 affect fat metabolism. All three of these proteins are thought to be involved in LCFA transport across the mitochondrial membranes, but not without controversy. Throughout this discussion, the interplay between CPTI, FAT/CD36 and UCP3 in conditions of low (resting) LCFA flux, and acute and chronically elevated LCFA flux will be discussed.

6.1 Summary of results

In the first study (Chapter Three), human and rat skeletal muscle were used to examine maximal CPTI activity, the sensitivity of CPTI to M-CoA, and the effects of exercise-related metabolites on CPTI activity in IMF and SS mitochondria. Although IMF mitochondria accounted for a greater proportion of total mitochondria, maximal CPTI activity and sensitivity to M-CoA were similar between the subfractions across all muscle groups examined. Up to 60% of CPTI activity was resistant to M-CoA inhibition *in vitro* supporting the idea that other regulators of CPTI must exist. However, when examining the effects of calcium and energy charge metabolites on CPTI activity in the presence of M-CoA, we found that none of these metabolites were capable of overriding M-CoA inhibition in human VL and rat Sol and RG muscle. This study implies that other mechanisms of CPTI regulation must exist.

The recent identification of FAT/CD36 and its association with CPTI in rat skeletal muscle allowed us to follow up on Study One (Chapter Three) and investigate the presence of FAT/CD36 in human skeletal muscle mitochondria and its role in LCFA transport across the mitochondrial membrane (Chapter Four). We found that FAT/CD36

was present in pure human mitochondrial preparations and that its proper functioning was essential for palmitate oxidation. Using SSO, a specific FAT/CD36 inhibitor, we also determined that FAT/CD36 must be located downstream of CPTI, as SSO had no effect on CPTI activity but did inhibit oxidation when palmitoylcarnitine, the product of the CPTI reaction, was used as a substrate. Importantly, the interaction between FAT/CD36 and CPTI proved to be a strong predictor of mitochondrial palmitate oxidation.

In the final study (Chapter Five), the effects of mouse skeletal muscle UCP3 overexpression and ablation on LCFA transport and oxidation capacity were examined. A physiological two-fold increase in UCP3 expression did not affect body and fat pad weights of mice but did cause a shift toward increased fat oxidation at the whole body level and also decreased blood LCFA levels. More in depth analysis at the sarcolemmal and mitochondrial levels demonstrated increased LCFA uptake and binding capacity, increased oxidative capacity and decreased IMTG content with UCP3 overexpression while UCP3 ablated mice did not differ from WT. Together with increased levels of muscle CoA, carnitine, and high energy phosphagens, the results support the hypothesis that UCP3 may act as a LCFA anion exporter. Regardless of whether this hypothesis holds or not, the overexpression of UCP3 had a significant and positive impact on LCFA metabolism. Thus UCP3 should not be ignored when discussing the complex regulation of LCFA metabolism.

6.2 Mitochondrial subfractions

In studying the three proteins mentioned above, one recurring technique was mitochondrial isolation. The mitochondrial isolation techniques varied across the three

experimental studies. In two studies (Chapters Three and Five), the use of the protease nagarse was omitted despite it being commonly used in the literature to isolate IMF mitochondria. This decision was based on evidence that nagarse interferes with M-CoA – CPTI inhibition (25; 30-33). A major concern was that unknown effects on IMF mitochondria following nagarse treatment would cause artifactual differences between IMF and SS mitochondria. Given that the main aim of Study One (Chapter Three) was to investigate the differences in CPTI and M-CoA sensitivity between IMF and SS mitochondria, we avoided the use of the protease altogether. The main consequence was a reduced mitochondrial yield. In the second study (Chapter Four), we resorted to using nagarse to minimize the number of human muscle biopsies required to complete all analyses. Mitochondrial yield was increased by 3.6 fold when compared to study one and three. Concerns of artifactual differences between IMF and SS mitochondria were eliminated by pooling IMF and SS mitochondria following the isolation.

In the final study (Chapter Five), IMF and SS mitochondria were also pooled following their isolation since the already complex study design did not suit comparison of mitochondrial subfractions. Furthermore, the starting tissue mass from mice was approximately 5-fold greater than from a human muscle biopsy, thus the use of nagarse to increase available mitochondria was not judged necessary.

The examination of mitochondrial subfractions was limited to the first study of this thesis due to the complexity of the process and larger muscle sample size required. With or without using nagarse to isolate IMF mitochondria, some cross-contamination between the mitochondrial subfractions is possible and should be assumed. This is a result of the lack of specific mitochondrial subfraction markers to unequivocally assess the purity of

each preparation. Cross-contamination and the varying techniques used to isolate mitochondrial subfractions could explain the current ambiguity in the literature regarding SDH, COX and CS activity in IMF and SS mitochondria (18; 19; 21; 25). The controversy continues, as Koves et al (32) recently published findings of differential sensitivity to M-CoA, but similar CS activity, in IMF and SS mitochondria of rat RG, arguing against the findings presented in Chapter Three. Opposing results also can be found in the literature on the large majority of measurements performed in IMF and SS mitochondria. This situation is very perplexing and greatly reduces the credibility of such measurements. Until consistency in methods is applied and proper purity checks for IMF and SS mitochondria become available, functional assessment of oxidative capacity in IMF and SS mitochondria promises to become even more controversial.

6.3 Concerted regulation of CPTI, FAT/CD36 and UCP3 during low LCFA flux conditions

Skeletal muscle M-CoA IC₅₀ values and *in vivo* M-CoA levels at rest suggest that CPTI should be fully inhibited. But resting respiratory exchanges ratios and palmitate oxidation rates suggest otherwise (65; 219-221). The popular arguments against this paradox are the existence of M-CoA insensitive CPTI isoforms (64), bound or intramitochondrial M-CoA units resulting in an overestimation of extramitochondrial *in vivo* values, or simply that the rate-limiting regulation of CPTI is more complex than originally anticipated (222). In support of the latter, it has been shown in rat heart mitochondria that CPTI needs to be at least 50% inhibited before affecting β -oxidation flux (210). Thus it could be argued that, although not effective *in vitro*, *in vivo* M-CoA

levels could be such that CPTI is always partly inhibited, allowing it to have a high flux control coefficient over β -oxidation (222) (Figure 6.1). Our data supports all of these views but also provides additional evidence of another FA transporter protein, FAT/CD36, in human skeletal mitochondrial membrane. Our data suggest that in a resting low LCFA flux condition, FAT/CD36 appears to be playing a permissive role in LCFA transport across the mitochondrial membrane of human skeletal muscle. Findings from Chapter Four demonstrate that CPTI may still be the rate-limiting step in LCFA oxidation since palmitoylcarnitine oxidation rates were found to be four times greater than palmitate oxidation rates. However, located downstream of CPTI, it is possible to foresee FAT/CD36 chaperoning palmitoylcarnitine units to translocase (Figure 6.1). Assuming that the LCFA anion export hypothesis for UCP3 is correct, UCP3 would contribute little to LCFA metabolism in a resting low LCFA flux state since CPTI and cofactors should be fully capable of handling the relatively low LCFA flux (156) (Figure 6.1). Indeed, UCP3 mRNA and protein levels are low in rat and human skeletal muscle in such conditions (134; 141; 148).

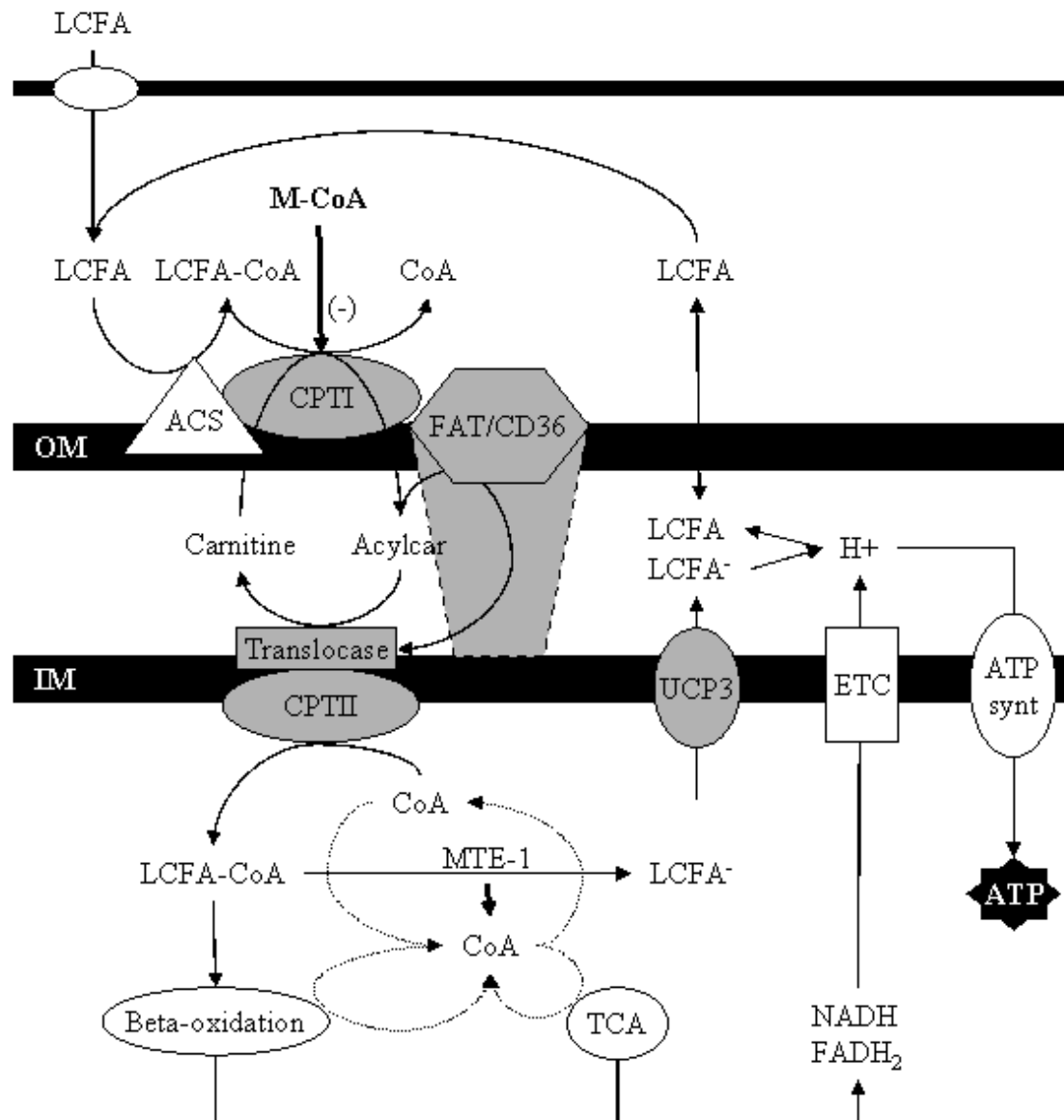


Figure 6.1. Concerted regulation of CPTI, FAT/CD36 and UCP3 in conditions of resting low LCFA flux. M-CoA partially inhibits CPTI activity resulting in low LCFA transport rates across the mitochondrial membrane. FAT/CD36 is essential in this process. UCP3 is minimally involved. Acylcar: Acylcarnitine; ATP synt: ATP synthase.

6.4 Concerted regulation of CPTI, FAT/CD36 and UCP3 during acutely elevated LCFA flux conditions

A strong link between CPTI, FAT/CD36 and UCP3 is that they respond similarly to increased LCFA levels. All three proteins contain PPAR-response elements (PPRE), meaning that their regulation is dependent on LCFA levels such that acutely elevated LCFA flux conditions like acute exercise increase their gene transcription (see Gilde AJ and Van Bilsen M 2003 for review (223)). Upregulation of CPTI gene transcription in response to acute exercise has been shown in human skeletal muscle (145) but CPTI regulation is also post-translational (Figure 6.2). For years, M-CoA has been known as the only allosteric exercise regulator of CPTI in rat skeletal muscle (38). But it has repeatedly been shown that M-CoA levels do not decrease during moderate intensity exercise in humans (65-67). From this thesis (Chapter Three), we also know that other exercise-related metabolites such as calcium and energy charge nucleotides have no effect on CPTI activity (181). Aside from a decrease in pH during high intensity exercise, there are no known additional direct effectors of CPTI activity in human skeletal muscle (69; 181). The answer may be control or rate limitation of LCFA transport into the mitochondria may lie distal to CPTI activity or at another site. Although this thesis did not examine the effect of acutely elevated LCFA flux conditions on FAT/CD36, acute exercise-induced translocation of FAT/CD36 has been shown in rat skeletal muscle mitochondria and should be considered (3) (Figure 6.2). Thus, there is a possibility that calcium and the exercise-related energy nucleotides used in Chapter Three to attempt overriding M-CoA inhibition of CPTI could indirectly support the CPT system by acting as muscle contraction signals to induce the translocation of FAT/CD36 to the

mitochondria. In rodents and humans, UCP3, just like FAT/CD36, is upregulated up to 4-fold at the mRNA and protein level in response to acute exercise and fasting (131; 133; 135; 145; 148; 197) (Figure 6.2). The two-fold physiological upregulation of UCP3 used in Chapter Five resulted in increased LCFA uptake and oxidation capacity as well as cofactors CoA and carnitine in mice skeletal muscle, possibly to allow greater flux through CPTI and increased rates of fat oxidation. Thus together, CPTI, FAT/CD36 and UCP3 could handle increased cytosolic LCFA-CoA levels, leading to greater shuttling of LCFA to the matrix and subsequent energy production.

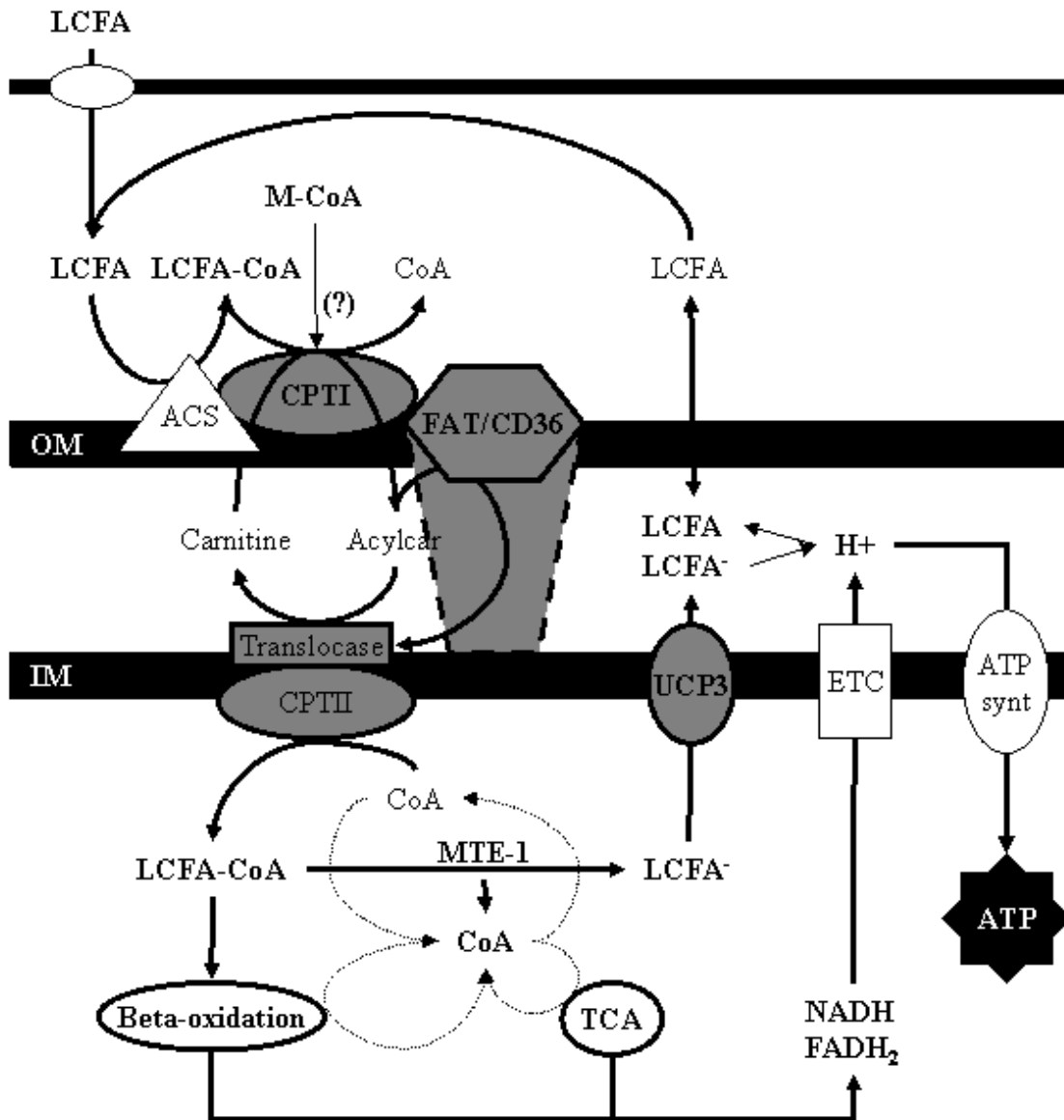


Figure 6.2. Concerted regulation of CPTI, FAT/CD36 and UCP3 in conditions of acutely elevated LCFA flux. CPTI activity is elevated (indicated by darker shade). FAT/CD36 content may be increased as a result of translocation from cytosolic pool. LCFA-CoA accumulate in the matrix. MTE-1 and UCP3 are required for CoA cleavage LCFA anion export, respectively, allowing greater rates of LCFA oxidation.

6.5 Concerted regulation of CPTI, FAT/CD36 and UCP3 during chronically elevated LCFA flux

Upregulation of CPTI activity has previously been shown in human skeletal muscle following chronic elevations of LCFA flux such as long term endurance training (69; 193; 224) and is partially a result of mitochondrial biogenesis (175; 224). Chronic exercise also affects CPTI activity indirectly by decreasing ACC activity (65) and altering M-CoA sensitivity to CPTI in human skeletal muscle, but results are far from consistent (32; 69; 181). Nonetheless, results from Chapter Four demonstrate that CPTI activity can be up to four times greater in individuals who are more aerobically fit (Figure 6.3). Whether a similar increase in mitochondrial FAT/CD36 protein also occurs in such individuals cannot be concluded from the present thesis due to the limited sample size. Previous studies have found an increase (193) or no change in FAT/CD36 protein content with endurance training (225; 226) but these measurements were made in whole muscle, disregarding subcellular localization. Only in rats has mitochondrial FAT/CD36 content been examined and shown to increase in response to chronic electrical stimulation (3) (Figure 6.3). Whether a similar upregulation is occurring in human skeletal muscle or is simply undetectable using currently available techniques cannot presently be answered. Less ambiguity surrounds the effects of chronic exercise on UCP3 protein content. Surprising at first, aerobically trained individuals have less UCP3 protein than untrained individuals (217; 227). This observation is similar to the decreased UCP3 content found in more oxidative than glycolytic tissues and may be interpreted as an adaptation to greater fat oxidation capacity (69; 181; 193) such that the export of LCFA anions is not required (Figure 6.3). With some questions remaining in regards to the regulatory roles

that FAT/CD36, CPTI and UCP3 play, it has clearly been shown that these proteins are capable of adapting to chronic exercise to optimize LCFA oxidation.

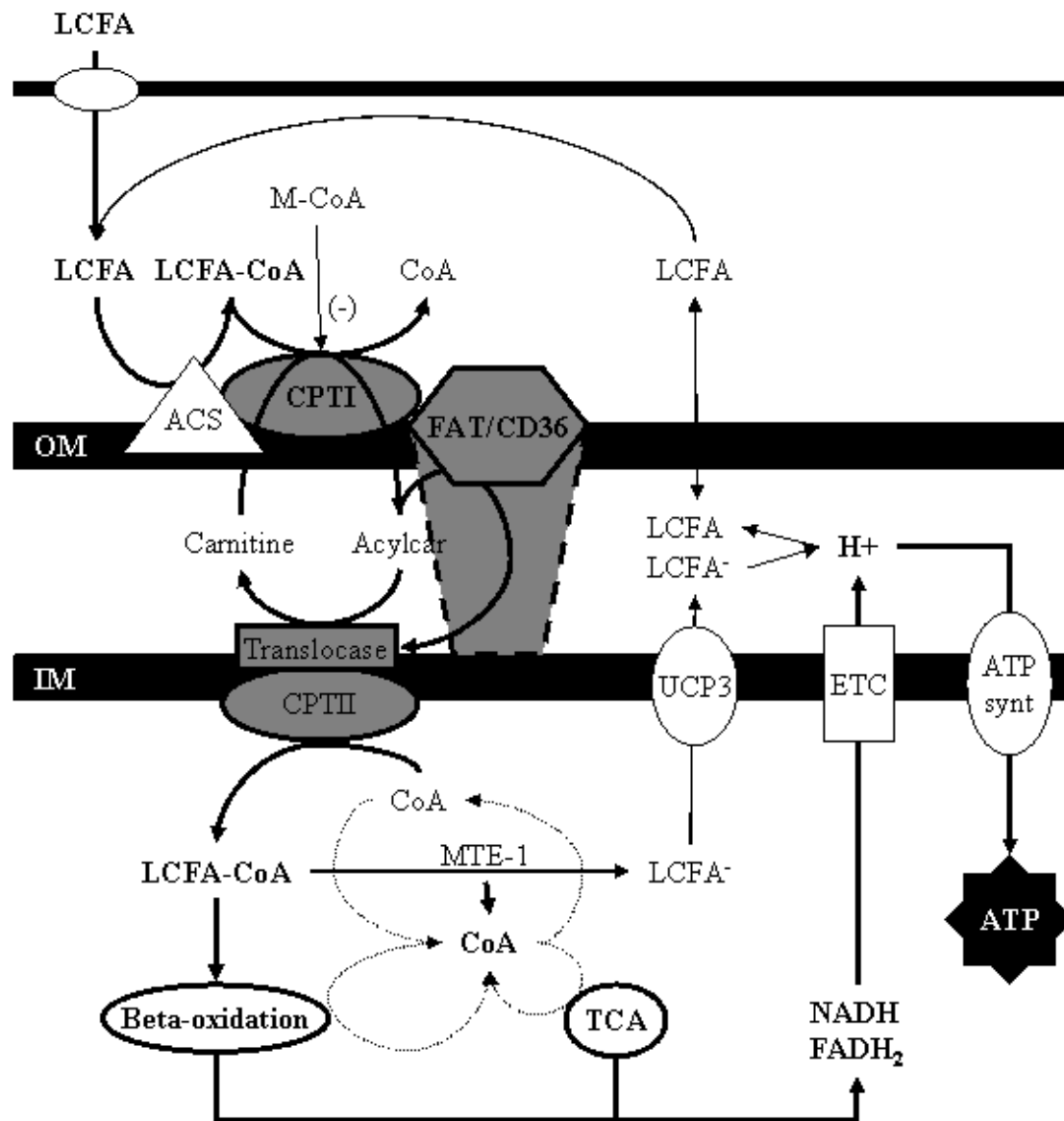


Figure 6.3. Concerted regulation of CPTI, FAT/CD36 and UCP3 in conditions of chronically elevated LCFA flux. Chronically increased CPTI activity and FAT/CD36 content allow for an elevated LCFA transport rate across the mitochondrial membranes. These adaptations are sufficient for LCFA oxidation handling thus LCFA anion export through UCP3 is not required.

6.6 Future work

Future work in the areas of CPTI, FAT/CD36 and UCP3 is required. Specifically, the cellular localization of M-CoA should be investigated to clarify human skeletal muscle regulation of CPTI activity at rest. The extent of M-CoA inhibition in the literature is inconsistent due to variety in the techniques used. Thus M-CoA sensitivity should be directly compared in mitochondria, muscle homogenate, and intact muscle strip preparations to address preparation artifacts issues. These may be at the source of the discrepancy between *in vivo* and *in vitro* M-CoA effects.

Future work is definitely needed in the area of FAT/CD36 regulation at rest and during acute and chronic exercise in human skeletal muscle. Firstly, resting muscle biopsies of very well trained, lean sedentary, obese and diabetic human subjects should be used to examine mitochondrial FAT/CD36 content in specific population groups, with varying muscle oxidative capacities. The subjects used in Chapter Four appeared to have been too similar in their background training status to provide a convincing answer on population differences. From the obese and diabetic groups, we would gain insight as to how FAT/CD36 adapts or contributes to depressed LCFA oxidation capacity and insulin resistance. Whether translocation of mitochondrial FAT/CD36 occurs with muscle contraction could be answered by sampling pre and post exercise muscle biopsies from subjects. An exercise time-course study could also provide clues regarding the type of exercise-induced regulation that is governing FAT/CD36. Lastly, the search for other *in vivo* effectors of FAT/CD36 is vital to further understand the regulation of LCFA transport across the mitochondrial membrane.

Finally, it was determined from this thesis that several important steps in LCFA uptake and oxidation are upregulated with a constitutive two-fold UCP3 overexpression in the mitochondrial membranes. These findings are consistent with idea that UCP3 acts as a LCFA anion exporter, but provided no direct evidence to support such a mechanism. Thus it is critical to conduct LCFA export studies with appropriate controls, in isolated mitochondria from UCP3 overexpressed and ablated mice to answer this question. Briefly, mitochondria should be loaded with labeled palmitate while blocking mitochondrial metabolism and incubating for increasing periods of time. Mitochondria should then be washed, centrifuged and resuspended to assess the level of radioactivity remaining in the mitochondria. If present, UCP3 export capacity could be emphasized by fasting UCP3 overexpressing mice. These experiments should provide some insight as to whether UCP3 is capable of LCFA anion export. If successful, these experiments should definitely be pursued in human skeletal mitochondria of lean, obese and diabetic subjects to assess the impact of the pathway on skeletal muscle and whole body fat oxidation and insulin resistance.

6.7 Conclusions

In summary, this thesis provides new information regarding the status of LCFA transport across the mitochondrial membranes in rodent and human skeletal muscle. Firstly, the controversy regarding the CPT system continues as common exercise metabolites failed to override M-CoA inhibition of CPTI activity in human and rat skeletal muscle *in vitro*. However, the identification of FAT/CD36 in highly purified human skeletal mitochondria and the demonstration that FAT/CD36 is essential for

mitochondrial LCFA transport may provide answers to the CPT system controversy. Although FAT/CD36 was only examined in resting conditions in this thesis, evidence in rat skeletal muscle suggests that FAT/CD36 appears to offer an additional level of regulation for LCFA transport across the mitochondrial membranes during exercise. Lastly, this thesis demonstrates for the first time that a constitutive physiological two fold overexpression of UCP3 content in mouse skeletal muscle significantly increases LCFA uptake and oxidation capacity in this tissue. This serves as a reminder of the complexity of skeletal muscle LCFA metabolism and oxidation.

REFERENCES

1. Luiken JJ, Glatz JF, Bonen A: Fatty acid transport proteins facilitate fatty acid uptake in skeletal muscle. *Can J Appl Physiol* 25:333-352, 2000
2. Turcotte LP, Swenberger JR, Tucker MZ, Yee AJ, Trump G, Luiken JJ, Bonen A: Muscle palmitate uptake and binding are saturable and inhibited by antibodies to FABP(PM). *Mol Cell Biochem* 210:53-63, 2000
3. Campbell SE, Tandon NN, Woldegiorgis G, Luiken JJ, Glatz JF, Bonen A: A novel function for fatty acid translocase (FAT)/CD36: involvement in long chain fatty acid transfer into the mitochondria. *J Biol Chem* 279:36235-36241, 2004
4. Luiken JJ, Coort SL, Willems J, Coumans WA, Bonen A, van der Vusse GJ, Glatz JF: Contraction-induced fatty acid translocase/CD36 translocation in rat cardiac myocytes is mediated through AMP-activated protein kinase signaling. *Diabetes* 52:1627-1634, 2003
5. Luiken JJ, Dyck DJ, Han XX, Tandon NN, Arumugam Y, Glatz JF, Bonen A: Insulin induces the translocation of the fatty acid transporter FAT/CD36 to the plasma membrane. *Am J Physiol Endocrinol Metab* 282:E491-495, 2002
6. Dyck DJ, Bonen A: Muscle contraction increases palmitate esterification and oxidation and triacylglycerol oxidation. *Am J Physiol* 275:E888-E896, 1998
7. Langfort J, Ploug T, Ihlemann J, Enevoldsen LH, Stallknecht B, Saldo M, Kjaer M, Holm C, Galbo H: Hormone-sensitive lipase (HSL) expression and regulation in skeletal muscle. *Adv Exp Med Biol* 441:219-228, 1998
8. Watt MJ, Spriet LL: Regulation and role of hormone-sensitive lipase activity in human skeletal muscle. *Proc Nutr Soc* 63:315-322, 2004

9. Kerner J, Hoppel C: Fatty acid import into mitochondria. *Biochim Biophys Acta* 1486:1-17, 2000
10. Stryer L: *Biochemistry*. New York, W. H. Freeman and Company, 1995
11. Kirkwood SP, Munn EA, Brooks GA: Mitochondrial reticulum in limb skeletal muscle. *Am J Physiol (Cell Physiol.)* 251:C395-C402, 1987
12. Kirkwood SP, Packer L, Brooks GA: Effects of endurance training on mitochondrial reticulum in limb skeletal muscle. *Arch Biochem Biophys* 255:80-88, 1987
13. Skulachev VP: Power transmission along biological membranes. *J Membr Biol* 114:97-112, 1990
14. Hoppeler H, Howald H, Conley K, Lindstedt SL, Claassen H, Vock P, Weibel ER: Endurance training in humans: aerobic capacity and structure of skeletal muscle. *J Appl Physiol* 59:320-327, 1985
15. Hoppeler H, Luthi P, Claassen H, Weibel ER, Howald H: The ultrastructure of the normal human skeletal muscle. A morphometric analysis on untrained men, women and well-trained orienteers. *Pflugers Arch* 344:217-232, 1973
16. Howald H, Hoppeler H, Claassen H, Mathieu O, Straub R: Influences of endurance training on the ultrastructural composition of the different muscle fiber types in humans. *Pflugers Arch* 403:369-376, 1985
17. Hoppeler H, Fluck M: Plasticity of skeletal muscle mitochondria: structure and function. *Med Sci Sports Exerc* 35:95-104, 2003
18. Bizeau ME, Willis WT, Hazel JR: Differential responses to endurance training in subsarcolemmal and intermyofibrillar mitochondria. *J Appl Physiol* 85:1279-1284, 1998

19. Cogswell AM, Stevens RJ, Hood DA: Properties of skeletal muscle mitochondria isolated from subsarcolemmal and intermyofibrillar regions. *Am J Physiol* 264:C383-389, 1993
20. Joffe M, Savage N, Isaacs H: Respiratory activities of subsarcolemmal and intermyofibrillar mitochondrial populations isolated from denervated and control rat soleus muscles. *Comp Biochem Physiol B* 76:783-787, 1983
21. Krieger DA, Tate CA, McMillin-Wood J, Booth FW: Populations of rat skeletal muscle mitochondria after exercise and immobilization. *J Appl Physiol* 48:23-28, 1980
22. Palmer JW, Tandler B, Hoppel CL: Biochemical properties of subsarcolemmal and interfibrillar mitochondria isolated from rat cardiac muscle. *J Biol Chem* 252:8731-8739, 1977
23. Goglia F, Lanni A, Duchamp C, Rouanet JL, Barre H: Effect of cold acclimation on oxidative capacity and respiratory properties of liver and muscle mitochondria in ducklings, *Cairina moschata*. *Comp Biochem Physiol B* 106:95-101, 1993
24. Lombardi A, Damon M, Vincent A, Goglia F, Herpin P: Characterisation of oxidative phosphorylation in skeletal muscle mitochondria subpopulations in pig: a study using top-down elasticity analysis. *FEBS Lett* 475:84-88, 2000
25. Jimenez M, Yvon C, Lehr L, Leger B, Keller P, Russell A, Kuhne F, Flandin P, Giacobino JP, Muzzin P: Expression of uncoupling protein-3 in subsarcolemmal and intermyofibrillar mitochondria of various mouse muscle types and its modulation by fasting. *Eur J Biochem* 269:2878-2884, 2002

26. Muller W: Subsarcolemmal mitochondria and capillarization of soleus muscle fibers in young rats subjected to an endurance training. A morphometric study of semithin sections. *Cell Tissue Res* 174:367-389, 1976
27. Kiessling KH, Pilstrom L, Karlsson J, Piehl K: Mitochondrial volume in skeletal muscle from young and old physically untrained and trained healthy men and from alcoholics. *Clin Sci* 44:547-554, 1973
28. Lopez-Mediavilla C, Orfao A, Gonzalez M, Medina JM: Identification by flow cytometry of two distinct rhodamine-123-stained mitochondrial populations in rat liver. *FEBS Lett* 254:115-120, 1989
29. Skulachev VP: Role of uncoupled and non-coupled oxidations in maintenance of safely low levels of oxygen and its one-electron reductants. *Q Rev Biophys* 29:169-202, 1996
30. Fraser F, Corstorphine CG, Zammit VA: Evidence that both the acyl-CoA- and malonyl-CoA binding sites of mitochondrial overt carnitine palmitoyltransferase (CPT I) are exposed on the cytosolic face of the outer membrane. *Biochem Soc Trans* 24:184S, 1996
31. Kashfi K, Cook GA: Proteinase treatment of intact hepatic mitochondria has differential effects on inhibition of carnitine palmitoyltransferase by different inhibitors. *Biochem J* 282 (Pt 3):909-914, 1992
32. Koves TR, Noland RC, Bates AL, Henes ST, Muoio DM, Cortright RN: Subsarcolemmal and Intermyo-fibrillar Mitochondria Play Distinct Roles in Regulating Skeletal Muscle Fatty Acid Metabolism. *Am J Physiol Cell Physiol*, 2005

33. Murthy MS, Pande SV: Malonyl-CoA binding site and the overt carnitine palmitoyltransferase activity reside on the opposite sides of the outer mitochondrial membrane. *Proc Natl Acad Sci U S A* 84:378-382, 1987
34. Pande SV: A mitochondrial carnitine acylcarnitine translocase system. *Proc Natl Acad Sci U S A* 72:883-887, 1975
35. Britton CH, Schultz RA, Zhang B, Esser V, Foster DW, McGarry JD: Human liver mitochondrial carnitine palmitoyltransferase I: characterization of its cDNA and chromosomal localization and partial analysis of the gene. *Proc Natl Acad Sci U S A* 92:1984-1988, 1995
36. Esser V, Brown NF, Cowan AT, Foster DW, McGarry JD: Expression of a cDNA isolated from rat brown adipose tissue and heart identifies the product as the muscle isoform of carnitine palmitoyltransferase I (M-CPT I). M-CPT I is the predominant CPT I isoform expressed in both white (epididymal) and brown adipocytes. *J Biol Chem* 271:6972-6977, 1996
37. McGarry JD, Mills SE, Long CS, Foster DW: Observations on the affinity for carnitine, and malonyl-CoA sensitivity, of carnitine palmitoyltransferase I in animal and human tissues. Demonstration of the presence of malonyl-CoA in non-hepatic tissues of the rat. *Biochem J* 214:21-28, 1983
38. McGarry JD, Brown NF: The mitochondrial carnitine palmitoyltransferase system. From concept to molecular analysis. *Eur J Biochem* 244:1-14, 1997
39. Woeltje KF, Esser V, Weis BC, Sen A, Cox WF, McPhaul MJ, Slaughter CA, Foster DW, McGarry JD: Cloning, sequencing, and expression of a cDNA encoding rat liver mitochondrial carnitine palmitoyltransferase II. *J Biol Chem* 265:10720-10725, 1990

40. Finocchiaro G, Taroni F, Rocchi M, Martin AL, Colombo I, Tarelli GT, DiDonato S: cDNA cloning, sequence analysis, and chromosomal localization of the gene for human carnitine palmitoyltransferase. *Proc Natl Acad Sci U S A* 88:661-665, 1991
41. McGarry D: Current concepts in carnitine research, Boca Raton: CRC Press, 1992
42. McGarry JD, Woeltje KF, Kuwajima M, Foster DW: Regulation of ketogenesis and the renaissance of carnitine palmitoyltransferase. *Diabetes Metab Rev* 5:271-284, 1989
43. Brown NF, Esser V, Foster DW, McGarry JD: Expression of a cDNA for rat liver carnitine palmitoyltransferase I in yeast establishes that catalytic activity and malonyl-CoA sensitivity reside in a single polypeptide. *J Biol Chem* 269:26438-26442, 1994
44. Yamazaki N, Shinohara Y, Shima A, Terada H: High expression of a novel carnitine palmitoyltransferase I like protein in rat brown adipose tissue and heart: isolation and characterization of its cDNA clone. *FEBS Lett* 363:41-45, 1995
45. Britton CH, Mackey DW, Esser V, Foster DW, Burns DK, Yarnall DP, Froguel P, McGarry JD: Fine chromosome mapping of the genes for human liver and muscle carnitine palmitoyltransferase I (CPT1A and CPT1B). *Genomics* 40:209-211, 1997
46. Yamazaki N, Shinohara Y, Shima A, Yamanaka Y, Terada H: Isolation and characterization of cDNA and genomic clones encoding human muscle type carnitine palmitoyltransferase I. *Biochim Biophys Acta* 1307:157-161, 1996
47. Fraser F, Corstorphine CG, Zammit VA: Topology of carnitine palmitoyltransferase I in the mitochondrial outer membrane. *Biochem J* 323 (Pt 3):711-718, 1997
48. Zammit VA, Corstorphine CG, Kolodziej MP, Fraser F: Lipid molecular order in liver mitochondrial outer membranes, and sensitivity of carnitine palmitoyltransferase I to malonyl-CoA. *Lipids* 33:371-376, 1998

49. Zammit VA: Carnitine acyltransferases: functional significance of subcellular distribution and membrane topology. *Prog Lipid Res* 38:199-224, 1999
50. Nic a' Bhaird N, Kumaravel G, Gandour RD, Krueger MJ, Ramsay RR: Comparison of the active sites of the purified carnitine acyltransferases from peroxisomes and mitochondria by using a reaction-intermediate analogue. *Biochem J* 294 (Pt 3):645-651, 1993
51. Woeltje KF, Esser V, Weis BC, Cox WF, Schroeder JG, Liao ST, Foster DW, McGarry JD: Inter-tissue and inter-species characteristics of the mitochondrial carnitine palmitoyltransferase enzyme system. *J Biol Chem* 265:10714-10719, 1990
52. McGarry JD, Brown NF, Inthanousay PP, Park DI, Cook BA, Foster DW: Insights into the topography of mitochondrial carnitine palmitoyltransferase gained from the use of proteases. *Prog Clin Biol Res* 375:47-61, 1992
53. Indiveri C, Tonazzi A, Palmieri F: Identification and purification of the carnitine carrier from rat liver mitochondria. *Biochim Biophys Acta* 1020:81-86, 1990
54. Palmieri F, Bisaccia F, Capobianco L, Dolce V, Fiermonte G, Iacobazzi V, Indiveri C, Palmieri L: Mitochondrial metabolite transporters. *Biochim Biophys Acta* 1275:127-132, 1996
55. A'Bhaird NN, Ramsay RR: Malonyl-CoA inhibition of peroxisomal carnitine octanoyltransferase. *Biochem J* 286 (Pt 2):637-640, 1992
56. Zierz S, Engel AG: Different sites of inhibition of carnitine palmitoyltransferase by malonyl-CoA, and by acetyl-CoA and CoA, in human skeletal muscle. *Biochem J* 245:205-209, 1987

57. Shi J, Zhu H, Arvidson DN, Cregg JM, Woldegiorgis G: Deletion of the conserved first 18 N-terminal amino acid residues in rat liver carnitine palmitoyltransferase I abolishes malonyl-CoA sensitivity and binding. *Biochemistry* 37:11033-11038, 1998
58. Shi J, Zhu H, Arvidson DN, Woldegiorgis G: A single amino acid change (substitution of glutamate 3 with alanine) in the N-terminal region of rat liver carnitine palmitoyltransferase I abolishes malonyl-CoA inhibition and high affinity binding. *J Biol Chem* 274:9421-9426, 1999
59. Mills SE, Foster DW, McGarry JD: Effects of pH on the interaction of substrates and malonyl-CoA with mitochondrial carnitine palmitoyltransferase I. *Biochem J* 219:601-608, 1984
60. Stephens TW, Cook GA, Harris RA: Effect of pH on malonyl-CoA inhibition of carnitine palmitoyltransferase I. *Biochem J* 212:521-524, 1983
61. Hardie DG: Regulation of fatty acid synthesis via phosphorylation of acetyl-CoA carboxylase. *Prog Lipid Res* 28:117-146, 1989
62. Winder WW, Arogyasami J, Barton RJ, Elayan IM, Vehrs PR: Muscle malonyl-CoA decreases during exercise. *J Appl Physiol* 67:2230-2233, 1989
63. McGarry JD: Malonyl-CoA and carnitine palmitoyltransferase I: an expanding partnership. *Biochem Soc Trans* 23:481-485, 1995
64. Kim JY, Koves TR, Yu GS, Gulick T, Cortright RN, Dohm GL, Muoio DM: Evidence of a malonyl-CoA-insensitive carnitine palmitoyltransferase I activity in red skeletal muscle. *Am J Physiol Endocrinol Metab* 282:E1014-1022, 2002

65. Dean D, Daugaard JR, Young ME, Saha A, Vavvas D, Asp S, Kiens B, Kim KH, Witters L, Richter EA, Ruderman N: Exercise diminishes the activity of acetyl-CoA carboxylase in human muscle. *Diabetes* 49:1295-1300, 2000
66. Odland LM, Heigenhauser GJ, Lopaschuk GD, Spriet LL: Human skeletal muscle malonyl-CoA at rest and during prolonged submaximal exercise. *Am J Physiol* 270:E541-544, 1996
67. Odland LM, Howlett RA, Heigenhauser GJ, Hultman E, Spriet LL: Skeletal muscle malonyl-CoA content at the onset of exercise at varying power outputs in humans. *Am J Physiol* 274:E1080-1085, 1998
68. Roepstorff C, Halberg N, Hillig T, Saha AK, Ruderman NB, Wojtaszewski JF, Richter EA, Kiens B: Malonyl-CoA and carnitine in regulation of fat oxidation in human skeletal muscle during exercise. *Am J Physiol Endocrinol Metab* 288:E133-142, 2005
69. Starritt EC, Howlett RA, Heigenhauser GJ, Spriet LL: Sensitivity of CPT I to malonyl-CoA in trained and untrained human skeletal muscle. *Am J Physiol Endocrinol Metab* 278:E462-468, 2000
70. Sahlin K, Harris RC, Ny Lind B, Hultman E: Lactate content and pH in muscle obtained after dynamic exercise. *Pflugers Arch* 367:143-149, 1976
71. Talle MA, Rao PE, Westberg E, Allegar N, Makowski M, Mittler RS, Goldstein G: Patterns of antigenic expression on human monocytes as defined by monoclonal antibodies. *Cell Immunol* 78:83-99, 1983
72. Abumrad NA, el-Maghrabi MR, Amri EZ, Lopez E, Grimaldi PA: Cloning of a rat adipocyte membrane protein implicated in binding or transport of long-chain fatty acids

that is induced during preadipocyte differentiation. Homology with human CD36. *J Biol Chem* 268:17665-17668, 1993

73. Tandon NN, Kralisz U, Jamieson GA: Identification of glycoprotein IV (CD36) as a primary receptor for platelet-collagen adhesion. *J Biol Chem* 264:7576-7583, 1989

74. Dawson DW, Pearce SF, Zhong R, Silverstein RL, Frazier WA, Bouck NP: CD36 mediates the In vitro inhibitory effects of thrombospondin-1 on endothelial cells. *J Cell Biol* 138:707-717, 1997

75. Endemann G, Stanton LW, Madden KS, Bryant CM, White RT, Protter AA: CD36 is a receptor for oxidized low density lipoprotein. *J Biol Chem* 268:11811-11816, 1993

76. Silverstein RL, Asch AS, Nachman RL: Glycoprotein IV mediates thrombospondin-dependent platelet-monocyte and platelet-U937 cell adhesion. *J Clin Invest* 84:546-552, 1989

77. Greenwalt DE, Watt KW, So OY, Jiwani N: PAS IV, an integral membrane protein of mammary epithelial cells, is related to platelet and endothelial cell CD36 (GP IV). *Biochemistry* 29:7054-7059, 1990

78. Knowles DM, 2nd, Tolidjian B, Marboe C, D'Agati V, Grimes M, Chess L: Monoclonal anti-human monocyte antibodies OKM1 and OKM5 possess distinctive tissue distributions including differential reactivity with vascular endothelium. *J Immunol* 132:2170-2173, 1984

79. Albert ML, Pearce SF, Francisco LM, Sauter B, Roy P, Silverstein RL, Bhardwaj N: Immature dendritic cells phagocytose apoptotic cells via alphavbeta5 and CD36, and cross-present antigens to cytotoxic T lymphocytes. *J Exp Med* 188:1359-1368, 1998

80. Ryeom SW, Sparrow JR, Silverstein RL: CD36 participates in the phagocytosis of rod outer segments by retinal pigment epithelium. *J Cell Sci* 109 (Pt 2):387-395, 1996
81. Luiken JJ, Schaap FG, van Nieuwenhoven FA, van der Vusse GJ, Bonen A, Glatz JF: Cellular fatty acid transport in heart and skeletal muscle as facilitated by proteins. *Lipids* 34 Suppl:S169-175, 1999
82. Bonen A, Luiken JJ, Liu S, Dyck DJ, Kiens B, Kristiansen S, Turcotte LP, Van Der Vusse GJ, Glatz JF: Palmitate transport and fatty acid transporters in red and white muscles. *Am J Physiol* 275:E471-478, 1998
83. Van Nieuwenhoven FA, Verstijnen CP, Abumrad NA, Willemsen PH, Van Eys GJ, Van der Vusse GJ, Glatz JF: Putative membrane fatty acid translocase and cytoplasmic fatty acid-binding protein are co-expressed in rat heart and skeletal muscles. *Biochem Biophys Res Commun* 207:747-752, 1995
84. Van Nieuwenhoven FA, Willemsen PH, Van der Vusse GJ, Glatz JF: Co-expression in rat heart and skeletal muscle of four genes coding for proteins implicated in long-chain fatty acid uptake. *Int J Biochem Cell Biol* 31:489-498, 1999
85. Pearce SF, Wu J, Silverstein RL: A carboxyl terminal truncation mutant of CD36 is secreted and binds thrombospondin: evidence for a single transmembrane domain. *Blood* 84:384-389, 1994
86. Tao N, Wagner SJ, Lublin DM: CD36 is palmitoylated on both N- and C-terminal cytoplasmic tails. *J Biol Chem* 271:22315-22320, 1996
87. Jochen A, Hays J: Purification of the major substrate for palmitoylation in rat adipocytes: N-terminal homology with CD36 and evidence for cell surface acylation. *J Lipid Res* 34:1783-1792, 1993

88. Crombie R, Silverstein R: Lysosomal integral membrane protein II binds thrombospondin-1. Structure-function homology with the cell adhesion molecule CD36 defines a conserved recognition motif. *J Biol Chem* 273:4855-4863, 1998
89. Febbraio M, Hajjar DP, Silverstein RL: CD36: a class B scavenger receptor involved in angiogenesis, atherosclerosis, inflammation, and lipid metabolism. *J Clin Invest* 108:785-791, 2001
90. Duttaroy AK, Spener F: Cellular proteins and their fatty acids in health and disease. Weinheim; Cambridge, Wiley-VCH, 2003
91. Sorrentino D, Stump D, Potter BJ, Robinson RB, White R, Kiang CL, Berk PD: Oleate uptake by cardiac myocytes is carrier mediated and involves a 40-kD plasma membrane fatty acid binding protein similar to that in liver, adipose tissue, and gut. *J Clin Invest* 82:928-935, 1988
92. Stremmel W: Fatty acid uptake by isolated rat heart myocytes represents a carrier-mediated transport process. *J Clin Invest* 81:844-852, 1988
93. Turcotte LP, Kiens B, Richter EA: Saturation kinetics of palmitate uptake in perfused skeletal muscle. *FEBS Lett* 279:327-329, 1991
94. Luiken JJ, Turcotte LP, Bonen A: Protein-mediated palmitate uptake and expression of fatty acid transport proteins in heart giant vesicles. *J Lipid Res* 40:1007-1016, 1999
95. Van Nieuwenhoven FA, Luiken JJ, De Jong YF, Grimaldi PA, Van der Vusse GJ, Glatz JF: Stable transfection of fatty acid translocase (CD36) in a rat heart muscle cell line (H9c2). *J Lipid Res* 39:2039-2047, 1998
96. Ibrahimi A, Bonen A, Blinn WD, Hajri T, Li X, Zhong K, Cameron R, Abumrad NA: Muscle-specific overexpression of FAT/CD36 enhances fatty acid oxidation by

- contracting muscle, reduces plasma triglycerides and fatty acids, and increases plasma glucose and insulin. *J Biol Chem* 274:26761-26766, 1999
97. Febbraio M, Guy E, Coburn C, Knapp FF, Jr., Beets AL, Abumrad NA, Silverstein RL: The impact of overexpression and deficiency of fatty acid translocase (FAT)/CD36. *Mol Cell Biochem* 239:193-197, 2002
98. Bonen A, Luiken JJ, Arumugam Y, Glatz JF, Tandon NN: Acute regulation of fatty acid uptake involves the cellular redistribution of fatty acid translocase. *J Biol Chem* 275:14501-14508, 2000
99. Luiken JJ, Koonen DP, Willems J, Zorzano A, Becker C, Fischer Y, Tandon NN, Van Der Vusse GJ, Bonen A, Glatz JF: Insulin stimulates long-chain fatty acid utilization by rat cardiac myocytes through cellular redistribution of FAT/CD36. *Diabetes* 51:3113-3119, 2002
100. James G, Olson EN: Fatty acylated proteins as components of intracellular signaling pathways. *Biochemistry* 29:2623-2634, 1990
101. Vistisen B, Roepstorff K, Roepstorff C, Bonen A, van Deurs B, Kiens B: Sarcolemmal FAT/CD36 in human skeletal muscle colocalizes with caveolin-3 and is more abundant in type 1 than in type 2 fibers. *J Lipid Res* 45:603-609, 2004
102. Lisanti MP, Scherer PE, Vidugiriene J, Tang Z, Hermanowski-Vosatka A, Tu YH, Cook RF, Sargiacomo M: Characterization of caveolin-rich membrane domains isolated from an endothelial-rich source: implications for human disease. *J Cell Biol* 126:111-126, 1994
103. Brand MD, Chien LF, Ainscow EK, Rolfe DF, Porter RK: The causes and functions of mitochondrial proton leak. *Biochim Biophys Acta* 1187:132-139, 1994

104. Rolfe DF, Brand MD: Contribution of mitochondrial proton leak to skeletal muscle respiration and to standard metabolic rate. *Am J Physiol* 271:C1380-1389, 1996
105. Brand MD: Regulation analysis of energy metabolism. *J Exp Biol* 200:193-202, 1997
106. Bouillaud F, Raimbault S, Ricquier D: The gene for rat uncoupling protein: complete sequence, structure of primary transcript and evolutionary relationship between exons. *Biochem Biophys Res Commun* 157:783-792, 1988
107. Kozak LP, Britton JH, Kozak UC, Wells JM: The mitochondrial uncoupling protein gene. Correlation of exon structure to transmembrane domains. *J Biol Chem* 263:12274-12277, 1988
108. Nicholls DG, Locke RM: Thermogenic mechanisms in brown fat. *Physiol Rev* 64:1-64, 1984
109. Seldin MF, Mott D, Bhat D, Petro A, Kuhn CM, Kingsmore SF, Bogardus C, Opara E, Feinglos MN, Surwit RS: Glycogen synthase: a putative locus for diet-induced hyperglycemia. *J Clin Invest* 94:269-276, 1994
110. Solanes G, Vidal-Puig A, Grujic D, Flier JS, Lowell BB: The human uncoupling protein-3 gene. Genomic structure, chromosomal localization, and genetic basis for short and long form transcripts. *J Biol Chem* 272:25433-25436, 1997
111. Warden CH, Fisler JS, Pace MJ, Svenson KL, Lusis AJ: Coincidence of genetic loci for plasma cholesterol levels and obesity in a multifactorial mouse model. *J Clin Invest* 92:773-779, 1993

112. Boss O, Samec S, Paoloni-Giacobino A, Rossier C, Dulloo A, Seydoux J, Muzzin P, Giacobino JP: Uncoupling protein-3: a new member of the mitochondrial carrier family with tissue-specific expression. *FEBS Lett* 408:39-42, 1997
113. Fleury C, Neverova M, Collins S, Raimbault S, Champigny O, Levi-Meyrueis C, Bouillaud F, Seldin MF, Surwit RS, Ricquier D, Warden CH: Uncoupling protein-2: a novel gene linked to obesity and hyperinsulinemia. *Nat Genet* 15:269-272, 1997
114. Gimeno RE, Dembski M, Weng X, Deng N, Shyjan AW, Gimeno CJ, Iris F, Ellis SJ, Woolf EA, Tartaglia LA: Cloning and characterization of an uncoupling protein homolog: a potential molecular mediator of human thermogenesis. *Diabetes* 46:900-906, 1997
115. Gong DW, He Y, Karas M, Reitman M: Uncoupling protein-3 is a mediator of thermogenesis regulated by thyroid hormone, beta3-adrenergic agonists, and leptin. *J Biol Chem* 272:24129-24132, 1997
116. Vidal-Puig A, Solanes G, Grujic D, Flier JS, Lowell BB: UCP3: an uncoupling protein homologue expressed preferentially and abundantly in skeletal muscle and brown adipose tissue. *Biochem Biophys Res Commun* 235:79-82, 1997
117. Cadenas S, Echtay KS, Harper JA, Jekabsons MB, Buckingham JA, Grau E, Abuin A, Chapman H, Clapham JC, Brand MD: The basal proton conductance of skeletal muscle mitochondria from transgenic mice overexpressing or lacking uncoupling protein-3. *J Biol Chem* 277:2773-2778, 2002
118. Gong DW, Monemdjou S, Gavrilova O, Leon LR, Marcus-Samuels B, Chou CJ, Everett C, Kozak LP, Li C, Deng C, Harper ME, Reitman ML: Lack of obesity and

- normal response to fasting and thyroid hormone in mice lacking uncoupling protein-3. *J Biol Chem* 275:16251-16257, 2000
119. Vidal-Puig AJ, Grujic D, Zhang CY, Hagen T, Boss O, Ido Y, Szczepanik A, Wade J, Mootha V, Cortright R, Muoio DM, Lowell BB: Energy metabolism in uncoupling protein 3 gene knockout mice. *J Biol Chem* 275:16258-16266, 2000
120. Horvath B, Spies C, Warden CH, Diano S, Horvath TL: Uncoupling protein 2 in primary pain and temperature afferents of the spinal cord. *Brain Res* 955:260-263, 2002
121. Krauss S, Zhang CY, Lowell BB: A significant portion of mitochondrial proton leak in intact thymocytes depends on expression of UCP2. *Proc Natl Acad Sci U S A* 99:118-122, 2002
122. Pecqueur C, Alves-Guerra MC, Gelly C, Levi-Meyrueis C, Couplan E, Collins S, Ricquier D, Bouillaud F, Miroux B: Uncoupling protein 2, in vivo distribution, induction upon oxidative stress, and evidence for translational regulation. *J Biol Chem* 276:8705-8712, 2001
123. Zhang CY, Baffy G, Perret P, Krauss S, Peroni O, Grujic D, Hagen T, Vidal-Puig AJ, Boss O, Kim YB, Zheng XX, Wheeler MB, Shulman GI, Chan CB, Lowell BB: Uncoupling protein-2 negatively regulates insulin secretion and is a major link between obesity, beta cell dysfunction, and type 2 diabetes. *Cell* 105:745-755, 2001
124. Hagen T, Zhang CY, Vianna CR, Lowell BB: Uncoupling proteins 1 and 3 are regulated differently. *Biochemistry* 39:5845-5851, 2000
125. Hinz W, Faller B, Gruninger S, Gazzotti P, Chiesi M: Recombinant human uncoupling protein-3 increases thermogenesis in yeast cells. *FEBS Lett* 448:57-61, 1999

126. Hinz W, Gruninger S, De Pover A, Chiesi M: Properties of the human long and short isoforms of the uncoupling protein-3 expressed in yeast cells. *FEBS Lett* 462:411-415, 1999
127. Jaburek M, Varecha M, Gimeno RE, Dembski M, Jezek P, Zhang M, Burn P, Tartaglia LA, Garlid KD: Transport function and regulation of mitochondrial uncoupling proteins 2 and 3. *J Biol Chem* 274:26003-26007, 1999
128. Matthias A, Ohlson KB, Fredriksson JM, Jacobsson A, Nedergaard J, Cannon B: Thermogenic responses in brown fat cells are fully UCP1-dependent. UCP2 or UCP3 do not substitute for UCP1 in adrenergically or fatty acid-induced thermogenesis. *J Biol Chem* 275:25073-25081, 2000
129. Harper JA, Stuart JA, Jekabsons MB, Roussel D, Brindle KM, Dickinson K, Jones RB, Brand MD: Artfactual uncoupling by uncoupling protein 3 in yeast mitochondria at the concentrations found in mouse and rat skeletal-muscle mitochondria. *Biochem J* 361:49-56, 2002
130. Stuart JA, Harper JA, Brindle KM, Jekabsons MB, Brand MD: A mitochondrial uncoupling artifact can be caused by expression of uncoupling protein 1 in yeast. *Biochem J* 356:779-789, 2001
131. Bezaire V, Hofmann W, Kramer JK, Kozak LP, Harper ME: Effects of fasting on muscle mitochondrial energetics and fatty acid metabolism in Ucp3(-/-) and wild-type mice. *Am J Physiol Endocrinol Metab* 281:E975-982, 2001
132. Clapham JC, Arch JR, Chapman H, Haynes A, Lister C, Moore GB, Piercy V, Carter SA, Lehner I, Smith SA, Beeley LJ, Godden RJ, Herrity N, Skehel M, Changani KK, Hockings PD, Reid DG, Squires SM, Hatcher J, Trail B, Latcham J, Rastan S,

- Harper AJ, Cadenas S, Buckingham JA, Brand MD, Abuin A: Mice overexpressing human uncoupling protein-3 in skeletal muscle are hyperphagic and lean. *Nature* 406:415-418, 2000
133. Boss O, Samec S, Kuhne F, Bijlenga P, Assimacopoulos-Jeannet F, Seydoux J, Giacobino JP, Muzzin P: Uncoupling protein-3 expression in rodent skeletal muscle is modulated by food intake but not by changes in environmental temperature. *J Biol Chem* 273:5-8, 1998
134. Weigle DS, Selfridge LE, Schwartz MW, Seeley RJ, Cummings DE, Havel PJ, Kuijper JL, BeltrandelRio H: Elevated free fatty acids induce uncoupling protein 3 expression in muscle: a potential explanation for the effect of fasting. *Diabetes* 47:298-302, 1998
135. Cadenas S, Buckingham JA, Samec S, Seydoux J, Din N, Dulloo AG, Brand MD: UCP2 and UCP3 rise in starved rat skeletal muscle but mitochondrial proton conductance is unchanged. *FEBS Lett* 462:257-260, 1999
136. Powers SK, Lennon SL: Analysis of cellular responses to free radicals: focus on exercise and skeletal muscle. *Proc Nutr Soc* 58:1025-1033, 1999
137. Arsenijevic D, Onuma H, Pecqueur C, Raimbault S, Manning BS, Miroux B, Couplan E, Alves-Guerra MC, Gubern M, Surwit R, Bouillaud F, Richard D, Collins S, Ricquier D: Disruption of the uncoupling protein-2 gene in mice reveals a role in immunity and reactive oxygen species production. *Nat Genet* 26:435-439, 2000
138. Brand MD, Pamplona R, Portero-Otin M, Requena JR, Roebuck SJ, Buckingham JA, Clapham JC, Cadenas S: Oxidative damage and phospholipid fatty acyl composition

in skeletal muscle mitochondria from mice underexpressing or overexpressing uncoupling protein 3. *Biochem J* 368:597-603, 2002

139. Echtay KS, Esteves TC, Pakay JL, Jekabsons MB, Lambert AJ, Portero-Otin M, Pamplona R, Vidal-Puig AJ, Wang S, Roebuck SJ, Brand MD: A signalling role for 4-hydroxy-2-nonenal in regulation of mitochondrial uncoupling. *Embo J* 22:4103-4110, 2003

140. Couplan E, del Mar Gonzalez-Barroso M, Alves-Guerra MC, Ricquier D, Goubern M, Bouillaud F: No evidence for a basal, retinoic, or superoxide-induced uncoupling activity of the uncoupling protein 2 present in spleen or lung mitochondria. *J Biol Chem* 277:26268-26275, 2002

141. Samec S, Seydoux J, Dulloo AG: Role of UCP homologues in skeletal muscles and brown adipose tissue: mediators of thermogenesis or regulators of lipids as fuel substrate? *Faseb J* 12:715-724, 1998

142. Schrauwen P, Hoppeler H, Billeter R, Bakker AH, Pendergast DR: Fiber type dependent upregulation of human skeletal muscle UCP2 and UCP3 mRNA expression by high-fat diet. *Int J Obes Relat Metab Disord* 25:449-456, 2001

143. Tunstall RJ, Mehan KA, Hargreaves M, Spriet LL, Cameron-Smith D: Fasting activates the gene expression of UCP3 independent of genes necessary for lipid transport and oxidation in skeletal muscle. *Biochem Biophys Res Commun* 294:301-308, 2002

144. Cortright RN, Zheng D, Jones JP, Fluckey JD, DiCarlo SE, Grujic D, Lowell BB, Dohm GL: Regulation of skeletal muscle UCP-2 and UCP-3 gene expression by exercise and denervation. *Am J Physiol* 276:E217-221, 1999

145. Pilegaard H, Ordway GA, Saltin B, Neufer PD: Transcriptional regulation of gene expression in human skeletal muscle during recovery from exercise. *Am J Physiol Endocrinol Metab* 279:E806-814, 2000
146. Tsuboyama-Kasaoka N, Tsunoda N, Maruyama K, Takahashi M, Kim H, Ikemoto S, Ezaki O: Up-regulation of uncoupling protein 3 (UCP3) mRNA by exercise training and down-regulation of UCP3 by denervation in skeletal muscle. *Biochem Biophys Res Commun* 247:498-503, 1998
147. Zhou M, Bao-Zhen L, Coughlin S, Vallega G, Pilch PF: UCP-3 expression in skeletal muscle: effects of exercise, hypoxia, and AMP-activated protein kinase. *Am J Physiol* 279:E622-E629, 2000
148. Schrauwen P, Hesselink MK, Vaartjes I, Kornips E, Saris WH, Giacobino JP, Russell A: Effect of acute exercise on uncoupling protein 3 is a fat metabolism-mediated effect. *Am J Physiol Endocrinol Metab* 282:E11-17, 2002
149. Schrauwen P, Saris WH, Hesselink MK: An alternative function for human uncoupling protein 3: protection of mitochondria against accumulation of nonesterified fatty acids inside the mitochondrial matrix. *Faseb J* 15:2497-2502, 2001
150. Schrauwen P, Schaart G, Saris WH, Slieker LJ, Glatz JF, Vidal H, Blaak EE: The effect of weight reduction on skeletal muscle UCP2 and UCP3 mRNA expression and UCP3 protein content in Type II diabetic subjects. *Diabetologia* 43:1408-1416, 2000
151. Nagase I, Yoshida S, Canas X, Irie Y, Kimura K, Yoshida T, Saito M: Up-regulation of uncoupling protein 3 by thyroid hormone, peroxisome proliferator-activated receptor ligands and 9-cis retinoic acid in L6 myotubes. *FEBS Lett* 461:319-322, 1999

152. Argyropoulos G, Brown AM, Willi SM, Zhu J, He Y, Reitman M, Gevaio SM, Spruill I, Garvey WT: Effects of mutations in the human uncoupling protein 3 gene on the respiratory quotient and fat oxidation in severe obesity and type 2 diabetes. *J Clin Invest* 102:1345-1351, 1998
153. Otabe S, Clement K, Dubois S, Lepretre F, Pelloux V, Leibel R, Chung W, Boutin P, Guy-Grand B, Froguel P, Vasseur F: Mutation screening and association studies of the human uncoupling protein 3 gene in normoglycemic and diabetic morbidly obese patients. *Diabetes* 48:206-208, 1999
154. Son C, Hosoda K, Ishihara K, Bevilacqua L, Masuzaki H, Fushiki T, Harper ME, Nakao K: Reduction of diet-induced obesity in transgenic mice overexpressing uncoupling protein 3 in skeletal muscle. *Diabetologia* 47:47-54, 2004
155. Wang S, Subramaniam A, Cawthorne MA, Clapham JC: Increased fatty acid oxidation in transgenic mice overexpressing UCP3 in skeletal muscle. *Diabetes Obes Metab* 5:295-301, 2003
156. Himms-Hagen J, Harper ME: Physiological role of UCP3 may be export of fatty acids from mitochondria when fatty acid oxidation predominates: an hypothesis. *Exp Biol Med (Maywood)* 226:78-84, 2001
157. Alexson SE, Nedergaard J, Cannon B: Inhibition of acetyl-carnitine oxidation in rat brown-adipose-tissue mitochondria by erucoyl-carnitine is due to sequestration of CoA. *Biochim Biophys Acta* 834:149-158, 1985
158. Moore GB, Himms-Hagen J, Harper ME, Clapham JC: Overexpression of UCP-3 in skeletal muscle of mice results in increased expression of mitochondrial thioesterase mRNA. *Biochem Biophys Res Commun* 283:785-790, 2001

159. Stavinoha MA, Rayspellicy JW, Hart-Sailors ML, Mersmann HJ, Bray MS, Young ME: Diurnal variations in the responsiveness of cardiac and skeletal muscle to fatty acids. *Am J Physiol Endocrinol Metab* 287:E878-887, 2004
160. Moreno M, Lombardi A, De Lange P, Silvestri E, Ragni M, Lanni A, Goglia F: Fasting, lipid metabolism, and triiodothyronine in rat gastrocnemius muscle: interrelated roles of uncoupling protein 3, mitochondrial thioesterase, and coenzyme Q. *Faseb J* 17:1112-1114, 2003
161. Nedergaard J, Cannon B: The 'novel' 'uncoupling' proteins UCP2 and UCP3: what do they really do? Pros and cons for suggested functions. *Exp Physiol* 88:65-84, 2003
162. Saggerson ED, Carpenter CA: Effects of fasting and malonyl CoA on the kinetics of carnitine palmitoyltransferase and carnitine octanoyltransferase in intact rat liver mitochondria. *FEBS Lett* 132:166-168, 1981
163. Winder WW, Arogyasami J, Elayan IM, Cartmill D: Time course of exercise-induced decline in malonyl-CoA in different muscle types. *Am J Physiol* 259:E266-271, 1990
164. Odland LM, Heigenhauser GJ, Wong D, Hollidge-Horvat MG, Spriet LL: Effects of increased fat availability on fat-carbohydrate interaction during prolonged exercise in men. *Am J Physiol* 274:R894-902, 1998
165. Moyes CD, Hood DA: Origins and consequences of mitochondrial variation in vertebrate muscle. *Annu Rev Physiol* 65:177-201, 2003
166. Bereiter-Hahn J: Behavior of mitochondria in the living cell. *Int Rev Cytol* 122:1-63, 1990

167. Schmidt I, Herpin P: Postnatal changes in mitochondrial protein mass and respiration in skeletal muscle from the newborn pig. *Comp Biochem Physiol B Biochem Mol Biol* 118:639-647, 1997
168. Bergstrom J: Percutaneous needle biopsy of skeletal muscle in physiological and clinical research. *Scand J Clin Lab Invest* 35:609-616, 1975
169. Srere PA: Citrate synthase. In: *Methods in Enzymology*. Edited by Lowenstein JM. New York, Academic, 1969
170. Howlett RA, Parolin ML, Dyck DJ, Hultman E, Jones NL, Heigenhauser GJ, Spriet LL: Regulation of skeletal muscle glycogen phosphorylase and PDH at varying exercise power outputs. *Am J Physiol* 275:R418-425, 1998
171. Dudley GA, Tullson PC, Terjung RL: Influence of mitochondrial content on the sensitivity of respiratory control. *J Biol Chem* 262:9109-9114, 1987
172. Kushmerick MJ, Meyer RA: Chemical changes in rat leg muscle by phosphorus nuclear magnetic resonance. *Am J Physiol* 248:C542-549, 1985
173. Wibom R, Hultman E: ATP production rate in mitochondria isolated from microsamples of human muscle. *Am J Physiol* 259:E204-209, 1990
174. Rasmussen UF, Rasmussen HN, Krstrup P, Quistorff B, Saltin B, Bangsbo J: Aerobic metabolism of human quadriceps muscle: in vivo data parallel measurements on isolated mitochondria. *Am J Physiol Endocrinol Metab* 280:E301-307, 2001
175. Gollnick PD: Metabolic regulation in skeletal muscle: influence of endurance training as exerted by mitochondrial protein concentration. *Acta Physiol Scand Suppl* 556:53-66, 1986

176. Holloszy JO, Coyle EF: Adaptations of skeletal muscle to endurance exercise and their metabolic consequences. *J Appl Physiol* 56:831-838, 1984
177. Kraegen EW, Cooney GJ, Ye J, Thompson AL: Triglycerides, fatty acids and insulin resistance--hyperinsulinemia. *Exp Clin Endocrinol Diabetes* 109:S516-526, 2001
178. McGarry JD: What if Minkowski had been ageusic? An alternative angle on diabetes. *Science* 258:766-770, 1992
179. Alam N, Saggerson ED: Malonyl-CoA and the regulation of fatty acid oxidation in soleus muscle. *Biochem J* 334:233-241, 1998
180. Berthon PM, Howlett RA, Heigenhauser GJ, Spriet LL: Human skeletal muscle carnitine palmitoyltransferase I activity determined in isolated intact mitochondria. *J Appl Physiol* 85:148-153, 1998
181. Bezaire V, Heigenhauser GJ, Spriet LL: Regulation of CPT I activity in intermyofibrillar and subsarcolemmal mitochondria from human and rat skeletal muscle. *Am J Physiol Endocrinol Metab* 286:E85-91, 2004
182. Harmon CM, Abumrad NA: Binding of sulfosuccinimidyl fatty acids to adipocyte membrane proteins: isolation and amino-terminal sequence of an 88-kD protein implicated in transport of long-chain fatty acids. *J Membr Biol* 133:43-49, 1993
183. Coort SL, Willems J, Coumans WA, van der Vusse GJ, Bonen A, Glatz JF, Luiken JJ: Sulfo-N-succinimidyl esters of long chain fatty acids specifically inhibit fatty acid translocase (FAT/CD36)-mediated cellular fatty acid uptake. *Mol Cell Biochem* 239:213-219, 2002

184. Tanaka T, Kawamura K: Isolation of myocardial membrane long-chain fatty acid-binding protein: homology with a rat membrane protein implicated in the binding or transport of long-chain fatty acids. *J Mol Cell Cardiol* 27:1613-1622, 1995
185. Luiken JJ, Arumugam Y, Dyck DJ, Bell RC, Pelsers MM, Turcotte LP, Tandon NN, Glatz JF, Bonen A: Increased rates of fatty acid uptake and plasmalemmal fatty acid transporters in obese Zucker rats. *J Biol Chem* 276:40567-40573, 2001
186. Bonen A, Parolin ML, Steinberg GR, Calles-Escandon J, Tandon NN, Glatz JF, Luiken JJ, Heigenhauser GJ, Dyck DJ: Triacylglycerol accumulation in human obesity and type 2 diabetes is associated with increased rates of skeletal muscle fatty acid transport and increased sarcolemmal FAT/CD36. *Faseb J* 18:1144-1146, 2004
187. Bergmeyer HU: *Methods in Enzymatic Analysis*. New York, Weinheim Verlag Chemie, 1974
188. Matsuno K, Diaz-Ricart M, Montgomery RR, Aster RH, Jamieson GA, Tandon NN: Inhibition of platelet adhesion to collagen by monoclonal anti-CD36 antibodies. *Br J Haematol* 92:960-967, 1996
189. Bach AC, Babayan VK: Medium-chain triglycerides: an update. *Am J Clin Nutr* 36:950-962, 1982
190. Jong-Yeon K, Hickner RC, Dohm GL, Houmard JA: Long- and medium-chain fatty acid oxidation is increased in exercise-trained human skeletal muscle. *Metabolism* 51:460-464, 2002
191. Carter SL, Rennie CD, Hamilton SJ, Tarnopolsky: Changes in skeletal muscle in males and females following endurance training. *Can J Physiol Pharmacol* 79:386-392, 2001

192. Tremblay A, Simoneau JA, Bouchard C: Impact of exercise intensity on body fatness and skeletal muscle metabolism. *Metabolism* 43:814-818, 1994
193. Tunstall RJ, Mehan KA, Wadley GD, Collier GR, Bonen A, Hargreaves M, Cameron-Smith D: Exercise training increases lipid metabolism gene expression in human skeletal muscle. *Am J Physiol Endocrinol Metab* 283:E66-72, 2002
194. Zhang CY, Hagen T, Mootha VK, Sliker LJ, Lowell BB: Assessment of uncoupling activity of uncoupling protein 3 using a yeast heterologous expression system. *FEBS Lett* 449:129-134, 1999
195. Harper ME, Dent R, Monemdjou S, Bezaire V, Van Wyck L, Wells G, Kavaslar GN, Gauthier A, Tesson F, McPherson R: Decreased mitochondrial proton leak and reduced expression of uncoupling protein 3 in skeletal muscle of obese diet-resistant women. *Diabetes* 51:2459-2466, 2002
196. Millet L, Vidal H, Andreelli F, Larrouy D, Riou JP, Ricquier D, Laville M, Langin D: Increased uncoupling protein-2 and -3 mRNA expression during fasting in obese and lean humans. *J Clin Invest* 100:2665-2670, 1997
197. Boss O, Samec S, Desplanches D, Mayet MH, Seydoux J, Muzzin P, Giacobino JP: Effect of endurance training on mRNA expression of uncoupling proteins 1, 2, and 3 in the rat. *Faseb J* 12:335-339, 1998
198. Gong DW, He Y, Reitman ML: Genomic organization and regulation by dietary fat of the uncoupling protein 3 and 2 genes. *Biochem Biophys Res Commun* 256:27-32, 1999
199. Eaton S: Current views of fatty acid oxidation and ketogenesis: from organelles to point mutations. New York, 1999

200. Watt MJ, Heigenhauser GJ, O'Neill M, Spriet LL: Hormone-sensitive lipase activity and fatty acyl-CoA content in human skeletal muscle during prolonged exercise. *J Appl Physiol* 95:314-321, 2003
201. Harris RC, Hultman E, Nordesjo LO: Glycogen, glycolytic intermediates and high-energy phosphates determined in biopsy samples of musculus quadriceps femoris of man at rest. Methods and variance of values. *Scand J Clin Lab Invest* 33:109-120, 1974
202. Cederblad G, Carlin JI, Constantin-Teodosiu D, Harper P, Hultman E: Radioisotopic assays of CoASH and carnitine and their acetylated forms in human skeletal muscle. *Anal Biochem* 185:274-278, 1990
203. Frayn KN, Maycock PF: Skeletal muscle triacylglycerol in the rat: methods for sampling and measurement, and studies of biological variability. *J Lipid Res* 21:139-144, 1980
204. Schrauwen P, Hardie DG, Roorda B, Clapham JC, Abuin A, Thomason-Hughes M, Green K, Frederik PM, Hesselink MK: Improved glucose homeostasis in mice overexpressing human UCP3: a role for AMP-kinase? *Int J Obes Relat Metab Disord* 28:824-828, 2004
205. Bonen A, Benton CR, Campbell SE, Chabowski A, Clarke DC, Han XX, Glatz JF, Luiken JJ: Plasmalemmal fatty acid transport is regulated in heart and skeletal muscle by contraction, insulin and leptin, and in obesity and diabetes. *Acta Physiol Scand* 178:347-356, 2003
206. Schrauwen P, Hoeks J, Schaart G, Kornips E, Binas B, Van De Vusse GJ, Van Bilsen M, Luiken JJ, Coort SL, Glatz JF, Saris WH, Hesselink MK: Uncoupling protein 3 as a mitochondrial fatty acid anion exporter. *Faseb J* 17:2272-2274, 2003

207. Hardie DG, Salt IP, Hawley SA, Davies SP: AMP-activated protein kinase: an ultrasensitive system for monitoring cellular energy charge. *Biochem J* 338 (Pt 3):717-722, 1999
208. Ruderman NB, Saha AK, Kraegen EW: Minireview: malonyl CoA, AMP-activated protein kinase, and adiposity. *Endocrinology* 144:5166-5171, 2003
209. Holloszy JO: Biochemical adaptations in muscle. Effects of exercise on mitochondrial oxygen uptake and respiratory enzyme activity in skeletal muscle. *J Biol Chem* 242:2278-2282, 1967
210. Eaton S, Bartlett K, Quant PA: Carnitine palmitoyl transferase I and the control of beta-oxidation in heart mitochondria. *Biochem Biophys Res Commun* 285:537-539, 2001
211. Horie S, Isobe M, Suga T: Changes in CoA pools in hepatic peroxisomes of the rat under various conditions. *J Biochem (Tokyo)* 99:1345-1352, 1986
212. Conte A, Palmieri L, Segnini D, Ronca G: Antidyslipaemic action and role of CoA in lipid metabolism of mitochondria and peroxisomes. *Int J Tissue React* 13:33-36, 1991
213. Short KR, Nygren J, Barazzoni R, Levine J, Nair KS: T(3) increases mitochondrial ATP production in oxidative muscle despite increased expression of UCP2 and -3. *Am J Physiol Endocrinol Metab* 280:E761-769, 2001
214. Garcia-Martinez C, Sibille B, Solanes G, Darimont C, Mace K, Villarroya F, Gomez-Foix AM: Overexpression of UCP3 in cultured human muscle lowers mitochondrial membrane potential, raises ATP/ADP ratio, and favors fatty acid vs. glucose oxidation. *Faseb J* 15:2033-2035, 2001

215. Edstrom L, Hultman E, Sahlin K, Sjoholm H: The contents of high-energy phosphates in different fibre types in skeletal muscles from rat, guinea-pig and man. *J Physiol* 332:47-58, 1982
216. Kushmerick MJ, Moerland TS, Wiseman RW: Mammalian skeletal muscle fibers distinguished by contents of phosphocreatine, ATP, and Pi. *Proc Natl Acad Sci U S A* 89:7521-7525, 1992
217. Russell AP, Wadley G, Hesselink MK, Schaart G, Lo S, Leger B, Garnham A, Kornips E, Cameron-Smith D, Giacobino JP, Muzzin P, Snow R, Schrauwen P: UCP3 protein expression is lower in type I, Iia and Iix muscle fiber types of endurance-trained compared to untrained subjects. *Pflugers Arch* 445:563-569, 2003
218. Alexson SE, Nedergaard J: A novel type of short- and medium-chain acyl-CoA hydrolases in brown adipose tissue mitochondria. *J Biol Chem* 263:13564-13571, 1988
219. Hulver MW, Berggren JR, Cortright RN, Dudek RW, Thompson RP, Pories WJ, MacDonald KG, Cline GW, Shulman GI, Dohm GL, Houmard JA: Skeletal muscle lipid metabolism with obesity. *Am J Physiol Endocrinol Metab* 284:E741-747, 2003
220. Kimber NE, Heigenhauser GJ, Spriet LL, Dyck DJ: Skeletal muscle fat and carbohydrate metabolism during recovery from glycogen-depleting exercise in humans. *J Physiol* 548:919-927, 2003
221. Steinberg GR, Bonen A, Dyck DJ: Fatty acid oxidation and triacylglycerol hydrolysis are enhanced after chronic leptin treatment in rats. *Am J Physiol Endocrinol Metab* 282:E593-600, 2002
222. Eaton S: Control of mitochondrial beta-oxidation flux. *Prog Lipid Res* 41:197-239, 2002

223. Gilde AJ, Van Bilsen M: Peroxisome proliferator-activated receptors (PPARS): regulators of gene expression in heart and skeletal muscle. *Acta Physiol Scand* 178:425-434, 2003
224. Spina RJ, Chi MM, Hopkins MG, Nemeth PM, Lowry OH, Holloszy JO: Mitochondrial enzymes increase in muscle in response to 7-10 days of cycle exercise. *J Appl Physiol* 80:2250-2254, 1996
225. Bruce CR, Anderson MJ, Carey AL, Newman DG, Bonen A, Kriketos AD, Cooney GJ, Hawley JA: Muscle oxidative capacity is a better predictor of insulin sensitivity than lipid status. *J Clin Endocrinol Metab* 88:5444-5451, 2003
226. Kiens B, Roepstorff C, Glatz JF, Bonen A, Schjerling P, Knudsen J, Nielsen JN: Lipid-binding proteins and lipoprotein lipase activity in human skeletal muscle: influence of physical activity and gender. *J Appl Physiol* 97:1209-1218, 2004
227. Schrauwen P, Troost FJ, Xia J, Ravussin E, Saris WH: Skeletal muscle UCP2 and UCP3 expression in trained and untrained male subjects. *Int J Obes Relat Metab Disord* 23:966-972, 1999

APPENDIX 1

Raw Data: Study 1

Table 2 (Human VL)

	SS	IMF
CPTI activity	221	202
	270	221
	285	327
	136	125
	286	391
	405	150
	355	503
	186	276
	231	385
CS activity	2.69	1.92
	2.04	1.76
	2.69	3.56
	1.57	2.26
	5.41	1.98
	1.16	3.07
	1.83	1.86
	2.47	1.36
	1.87	1.86
Activity at 0.7 μM M-CoA	168	180
	130	190
	208	214
	107	105
	205	351
	324	88
	100	343
	98	162
	82	126

Figure 1 (Human VL)

	SS	IMF
No M-CoA	220	202
	270	221
	285	326
	135	125
	286	391
	404	150
	186	503
	355	276
	106	245
0.2 μM M-CoA	169	180
	141	201
	276	218
	120	106
	228	364
	369	130
	188	385
	319	224
	104	193
0.7 μM M-CoA	167	137
	130	190
	207	213
	107	105
	205	351
	323	88
	105	342
	274	162
	81	131
2.0 μM M-CoA	172	109
	116	172
	201	214
	123	88
	180	334
	198	86
	100	265
	149	149
	56	118

Figure 2 (Human VL)

	CON	M-CoA	Ca	AMP	ADP	Pi	All
SS	220	167	170	153	192	143	122
	270	130	107	137	147	102	113
	285	208	197	198	208	228	209
	136	107	137	140	87	106	90
	286	205	193	177	176	209	167
	404	324	323	254	238	233	281
	186	100	108	116	81	131	75
	355	274	274	205	189	185	232
	231	82	62	54	88	28	69
IMF	202	180	164	120	195	168	137
	221	190	209	209	247	205	193
	327	214	206	271	282	241	246
	125	105	64	115	111	105	128
	391	351	355	402	413	357	378
	150	88	70	53	90	89	64
	502	343	315	255	300	248	262
	133	71	54	37	74	73	47
	385	126	127	110	104	69	91

Figure 3 (Human VL)

	pH 7.1	pH 6.8
SS	442	207
	446	283
	165	109
	312	187
	670	457
IMF	683	637
	260	132
	140	89

Table 3 (Rat Sol and RG)

	SS		IMF	
	Sol	RG	Sol	RG
CPTI activity	367	876	347	395
	289	382	1318	482
	921	824	1338	603
	264	733	208	-
	306	1112	322	1035
	785	-	1008	-
	559	-	1041	-
	787	-	1226	-
CS activity	2.46	2.09	2.71	7.35
	5.53	5.14	2.71	5.45
	4.28	4.58	3.42	7.78
	4.95	5.53	3.34	-
	3.14	3.29	4.01	2.01
	2.74	-	3.32	-
	6.73	-	3.9	-
	2.71	-	2.17	-
Activity at 2 μM M-CoA	91	45	94	216
	119	217	557	258
	199	132	128	103
	217	449	198	-
	46	774	13	678
	185	-	369	-
	258	-	55	-
	440	-	730	-

Figure 4a, b (Rat Sol and RG)

	SS		IMF	
	Sol	RG	Sol	RG
No M-CoA	367	876	348	395
	288	382	1318	482
	921	824	1338	603
	264	732	208	-
	306	1112	322	1035
	785	-	1008	-
	559	-	1041	-
	787	-	1226	-
0.2 μM M-CoA	312	490	255	256
	224	334	1064	399
	769	761	1216	532
	251	654	198	-
	245	1028	195	714
	706	-	906	-
	510	-	787	-
	637	-	1234	-
0.7 μM M-CoA	94	456	190	236
	176	227	1028	327
	711	584	651	430
	226	538	154	-
	177	908	97	888
	486	-	873	-
	464	-	614	-
	643	-	1183	-
2.0 μM M-CoA	91	45	94	216
	119	217	557	258
	199	132	128	103
	217	449	136	-
	46	774	13	678
	185	-	369	-
	258	-	55	-
	440	-	730	-

Figure 5a, b (Rat Sol and RG)

	CON	M-CoA	Ca	AMP	ADP	Pi	All
Sol -SS	367	94	127	152	173	183	128
	289	223	227	212	260	179	179
	921	769	889	785	749	740	731
	264	226	209	246	171	157	143
	305	245	210	223	175	198	150
	785	706	462	231	500	400	473
	559	510	486	490	508	462	469
	786	643	566	590	561	633	586
Sol - IMF	347	190	84	108	95	124	148
	1318	1063	885	832	724	770	798
	1338	1216	915	1009	705	1063	975
	208	154	201	234	37	182	85
	322	195	133	103	85	75	81
	1008	873	754	860	967	982	875
	1041	787	675	658	644	683	584
	1226	1183	921	1150	1055	1131	1064
RG-SS	876	490	290	334	368	555	293
	381	334	317	258	232	240	184
	824	583	577	577	554	629	631
	732	654	633	653	698	724	762
	1112	1028	948	965	873	864	947
RG-IMF	394	256	235	235	245	174	205
	481	399	341	273	288	291	254
	602	531	490	525	473	-	-
	-	-	-	-	-	-	-
	1035	714	832	908	735	814	704

APPENDIX 2

Raw Data: Study 2

Figure 2 (SSO palmitate dose-response)

0 μM SSO	25 μM SSO	50 μM SSO	100 μM SSO	200 μM SSO
17.05	12.31	7.41	2.39	0
47.84	36.02	17.37	12.92	3.83
17.63	15.19	11.72	6.17	2.82
34.04	26.21	17.70	9.19	5.79

Figure 3 (Octanoate oxidation)

CON	200 μM SSO
21.53	19.59
32.14	30.85

Figure 4a (Max and submax CPTI activity)

300 μM P-CoA	150 P-CoA	75 P-CoA	39 P-CoA	18 P-CoA
Control				
426	213	139	67	31
173	117	97	63	37
138	86	44	20	6
137	81	61	29	12
200 μM SSO				
447	292	175	99	47
153	119	44	10	0
132	115	70	25	24
142	89	74	40	15

Figure 4b (Palmitoylcarnitine oxidation)

CON	200 μM SSO
17.29	2.54
31.54	0.07
49.33	1.09
86.81	14.34

Figure 5a, b, c, d (Correlations)

Oxidation	VO2	CPTI	b-HAD	CS
26.1	43.8	138.0	15.3	31.3
47.1	45.3	128.0	14.9	35.1
41.8	50.2	331.0	18.3	53.9
34.4	51.0	108.0	12.9	27.4
34.2	52.6	106.0	13.1	30.8
19.8	53.2	131.0	18.3	29.2
34.0	55.0	110.0	17.9	47.9
9.1	21.5	93.0	5.3	18.5
7.8	26.9	89.0	16.8	25.4
17.8	31.4	70.0	13.7	23.1
24.3	34.6	44.0	9.1	36.2
4.4	35.0	51.0	17.3	26.6
3.3	35.2	59.0	22.4	33.3
17.0	36.4	66.0	11.5	21.7

Figure 6 (Prediction)

Palmitate oxidation	CPTI activity	FAT/CD36 content
26.1	138.0	2.5
41.8	331.0	3.5
34.4	108.0	1.5
34.2	106.0	1.8
19.8	131.0	2.5
34.0	110.0	2.2
7.8	89.0	2.3
17.8	70.0	2.5

APPENDIX 3

Raw data: Study 3

Table 1 (Whole body)

	WT	Ucp3-tg	Ucp3 (-/-)		WT	Ucp3-tg	Ucp3(-/-)
Food Intake	3.28	3.40	3.44	I BAT	4.49	5.24	3.40
	2.77	2.22	2.64		5.30	5.30	3.27
	2.75	3.46	3.29		2.96	4.47	3.58
	3.58	3.30	3.25		3.34	5.18	2.95
	4.42	3.15	3.50		2.98	1.40	3.34
	3.36	3.00	3.75		5.68	3.93	2.25
	2.87	3.23	3.33		1.46	3.50	1.99
		3.28			2.23	2.20	1.31
Body Weights	17.50	18.43	18.16	P WAT	8.34	8.71	8.98
	18.60	15.76	15.46		11.22	5.28	8.61
	16.55	18.05	16.35		8.97	9.24	7.73
	18.71	17.15	17.62		7.09	2.27	7.34
	19.85	15.19	17.78		10.72	11.75	4.11
	22.16	12.77	14.78		3.37	6.11	4.79
	16.14	14.24	15.40		6.65	8.08	6.24
	16.61	16.17	17.36				

Table 2 (In vivo)

	WT	Ucp3-tg	Ucp3 (-/-)
VO ₂	3.88	3.60	4.23
	3.71	5.50	2.42
	4.21	3.60	3.56
	3.48	3.42	3.89
	3.46	4.03	3.53
RER	1.027	0.922	0.940
	0.925	0.930	0.940
	0.913	0.858	0.937
	0.939	0.881	1.020
	0.927	0.898	1.022

Table 3 (Serum)

Table 4 (Westerns)

	WT	Ucp3-tg	Ucp3(-/-)		WT	Ucp3-tg	Ucp3(-/-)
FFA	517	235.2	509.4	FAT/ CD36	1.71	1.36	1.19
	546.5	325.8	562.1		1.08	0.90	1.64
	451	414.4	578.7		0.67	0.90	0.80
	388.3	288.6	384		1.11	1.06	1.20
	422.7	243.5	333.6		0.71	0.80	1.15
	380.8	-	426.2		0.72	1.01	1.02
	550.9	-	339.6	FABPpm	0.94	1.51	1.24
	-	-	392.9		0.89	1.55	0.65
	-	-	363.4		1.08	1.58	1.51
	-	-	383.2		0.87	1.65	1.68
Glucose	11.08	15.13	19.87	FABPc	0.87	1.16	0.82
	17.73	13.3	27.11		1.36	1.99	0.40
	17.05	16.12	14.99	AMPK Phos/tot	1.05	1.59	1.32
	17.15	15.54	14.22		1.22	1.30	1.36
	9.8	21.29	15.56		0.70	1.16	0.98
	30.73	-	12.14		1.30	1.23	1.34
	13.14	-	13.44		0.64	1.13	0.59
	-	-	14.37		1.09	1.96	1.10
	-	-	13.54		1.16	1.08	0.27
	-	-	10.41		1.36	1.28	1.04
Ketones	216.7	248.4	355.6	AMPK Phos/tot	1.23	0.69	0.71
	335.2	172.1	481.7		0.69	0.54	0.86
	265.3	419	268.1		0.90	0.68	1.35
	206.7	255.1	186.3		1.02	1.03	0.90
	104.1	314.2	99.4				
	267.3	-	62.1				
	338.3	-	210.7				
	-	-	185.5				
	-	-	148.6				
	-	-	183.8				

Table 5 (Phosphagens)**Table 6 (Metabolites)**

	WT	Ucp3-tg	Ucp3(-/-)		WT	Ucp3-tg	Ucp3(-/-)
PCr	29.91	49.89	59.62	Free car	4.50	5.94	5.80
	28.74	67.67	38.23		4.14	6.69	5.55
	46.28	59.27	47.29		4.23	6.22	5.49
	19.87	45.22	41.24		3.98	5.79	4.95
	30.81	49.03	28.57		4.49	6.86	5.55
	27.86	30.55	10.12		-	6.01	4.56
	-	-	35.35		-	-	5.15
	-	-	37.86		-	-	-
Cr	75.11	63.32	37.37	Acetylcar	0.41	0.38	0.08
	63.40	54.66	64.24		0.27	0.25	0.16
	47.40	55.00	44.37		0.49	0.13	0.09
	78.40	69.70	57.66		0.60	0.39	0.15
	70.65	70.54	79.43		0.37	0.45	0.44
	78.13	96.41	85.29		-	0.50	0.34
	-	-	58.18		-	-	0.56
	-	-	71.63		-	-	-
Tot Cr	105.02	113.21	96.99	Tot car	4.90	6.32	5.89
	92.14	122.33	102.48		4.41	6.94	5.71
	93.68	114.27	91.66		4.72	6.35	5.57
	98.26	114.92	98.90		4.58	6.15	5.10
	101.45	119.57	108.00		4.86	7.31	6.00
	105.99	126.77	95.41		-	6.51	4.90
	-	-	93.53		-	-	5.71
	-	-	109.48		-	-	-
ATP	22.07	27.79	25.97	CoA	140.10	202.54	158.61
	16.87	29.66	26.14		124.64	178.25	92.90
	22.12	25.51	23.76		100.98	143.00	133.27
	18.88	24.97	22.39		95.60	173.20	112.22
	24.65	27.70	29.38		108.32	177.91	141.63
	20.20	28.64	23.35		-	141.15	115.81
	-	-	23.42		-	-	158.84
	-	-	27.04		-	-	140.60
ADP	2.99	3.90	3.03	Acetyl-CoA	8.54	11.31	6.36
	3.53	3.56	3.63		5.90	7.99	5.98
	3.05	3.83	2.89		7.10	5.22	4.80
	2.65	3.97	3.83		7.55	7.30	5.62
	3.18	3.90	3.63		8.07	10.92	13.06
	3.54	3.74	3.48		-	9.37	11.73
	3.83	-	3.14		-	-	10.00
	3.28	-	2.09		-	-	12.16
ATP/ ADP	6.26	7.13	8.58	Tot CoA	140.10	202.54	158.61
	6.37	8.32	7.20		124.64	178.25	92.90

	6.96	6.66	8.22		100.98	143.00	133.27
	5.34	6.29	8.13		95.60	173.20	112.22
	6.44	7.11	8.10		108.32	177.91	141.63
	6.16	7.66	6.72		-	141.15	115.81
	-	-	7.46		-	-	158.84
	-	-	12.94		-	-	140.60

Figure 2 (HSL)

Figure 3 (CPTI)

	WT	Ucp3-tg	Ucp3(-/-)		WT	Ucp3-tg	Ucp3(-/-)
HSL	0.90	0.55	0.65	CPTI	434	533	616
	0.80	0.78	0.79		197	672	339
	0.96	1.47	1.27		262	427	325
	1.27	0.73	0.89		344	279	305
	0.85	0.86	1.32		140	517	406
	0.99	1.04	0.60		224	224	199
	0.81	-	0.53		221	376	361
	0.91	-	0.88		180	346	218

Figure 4 (b-HAD)

Figure 5 (CS)

	WT	Ucp3-tg	Ucp3 (-/-)		WT	Ucp3-tg	Ucp3 (-/-)
b-HAD	2.82	9.87	7.14	CS	20.60	29.10	25.30
	3.59	7.93	7.88		22.50	40.70	30.50
	7.02	3.89	3.05		30.00	33.70	26.40
	4.43	3.95	5.25		23.20	22.90	15.80
	2.51	6.00	3.42		15.20	22.30	20.20
	3.75	7.31	5.86		22.00	20.50	17.30
	4.01	6.49	3.28		21.20	28.96	30.70
	-	-	-		22.80	33.50	19.20

Figure 6 (IMTG)

	WT	Ucp3-tg	Ucp3 (-/-)
IMTG	55.80	34.08	39.68
	66.44	25.70	48.74
	36.41	41.36	39.85
	48.28	21.42	65.07
	29.27	39.93	36.35
	41.01	23.57	49.96
	40.83	-	39.41
	-	-	51.84

